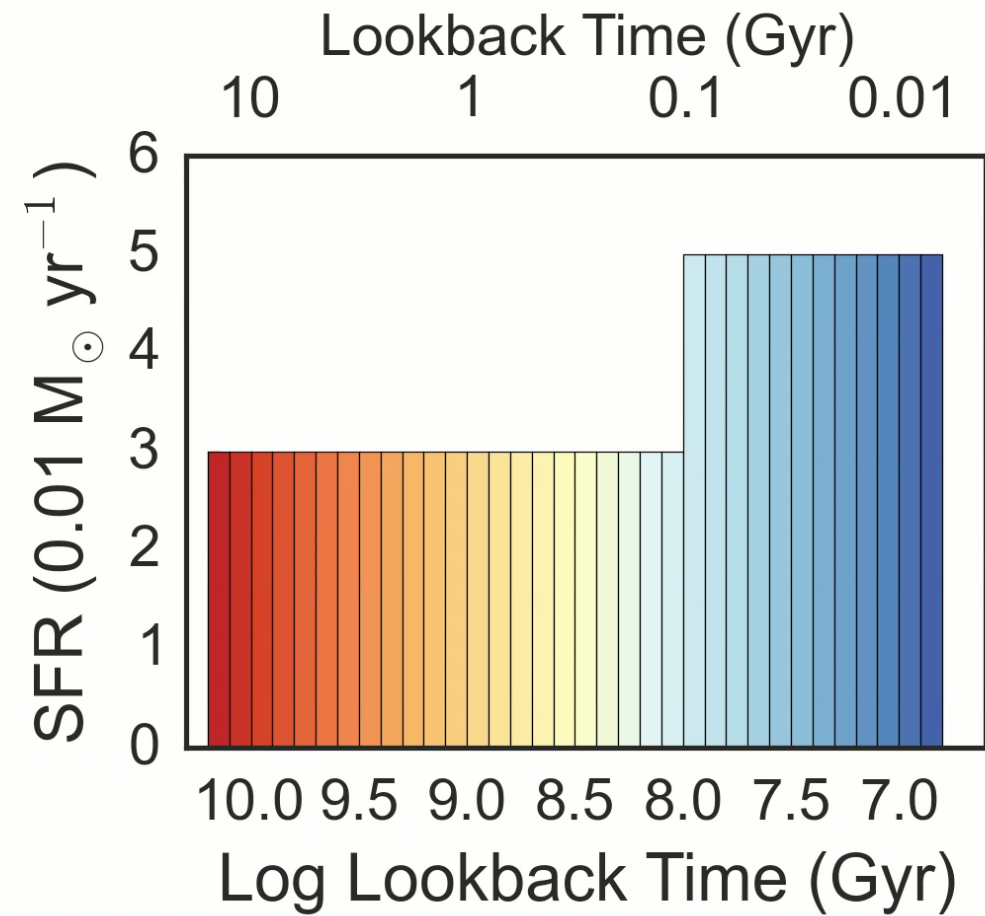
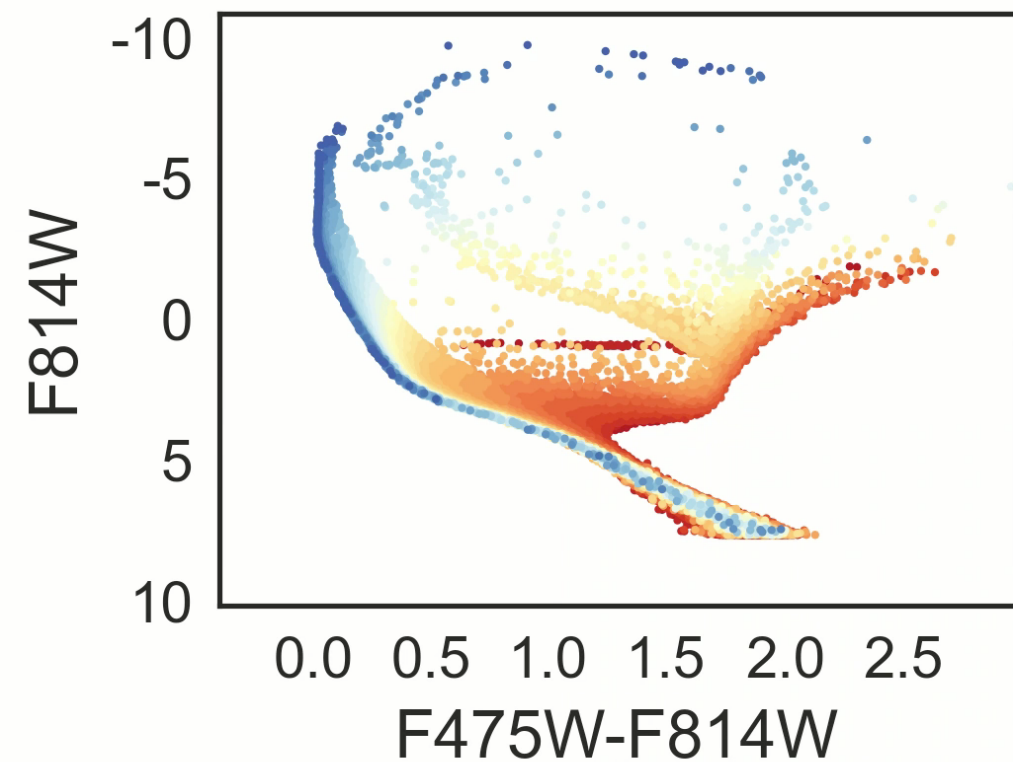


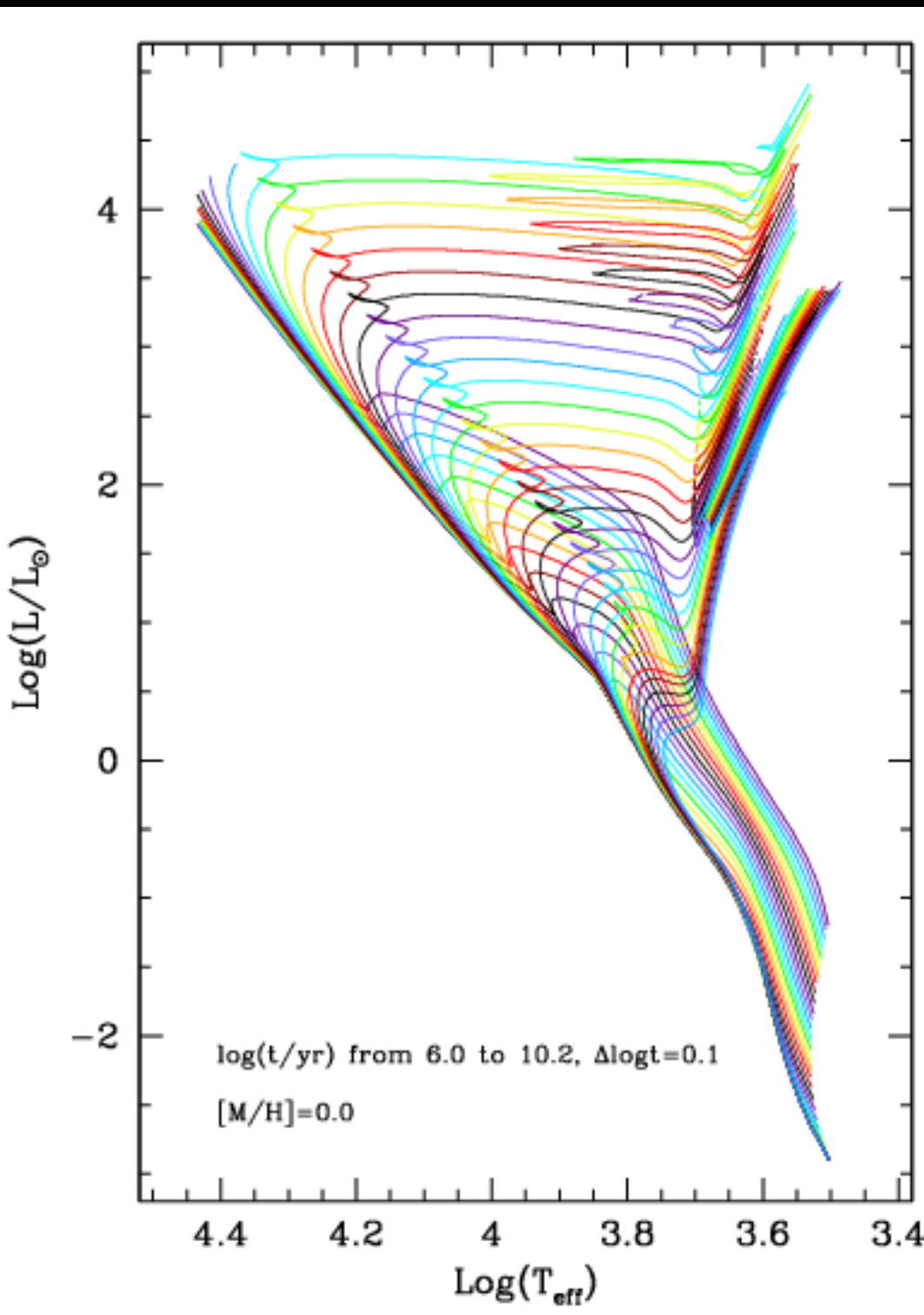
How do we measure galaxy ages*?

*more generally than just most recent 100 Myr

Essentially, how do we infer this from integrated light?

Movie Credit: Dan Weisz





Stellar isochrones as a function of age, for solar metallicity

Examples of theoretical isochrones in the HR diagram. {bf Left panel:} A sequence of solar-metallicity isochrones for ages going from $\log t = 6$ to 10.2 at equally spaced intervals of $\Delta \log t = 0.1$. {bf Right panel:} Three sequences of isochrones for a fixed age and at varying metallicity. The ages are $\log t = 6.3$, 8.0 and 10.1 . The sequence of metallicities goes from $[M/H] = -1.45$ to $+0.75$ at equally spaced intervals of $\Delta[M/H] = 0.2$. In all cases, the mass-loss parameter is assumed to be $\eta = 0.2$, and the sequences are completed down to $0.1 \sim M_{\odot}$. Notice the presence of the PMS phase in the youngest isochrones. Bressan et al 2012

Can fit the spectrum or spectral energy distribution with SPS models

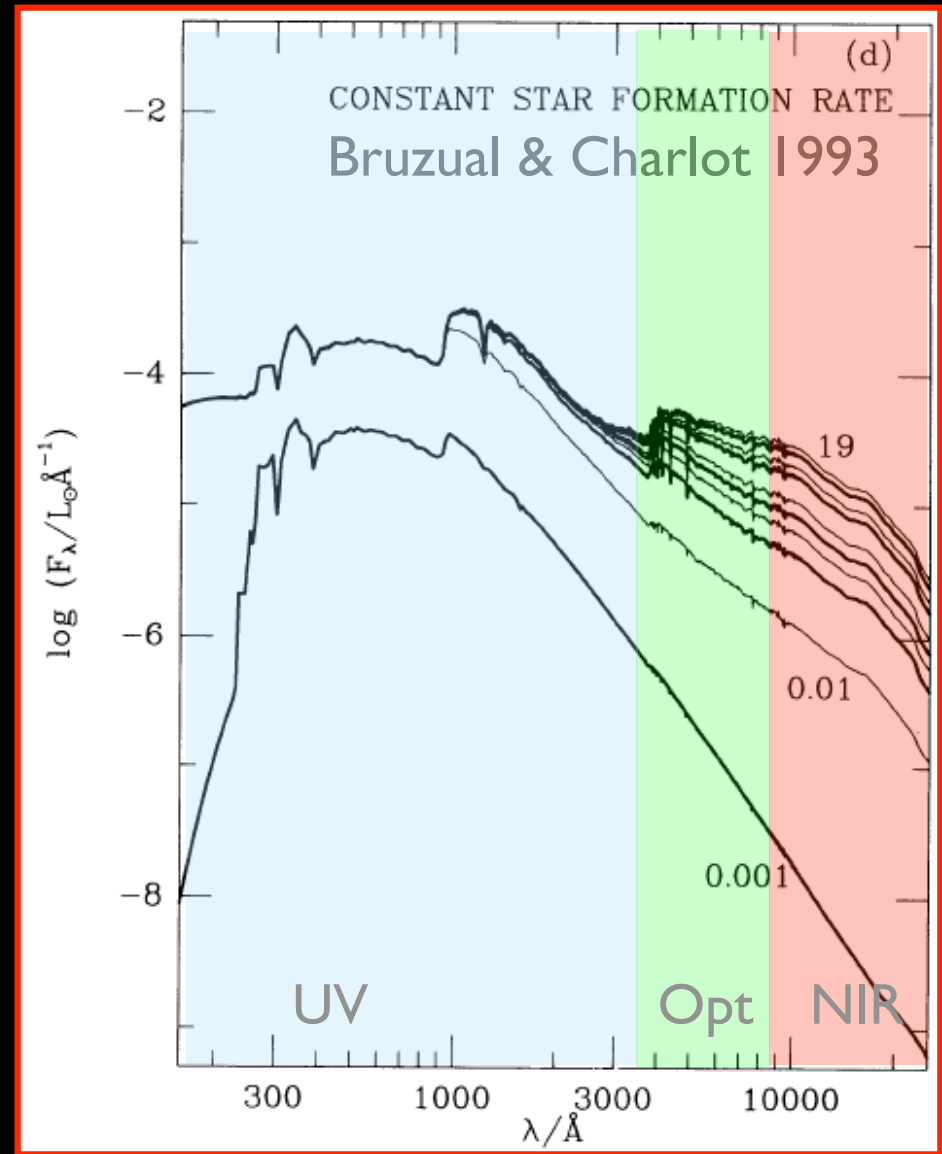
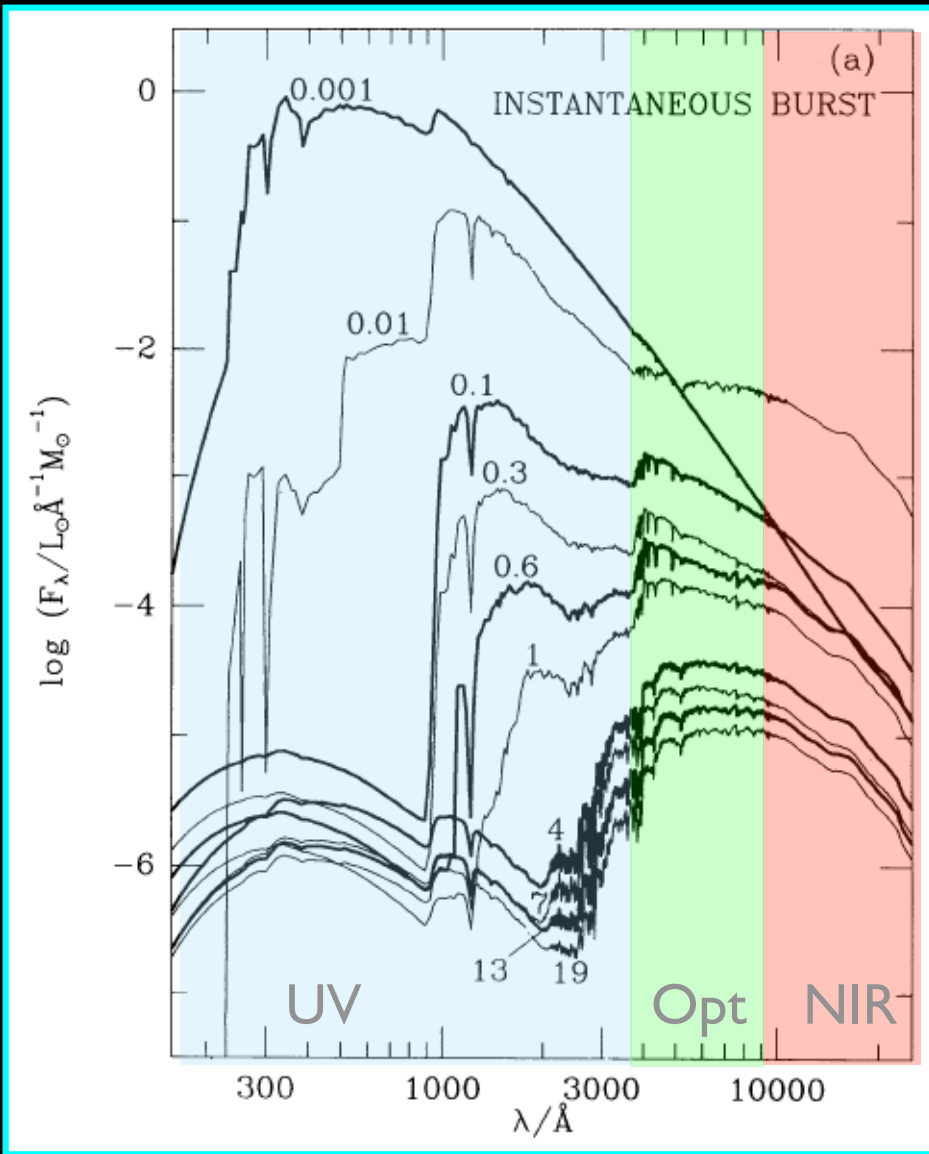
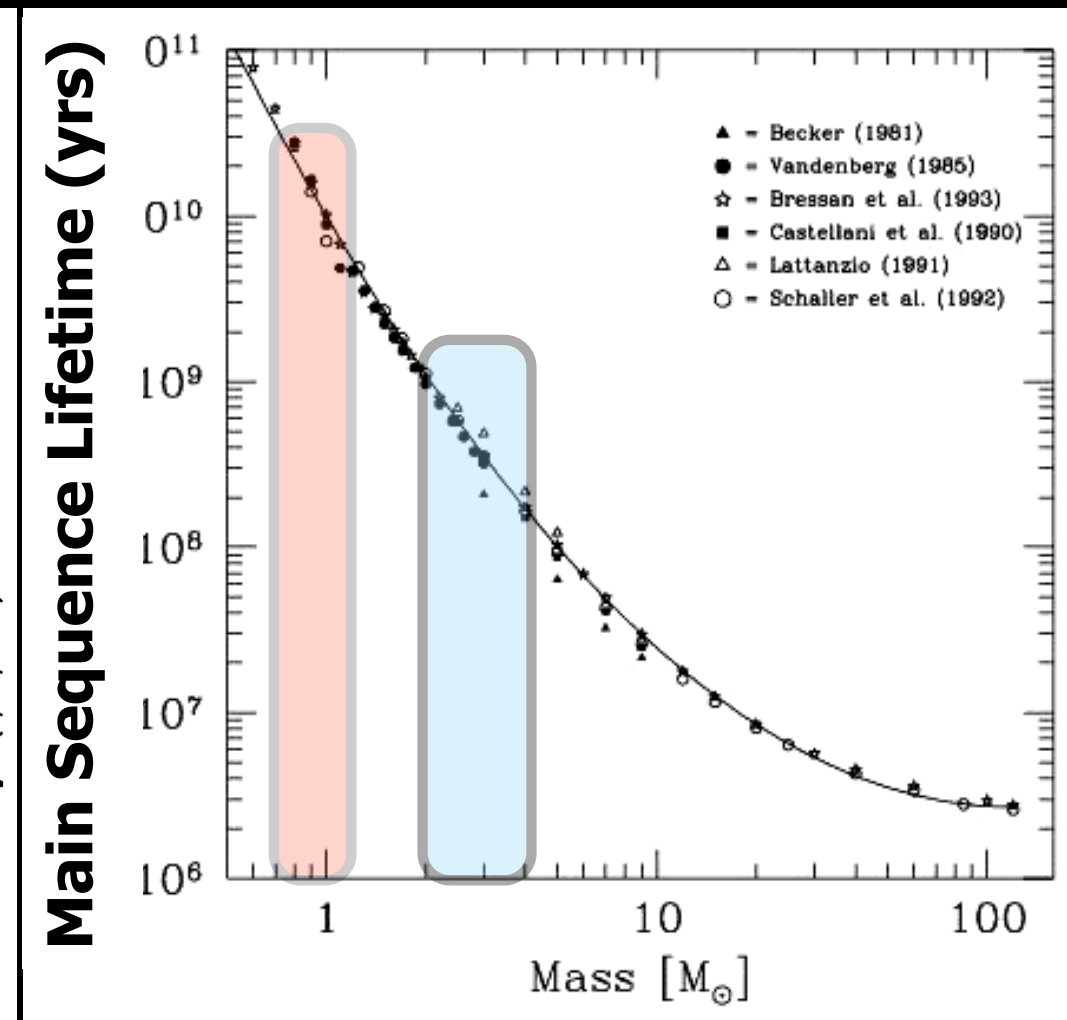
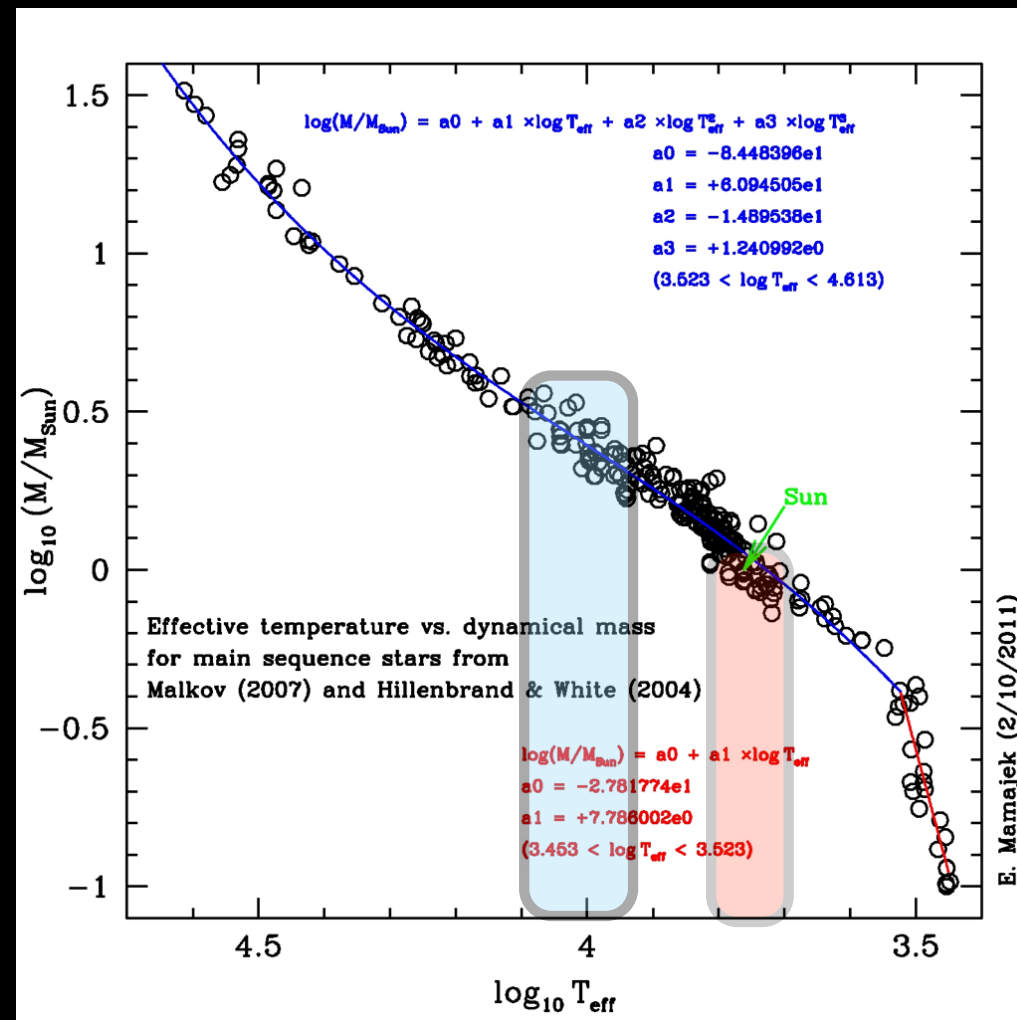


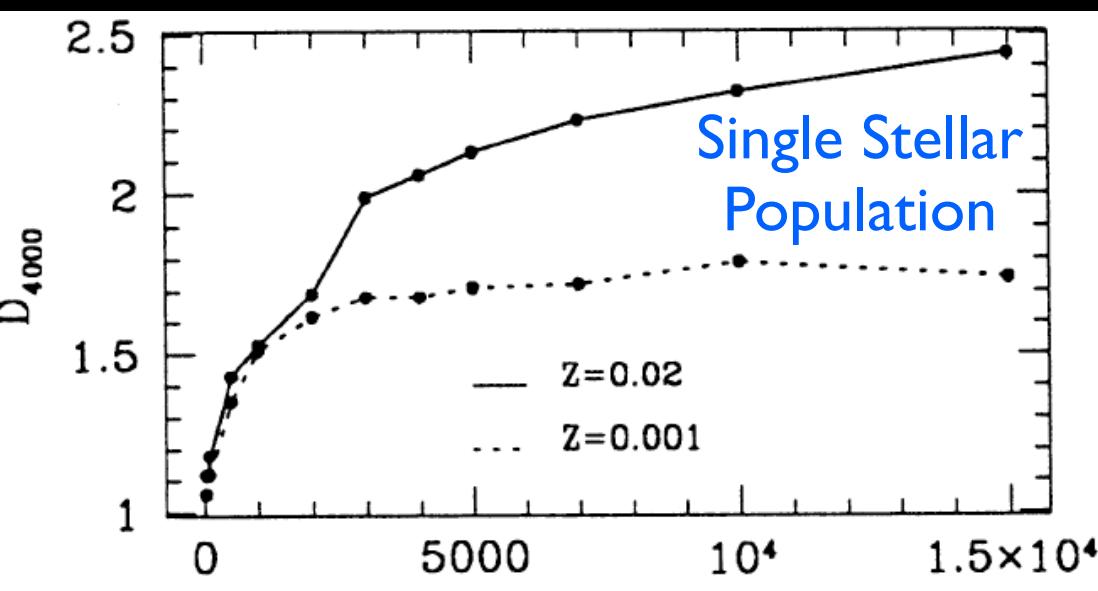
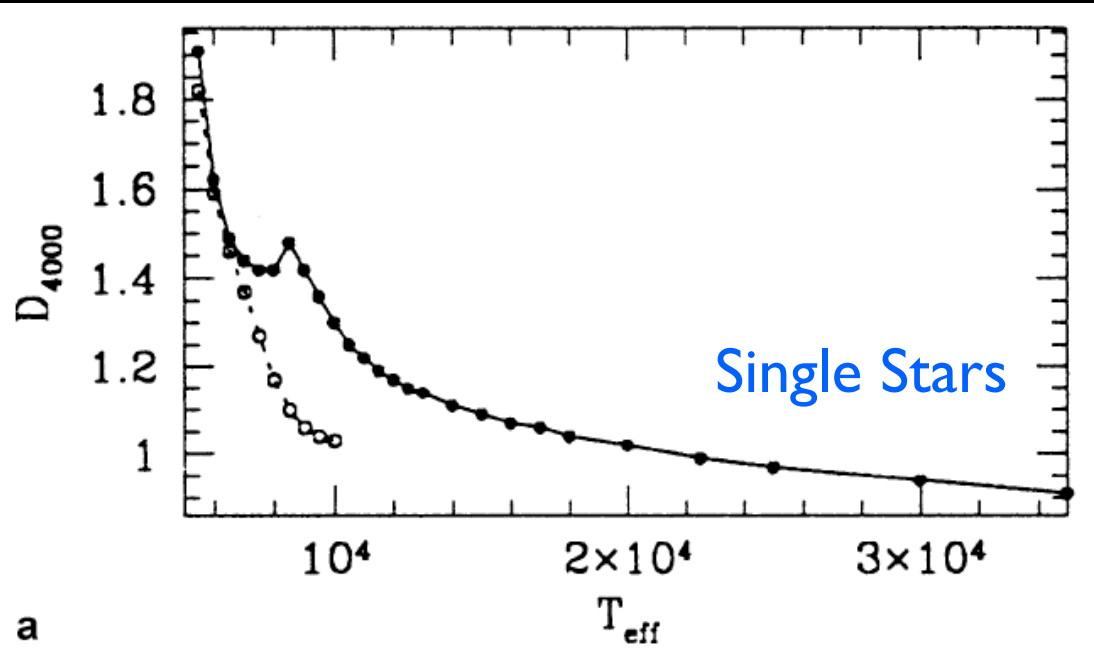
FIG. 4.—Spectral evolution of stellar populations with different star formation rates as predicted by the isochrone synthesis model: (a) instantaneous starburst; (b) eq. (2) with $\tau = 3$ Gyr; (c) eq. (2) with $\tau = 7$ Gyr; and (d) constant star formation. In each case, the age (in Gyr) is indicated next to the spectra. Thick lines and thin lines have been used alternatively for clarity. All models have the Salpeter IMF.

In practice, there are lots of shortcuts
one can take

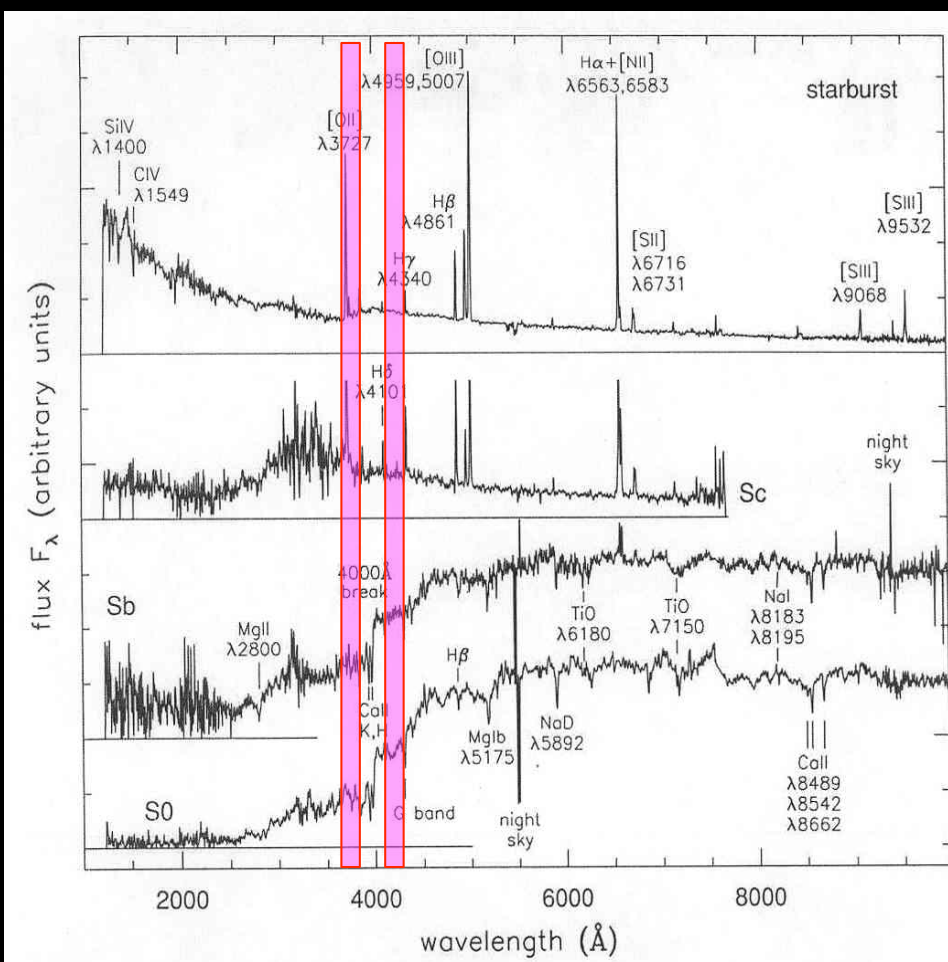
Age sensitivity comes from “what mass star is dominating spectrum”



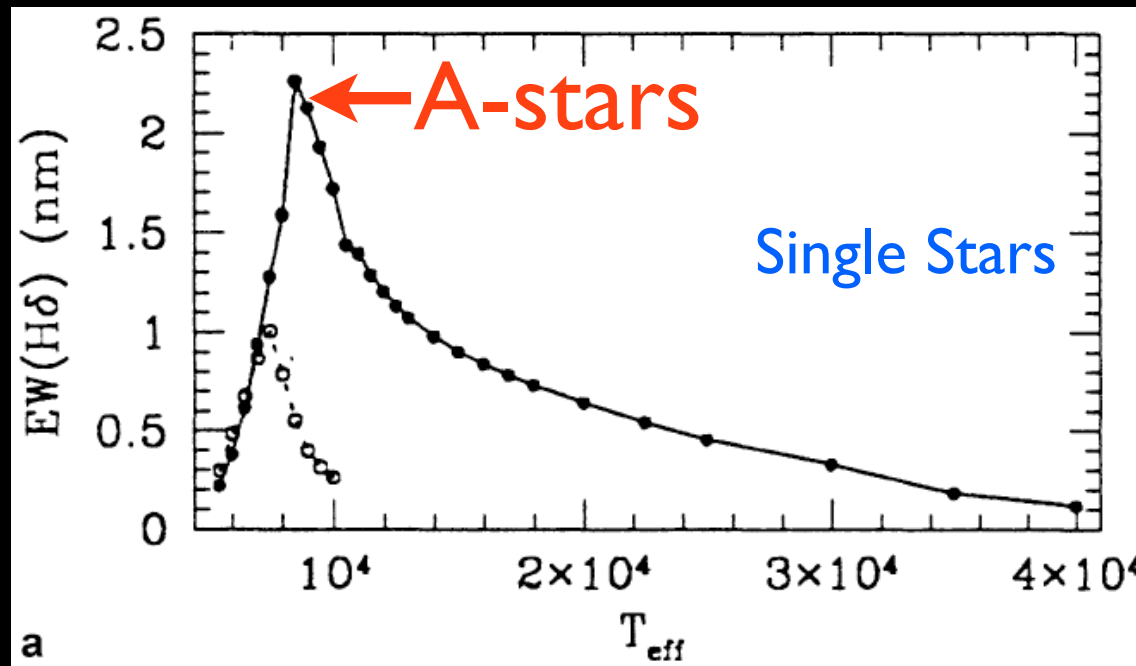
Ages from D₄₀₀₀: 4000 Angstrom Break Works to old ages, but metallicity issues



D_{4000} is largely used to determine the star formation characteristics of distant field and cluster galaxies. Hereafter the 4000 Å break is defined as the ratio between the average flux density in $\text{ergs s}^{-1}\text{cm}^{-2}\text{Hz}^{-1}$ between 4050 and 4250 Å and that between 3750 and 3950 Å (Bruzual 1983).

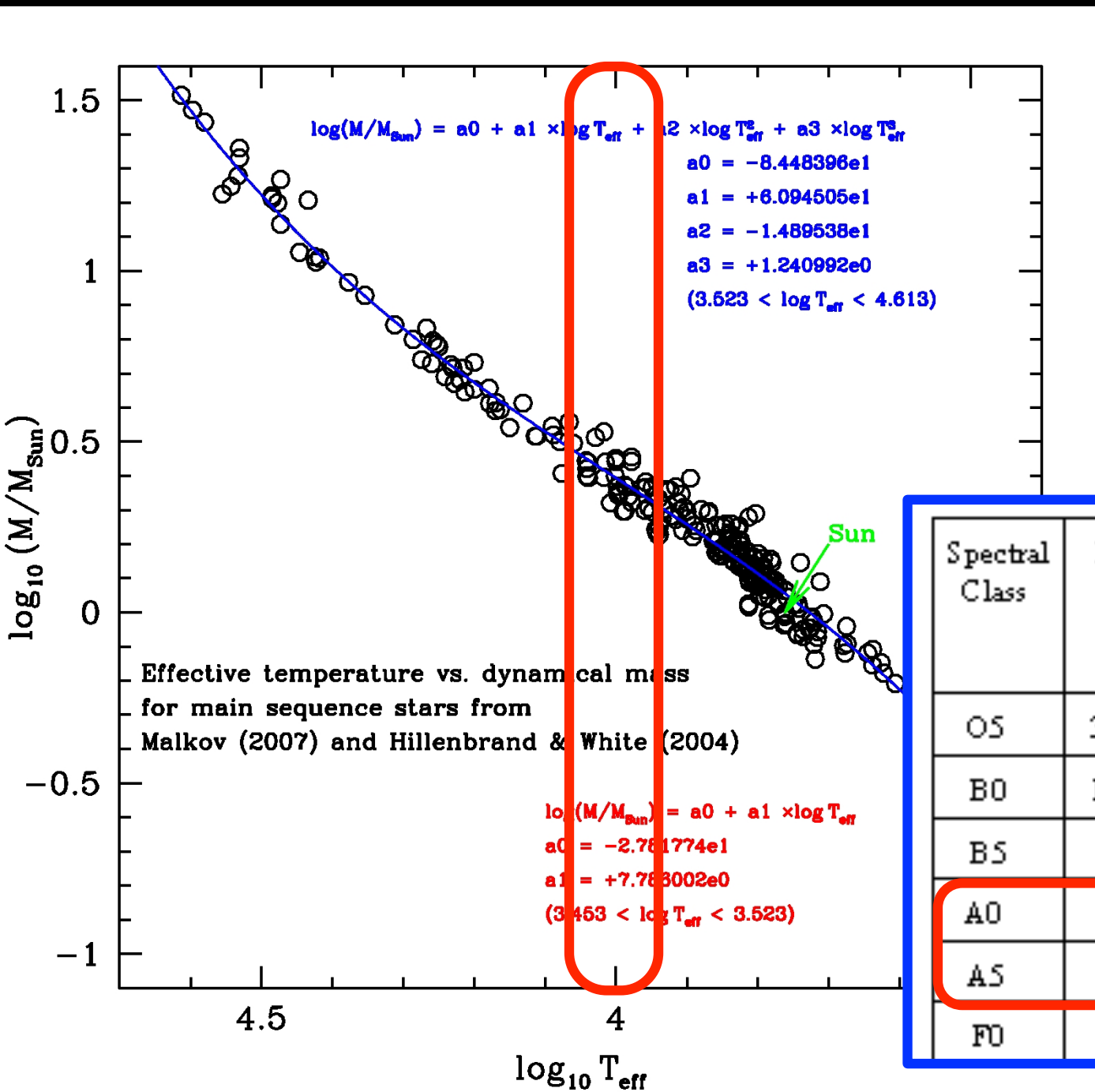


Ages from Balmer Absorption Lines: H δ



Strongest Balmer absorption lines are from A-stars with moderately high masses, and short (0.5-1 Gyr) lifetimes

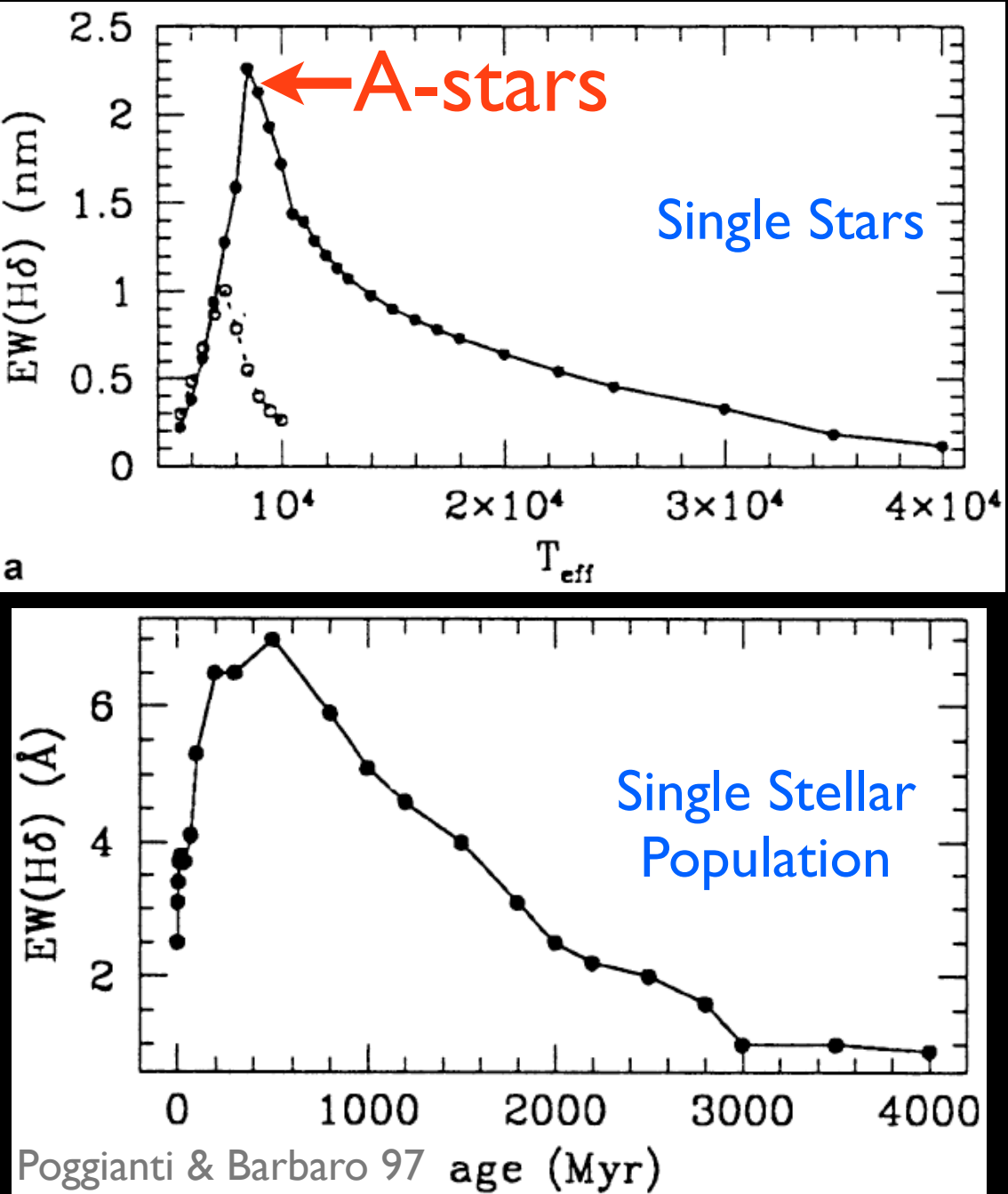
Ages from Balmer Absorption Lines: H δ



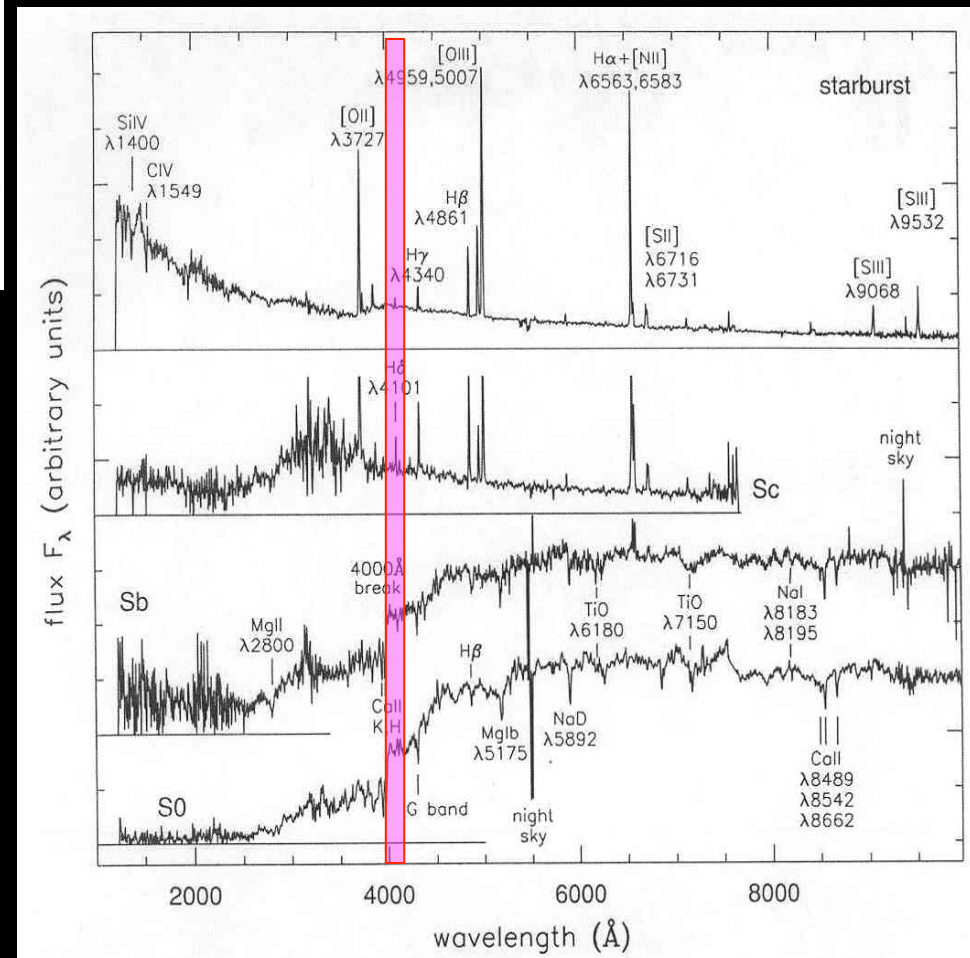
Peak Balmer
line strength
for $2-3 M_{\odot}$
stars

Spectral Class	Mass [M _⊙]	time to form [million years]	MS lifetime [million years]	time till He-flash [million years]
O5	32	0.01	1	
B0	16	0.1	10	2
B5	6		100	5
A0	3	1	500	30
A5	2		1,000	
F0	1.75		2,000	300

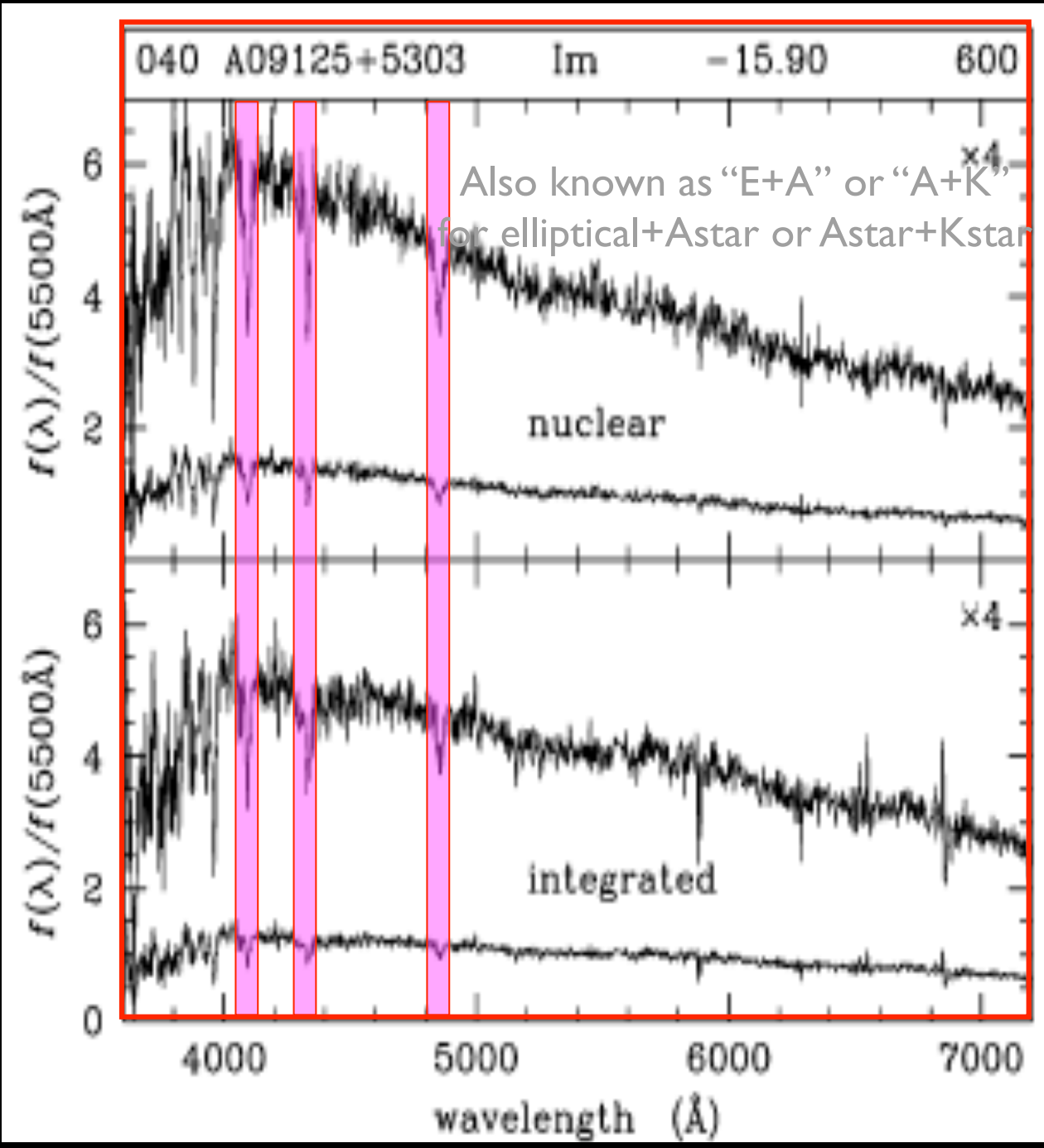
Ages from Balmer Absorption Lines: H δ



Note: Not sensitive past a few Gyrs

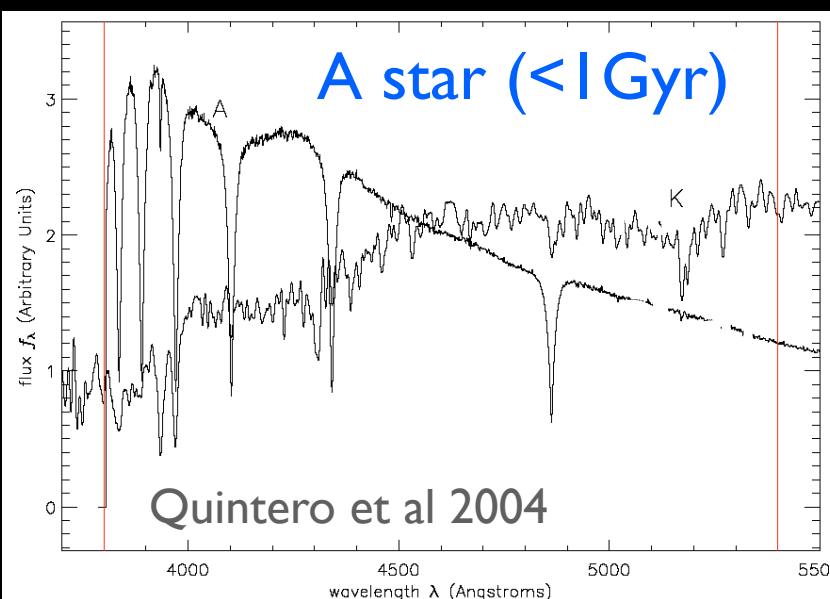


Example: “Post-Starburst” Spectrum



Blue stellar spectra, but no emission lines

strong Balmer absorption lines indicative of short lived A stars, but no sign of current SF



Metallicity

- Where do metals come from?
- What controls the metallicity of a galaxy?
- How do we measure it?
- Results.

Fast terminology

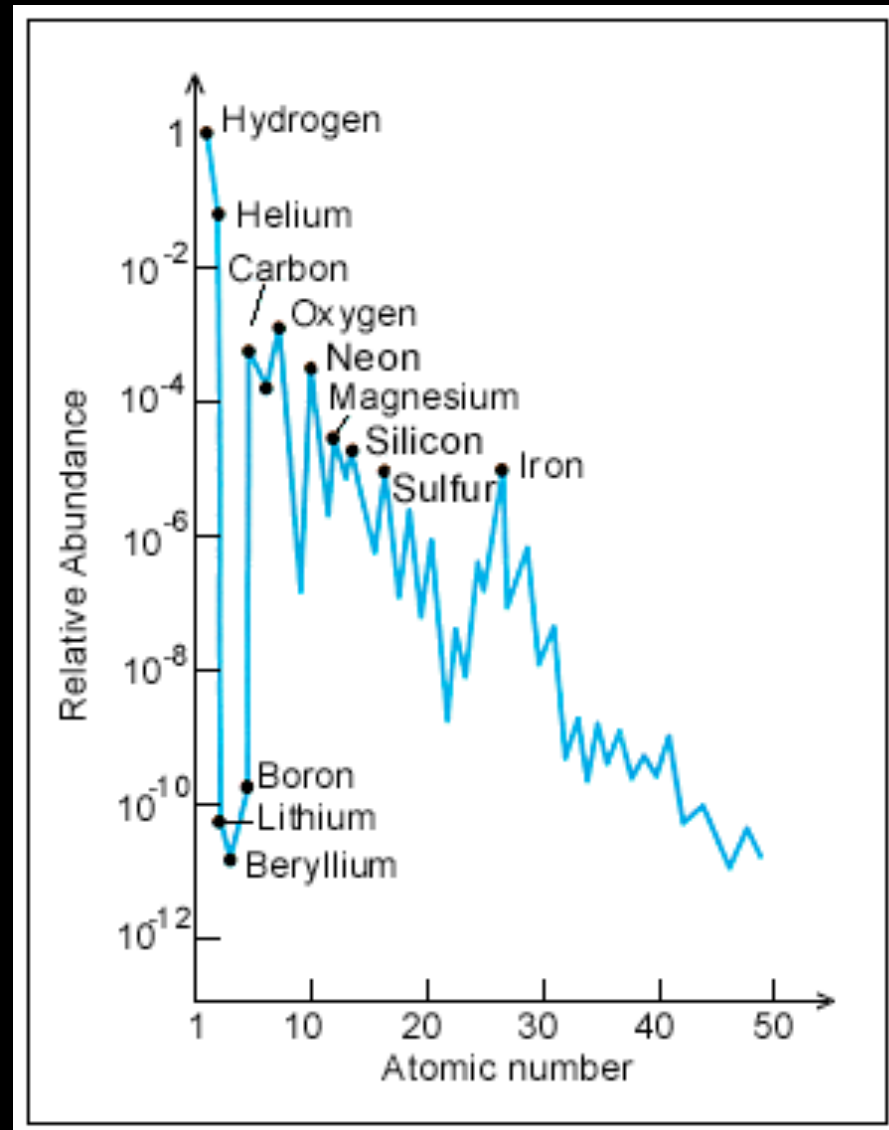
- “Metallicity”
 - For stars, usually refers to Fe
 - For gas, usually refers to O
 - Sometimes refers to all metals
- X = mass fraction of Hydrogen
- Y = mass fraction of Helium
- Z = mass fraction of metals
- “Abundance”
 - Usually refers to arbitrary elements

Abundance: Gas Phase

The gas phase abundance of an element X is defined:

$$l_2 + \log(X/H)$$

of atoms



Why l₂? In 1929 Henry Norris Russell arbitrarily chose $\log(N(H))=l_2$

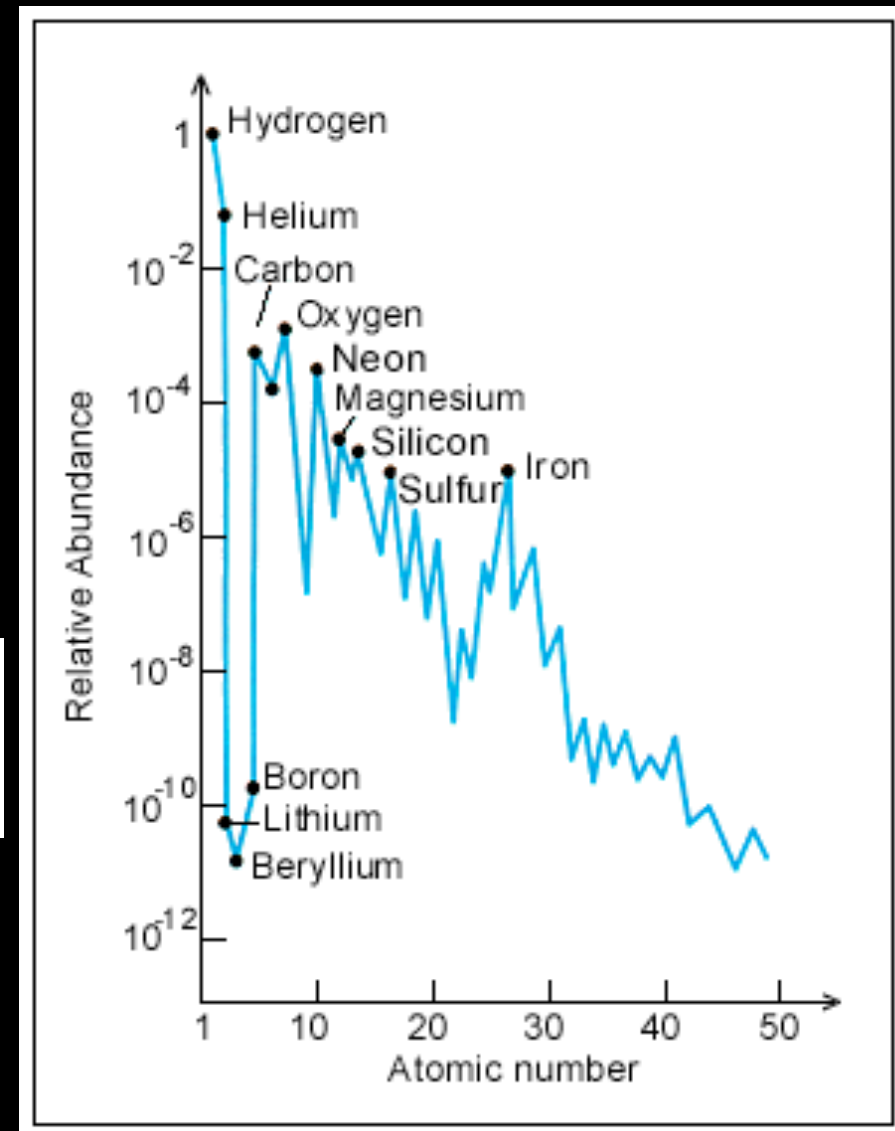
Solar Abundance from
Anders & Grevesse 1989

Abundance: Stars

Metal abundances in stars are defined relative to solar:

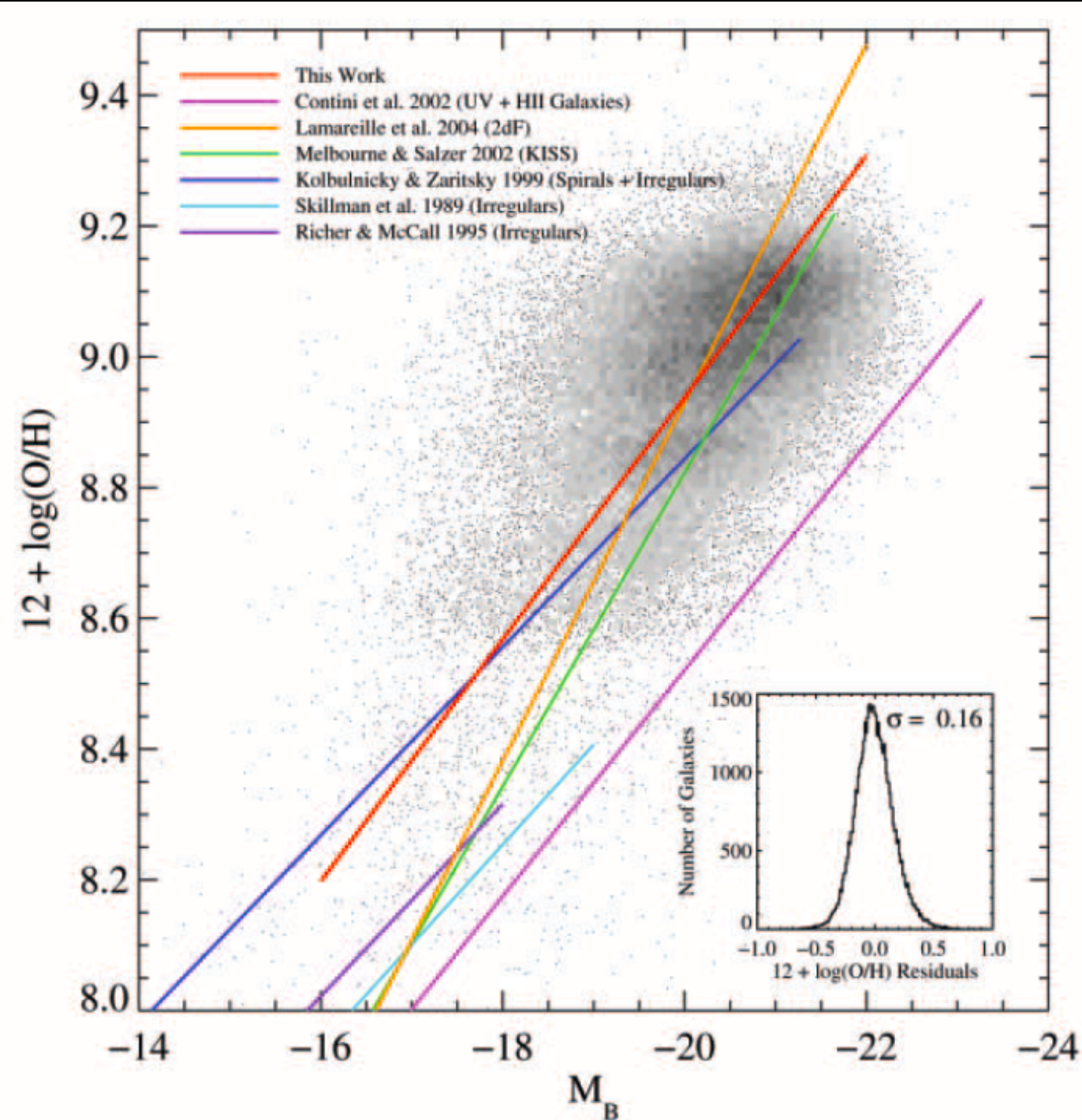
$$[\text{Fe}/\text{H}] = \log_{10} \left(\frac{N_{\text{Fe}}}{N_{\text{H}}} \right)_{\text{star}} - \log_{10} \left(\frac{N_{\text{Fe}}}{N_{\text{H}}} \right)_{\text{sun}}$$

of atoms



Can use any other species for “Fe” or “H” (i.e. [O/H], [O/Fe], etc)

Galaxies
follow a
luminosity-
metallicity
relation



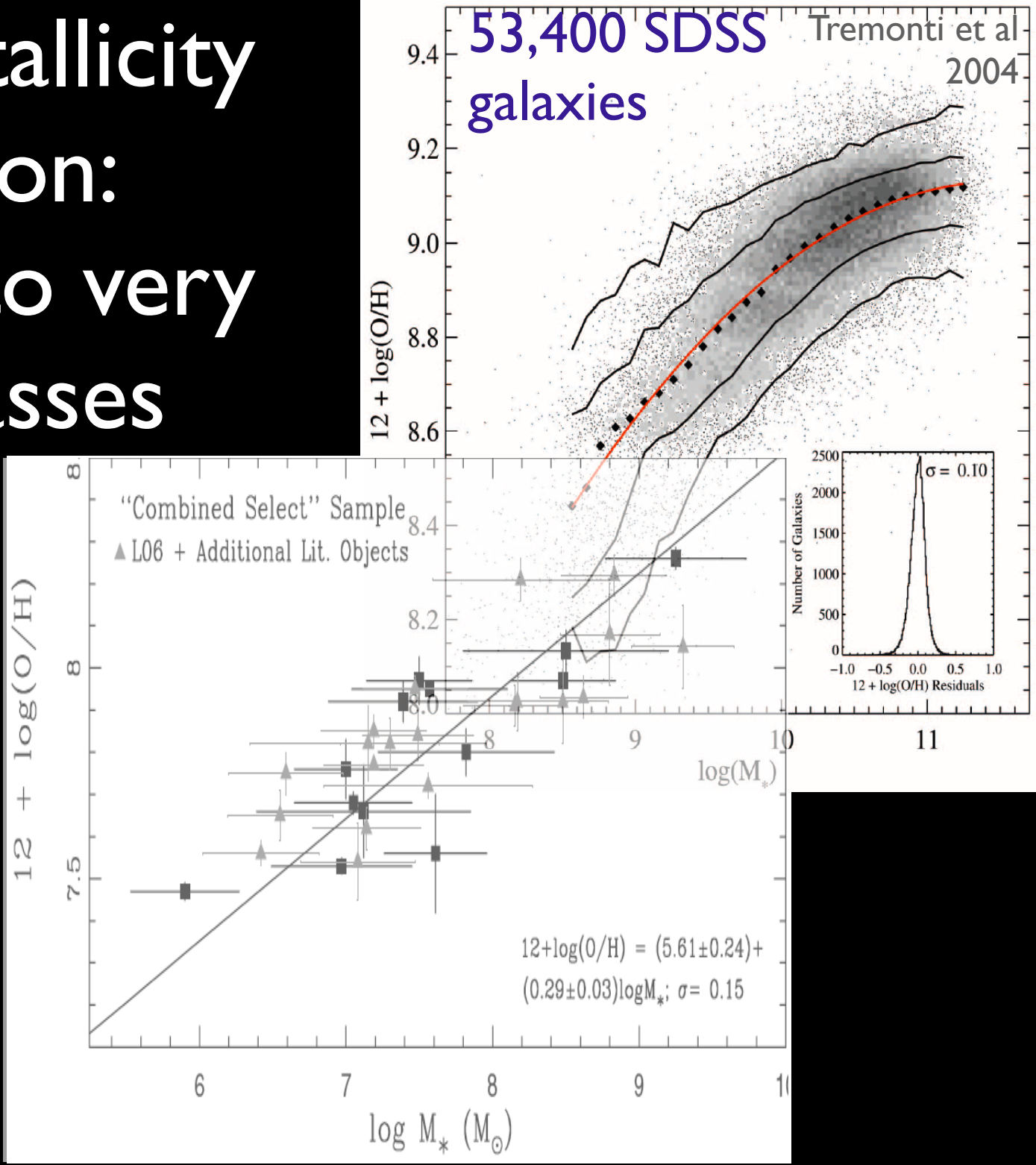
53,400 SDSS
galaxies: Note --
these metallicities
are biased high

Mass-Metallicity

Relation:

Extends to very
low masses

Berg et al 2012
Weak-line “gold
standard”
metallicities

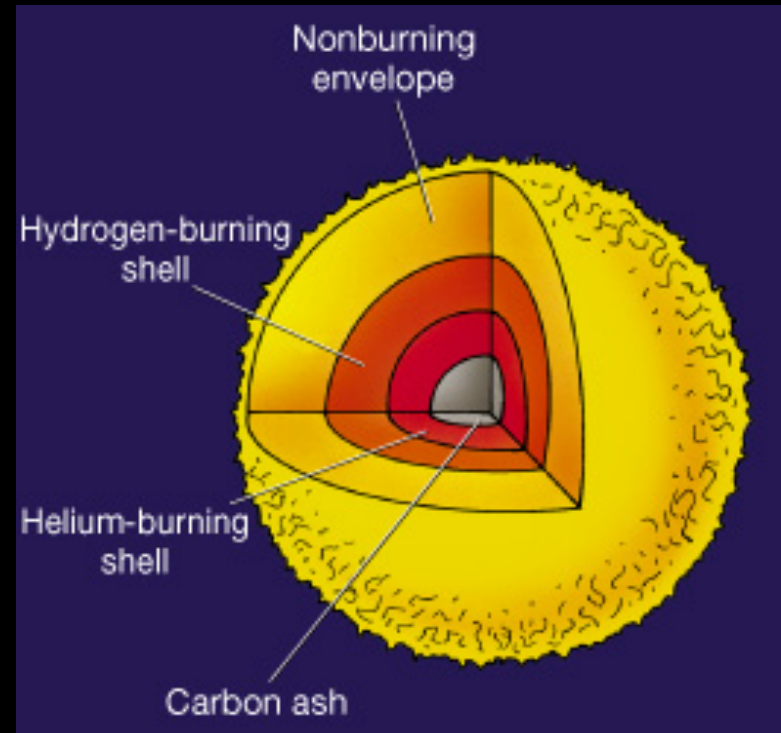


Two Ingredients Needed:

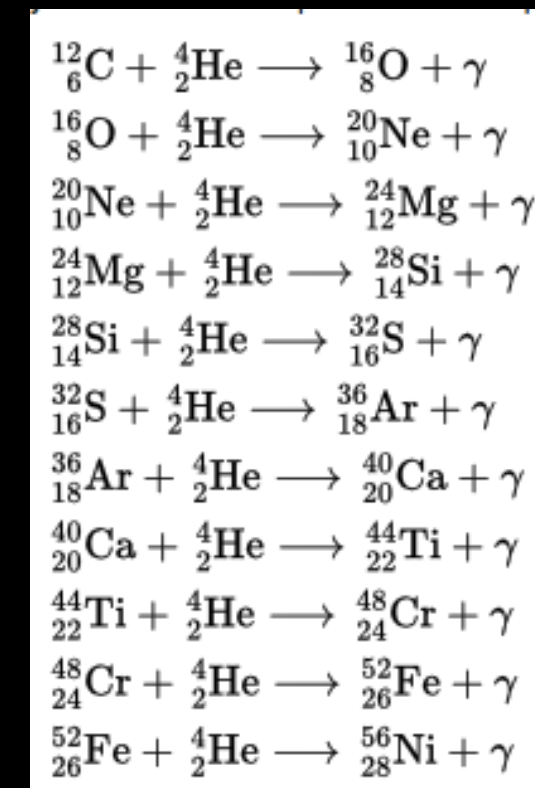
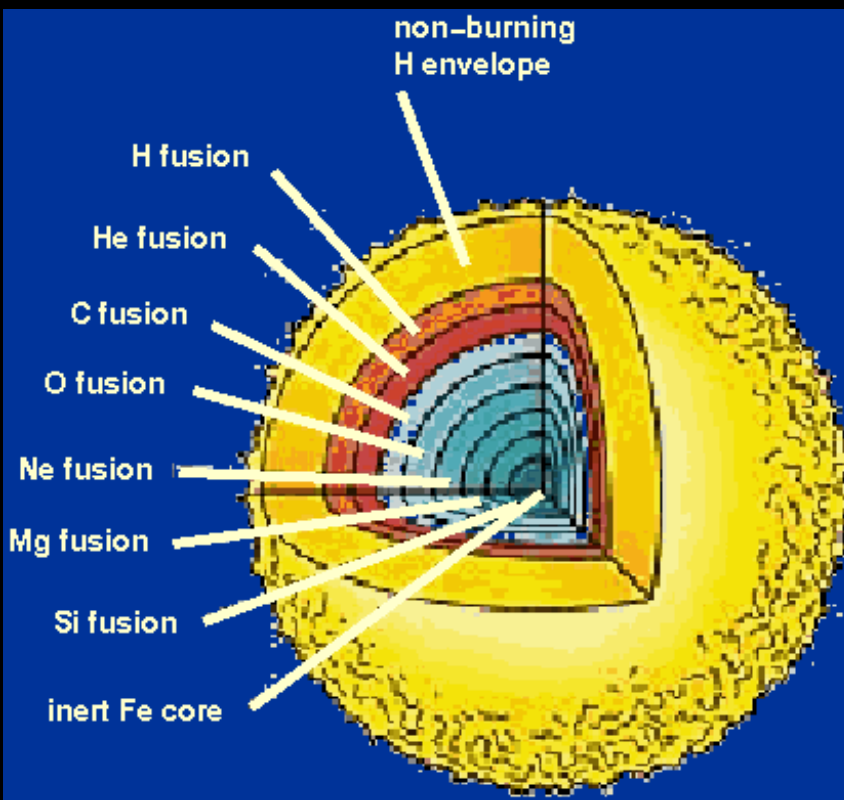
- Where do metals come from?
- What “chemical evolution” sets the observed metallicity of a galaxy

Main Nucleosynthetic Channels: Stellar Interior Processing

Nucleosynthesis inside Stars



Low mass stars:
C or C+O core fuses up
to Fe-peak when ignites



High mass
stars:
 α -elements
through “ α -
ladder”

Main Nucleosynthetic Channels: Supernovae

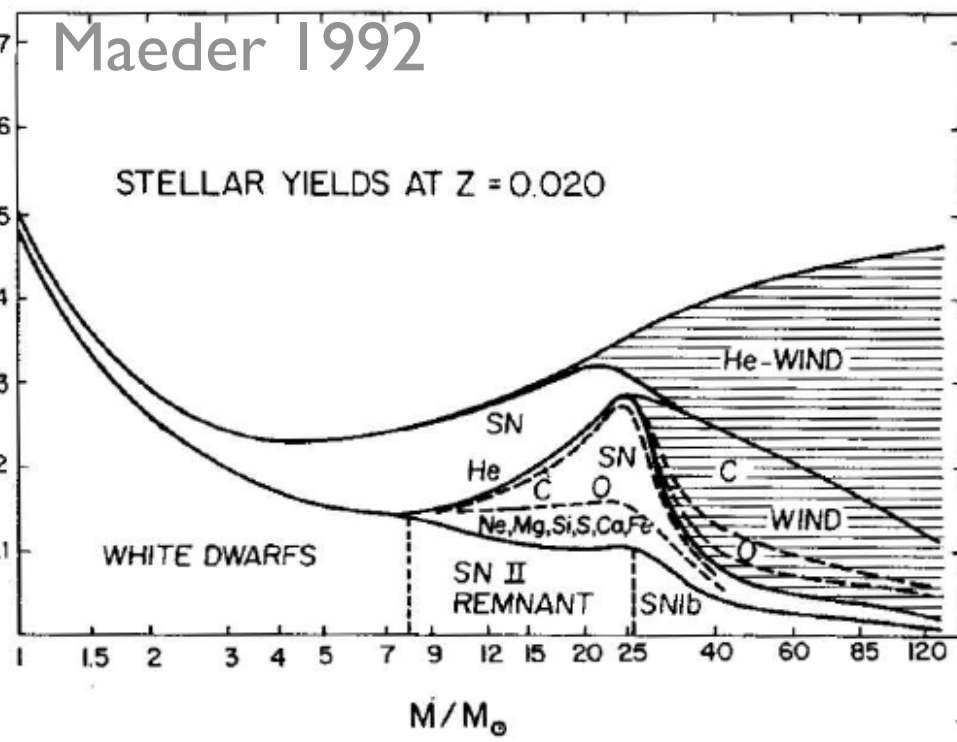
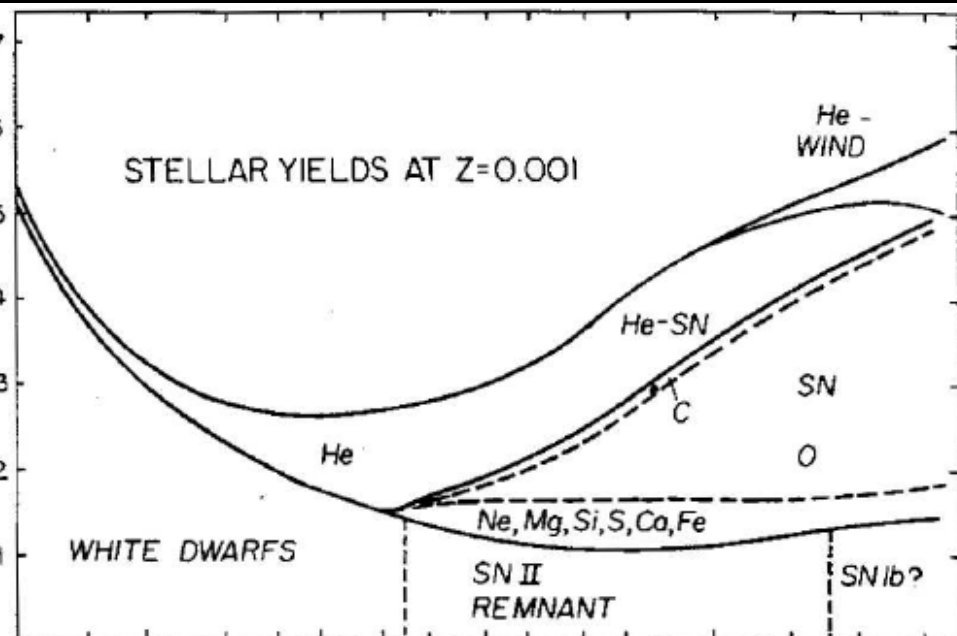
Production of Elements I.

Type II SNe
 $(M > 6-8 M_{\odot})$

- Fast enrichment (<50 Myrs)
- α -element enhanced compared to solar
 - (O, Ne, Mg, Si, S, Ar, Ca, Ti, Cr)
- Makes r-process elements heavier than Fe

Massive Star Element Production

- Depends on metallicity Z , the mass+rotation of the star, & mass loss before SN
- Need to integrate over IMF to get total production
- Oxygen and other α elements (Mg, Si, Ca, Ti) dominate
- Some elements from internal fusion, some in explosion



Exact Type II yield is uncertain

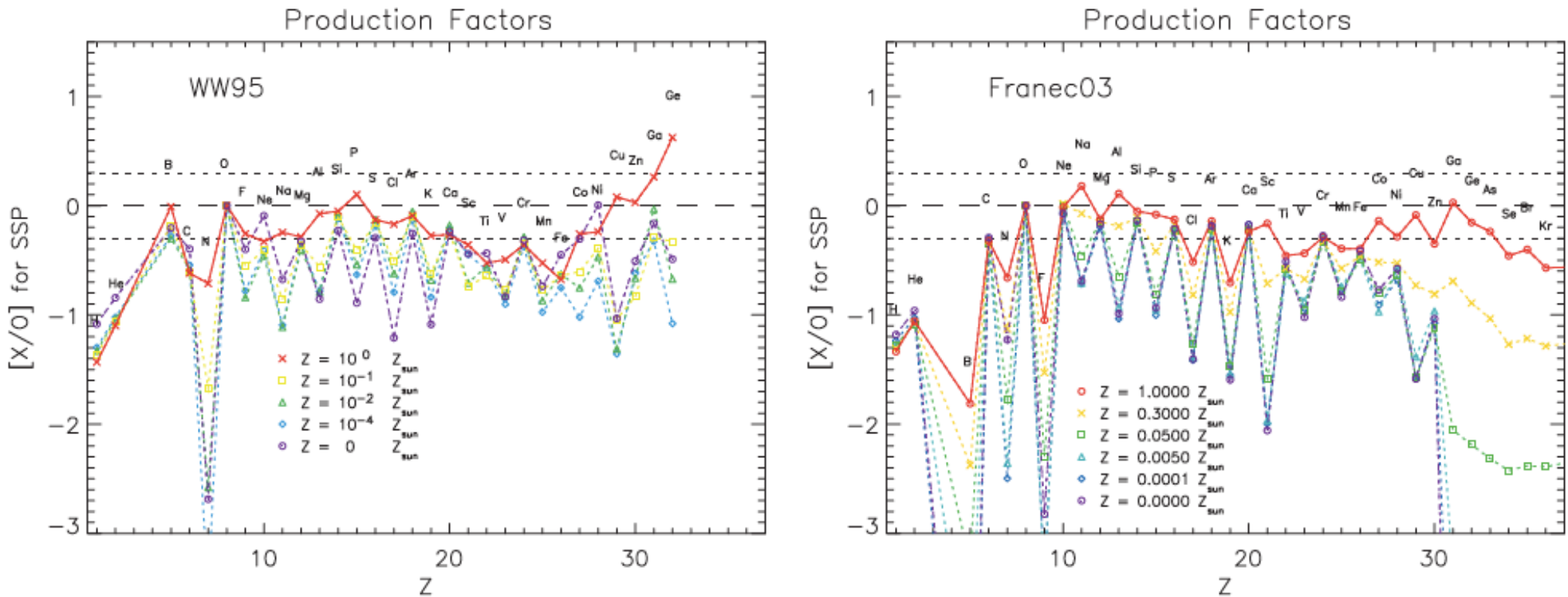


Figure 1 Production factors relative to O on a solar logarithmic scale from a single generation of massive stars using the metallicity-dependent yields of Woosley & Weaver 1995 (left panel) and those of FRANEC 2003 (right panel). The latter were kindly provided by A. Chieffi (2003, personal communication). Yields were integrated over a Salpeter (1955) IMF from 12 to $40 M_{\odot}$. The dashed line indicates the solar values (where $\log(N_O/N_H)_\odot + 12 = 8.73$, Holweger 2001) and dotted lines indicate deviations from scaled solar by a factor of two. For both sets of yields C, N, and some of the iron-peak elements are subsolar because they require additional sources such as lower mass stars and Type Ia SNe. The strength of the ‘odd-even’ effect increases with decreasing metallicity in both cases, however the effect is more pronounced for FRANEC 2003.

Depends on nucleosynthetic
models, metallicity, IMF

From review by
Gibson et al 2003

Production of Elements I.

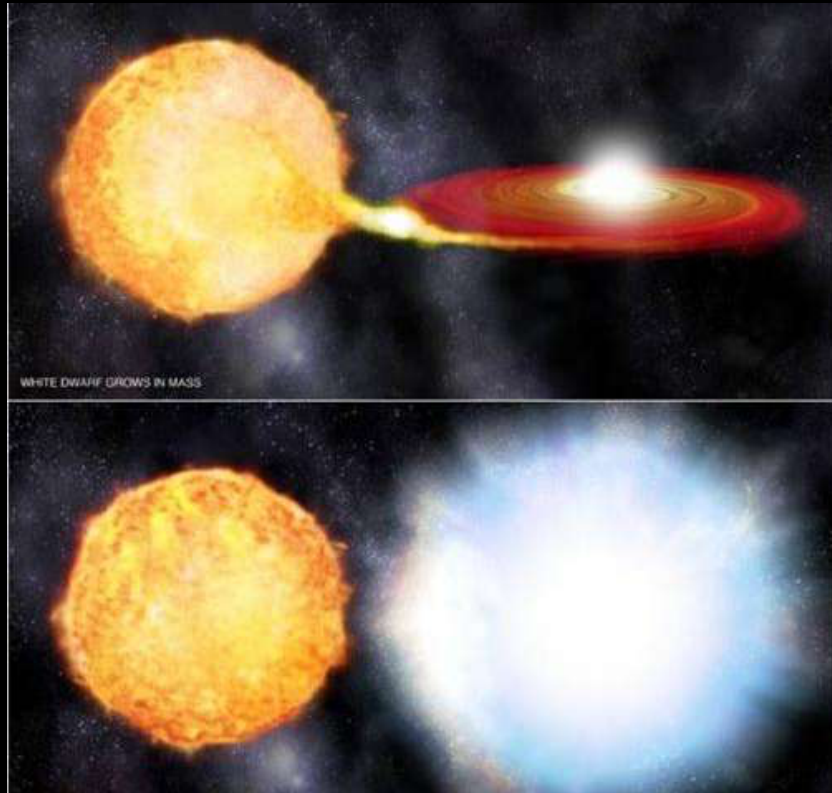
Type II SNe
($M > 6\text{-}8 M_\odot$)

Type Ia SNe
(Range of masses)

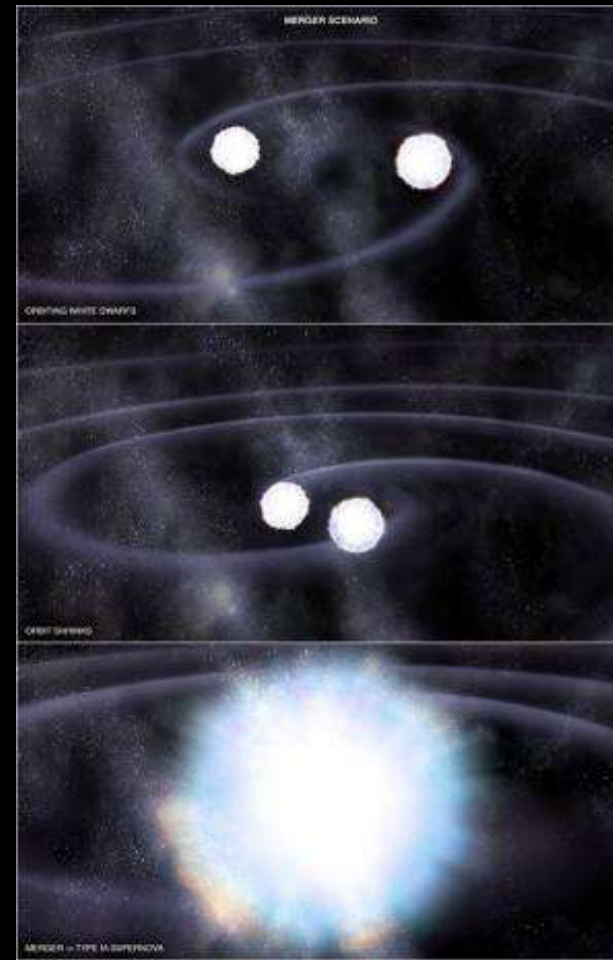
- Fast enrichment (<50 Myrs)
- α -element enhanced compared to solar (O, Ne, Mg, Si, S, Ar, Ca, Ti, Cr)
- Some prompt, but most delayed
- Fe-peak elements are dominant products

Multiple possible channels for Type Ia

All involve detonation of at least one white dwarf near the Chandrasekhar limit

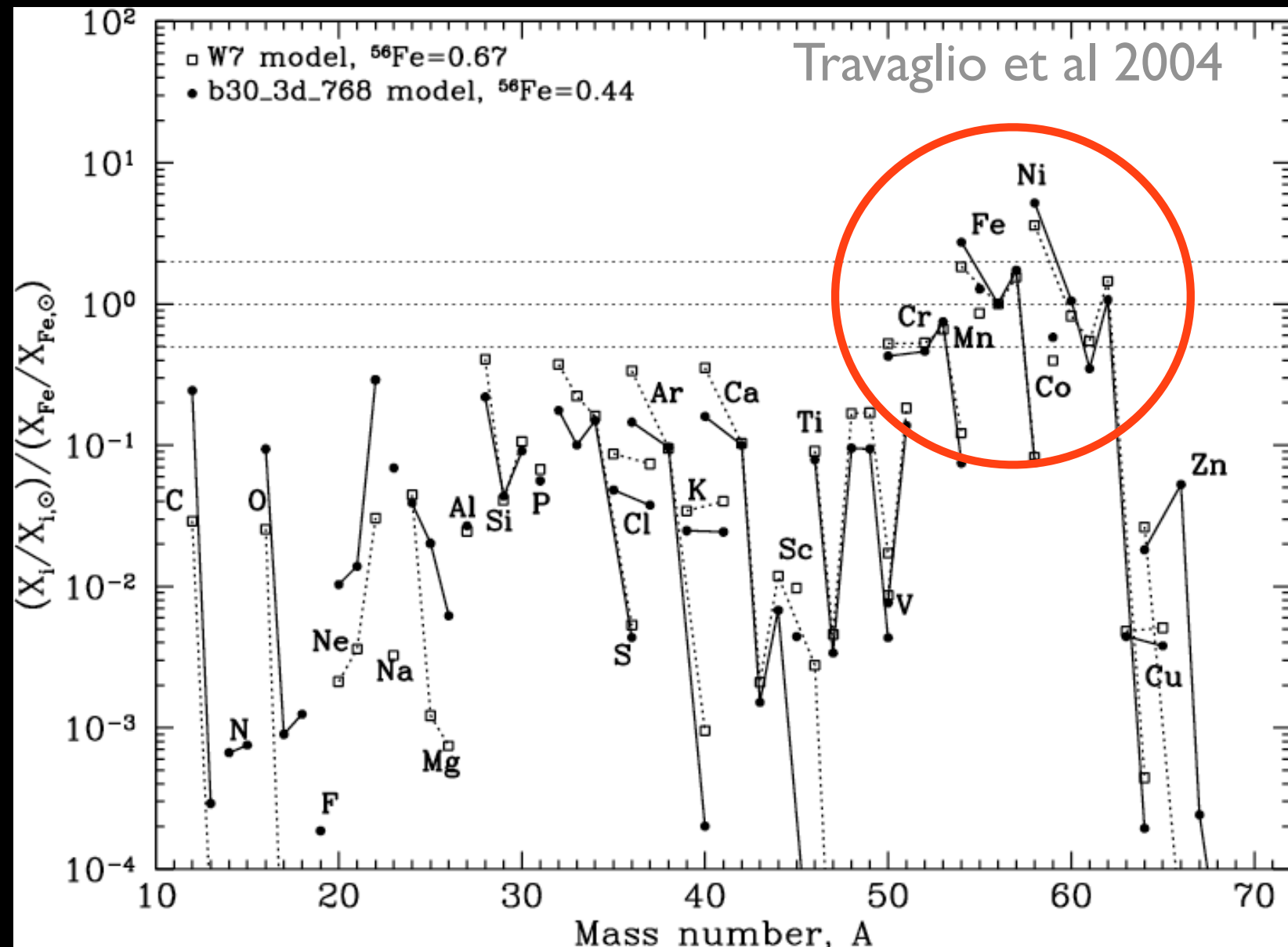


Single-degenerate
channel



Double-degenerate
channel

Type Ia Yields: Primarily Iron Peak



Note: Explosion models uncertain

Other sources of elements beyond the “iron peak”

Main Nucleosynthetic Channels: Beyond the Fe-peak

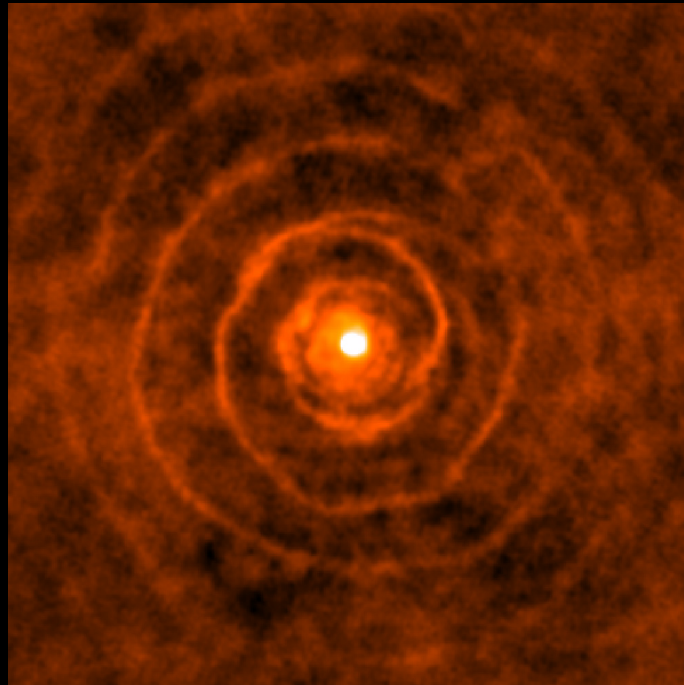
- “s-process” due to *slow* accretion of neutrons interspersed with decay to stable nuclei (starts w/ Fe)
- “r-process” due to *rapid* accretion of neutrons, followed by subsequent β -decay to stable nuclei (starts w/ Fe)
- Cosmic ray spallation (induces fission)

s-process

Slow accretion of individual neutrons,
followed rapidly by β decay

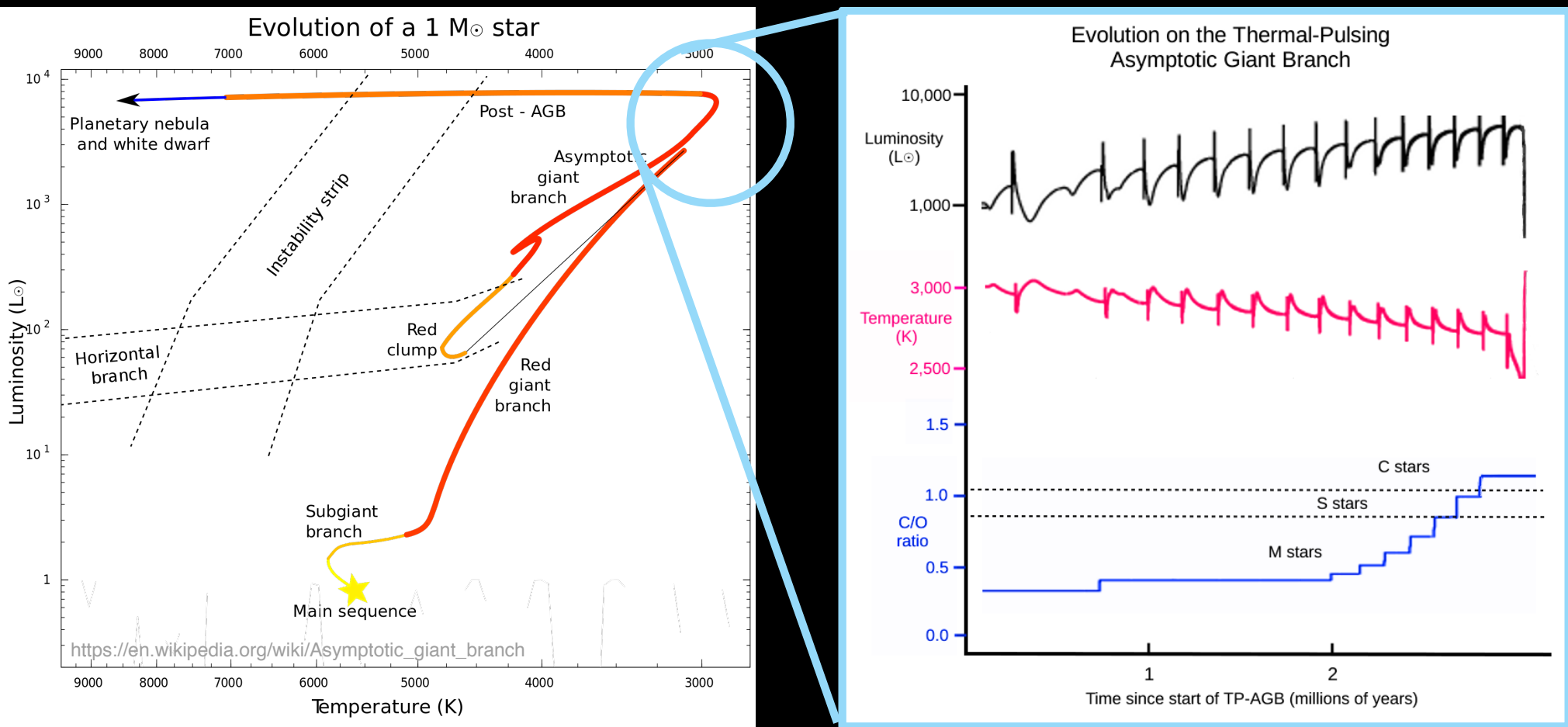
S-Process Production

AGB Winds
(Range of masses)

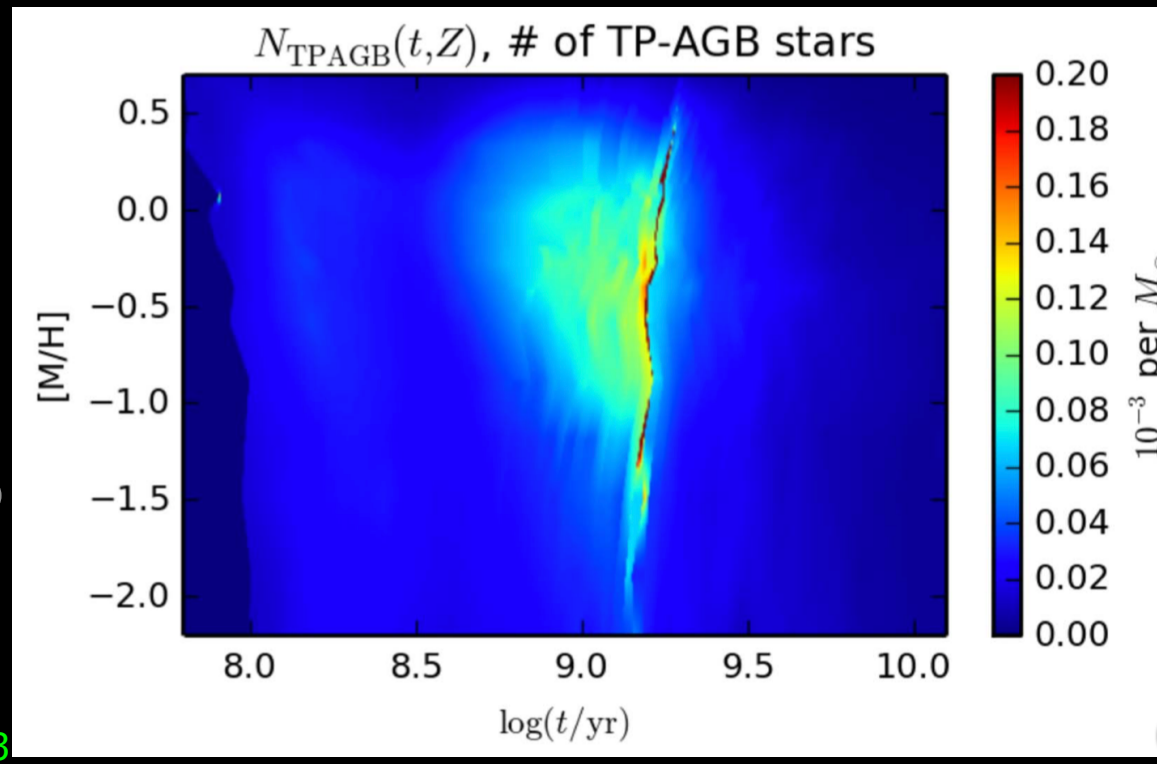
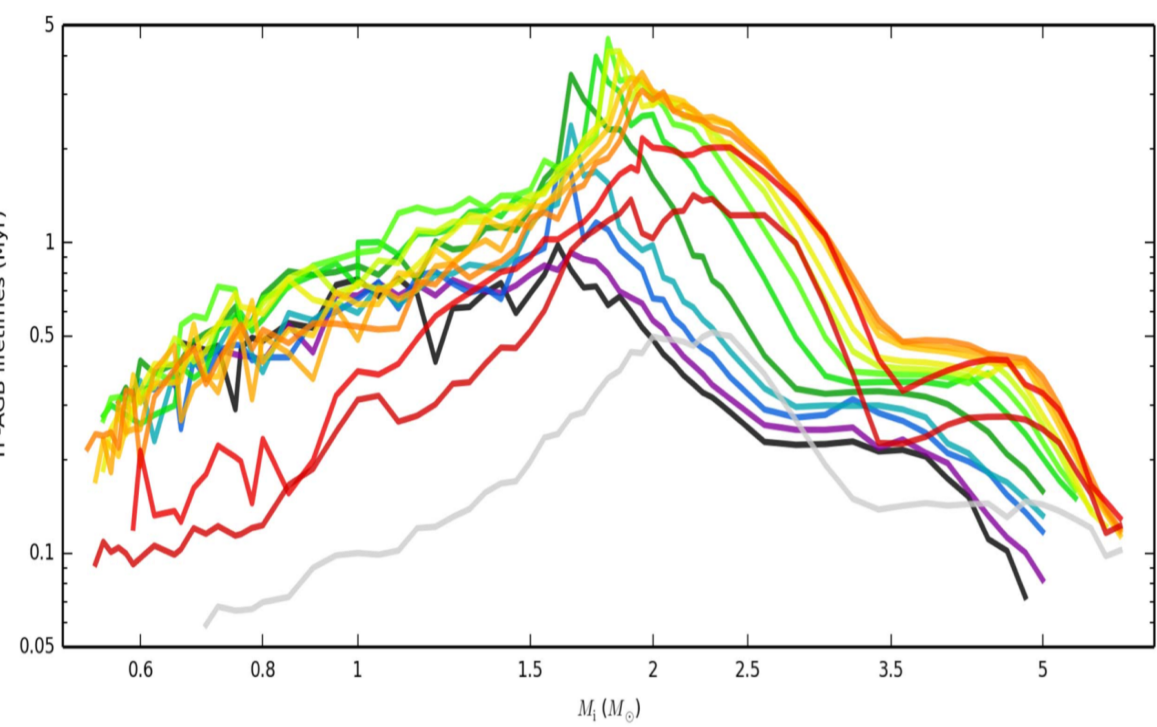


- Pulsation + dredging
- Important for s-process (slow neutron capture) elements beyond Fe-peak

Asymptotic Giant Branch (AGB) Stars



- Double shell burning around a C/O core
- Thermal pulsation & mass loss at late stages



TP-AGB: Intermediate & low mass stars

During TP-AGB, material dredges in and out of core, enriching envelope

Rauch et al 2008

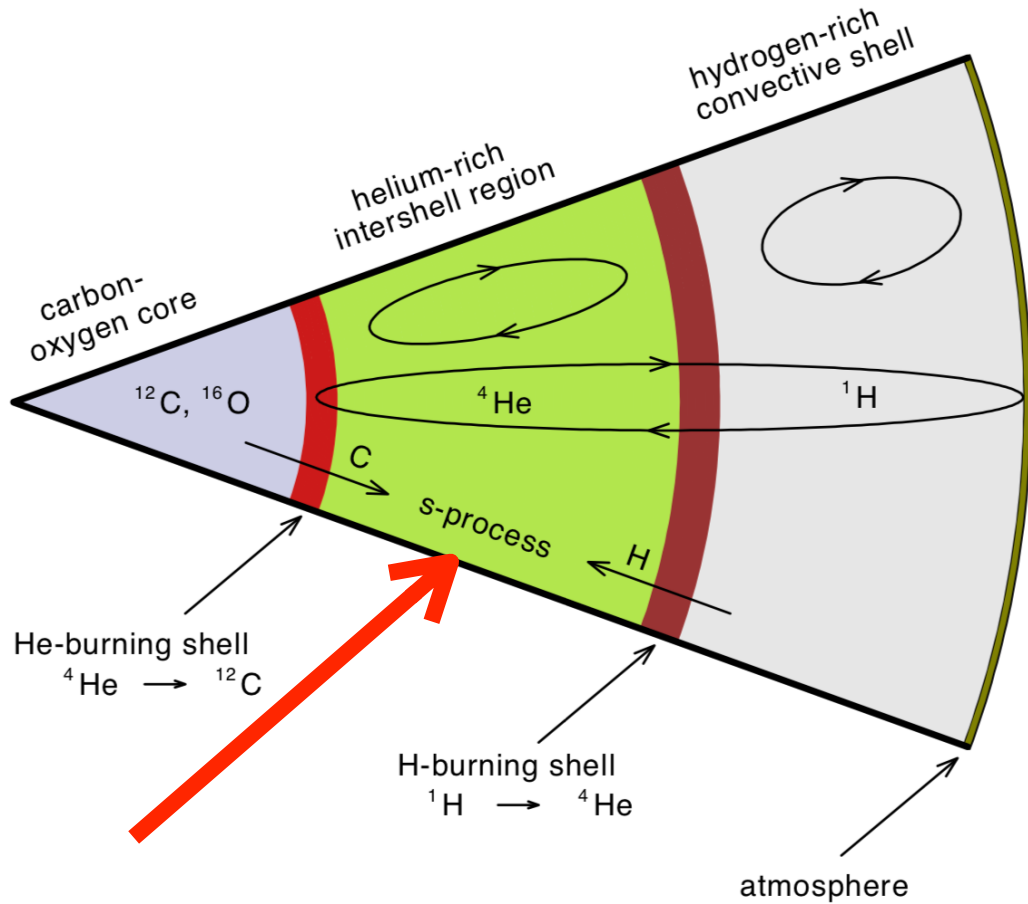
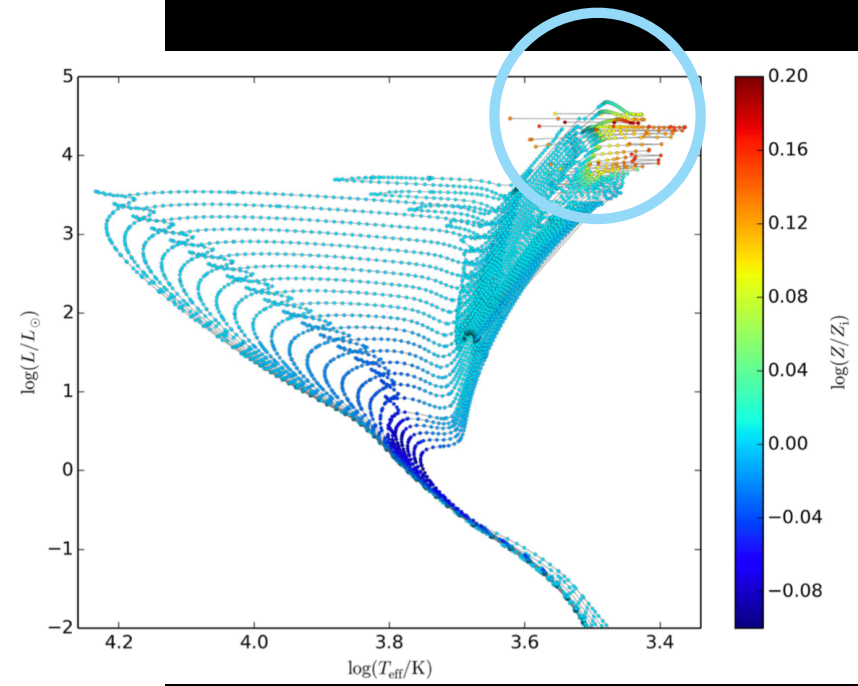


Figure 1. Inner structure of an AGB star. Note that the convection zone from the surface to the bottom of the helium-burning shell is established during a TP only.



Marigo et al 2017

Winds carry enriched material away

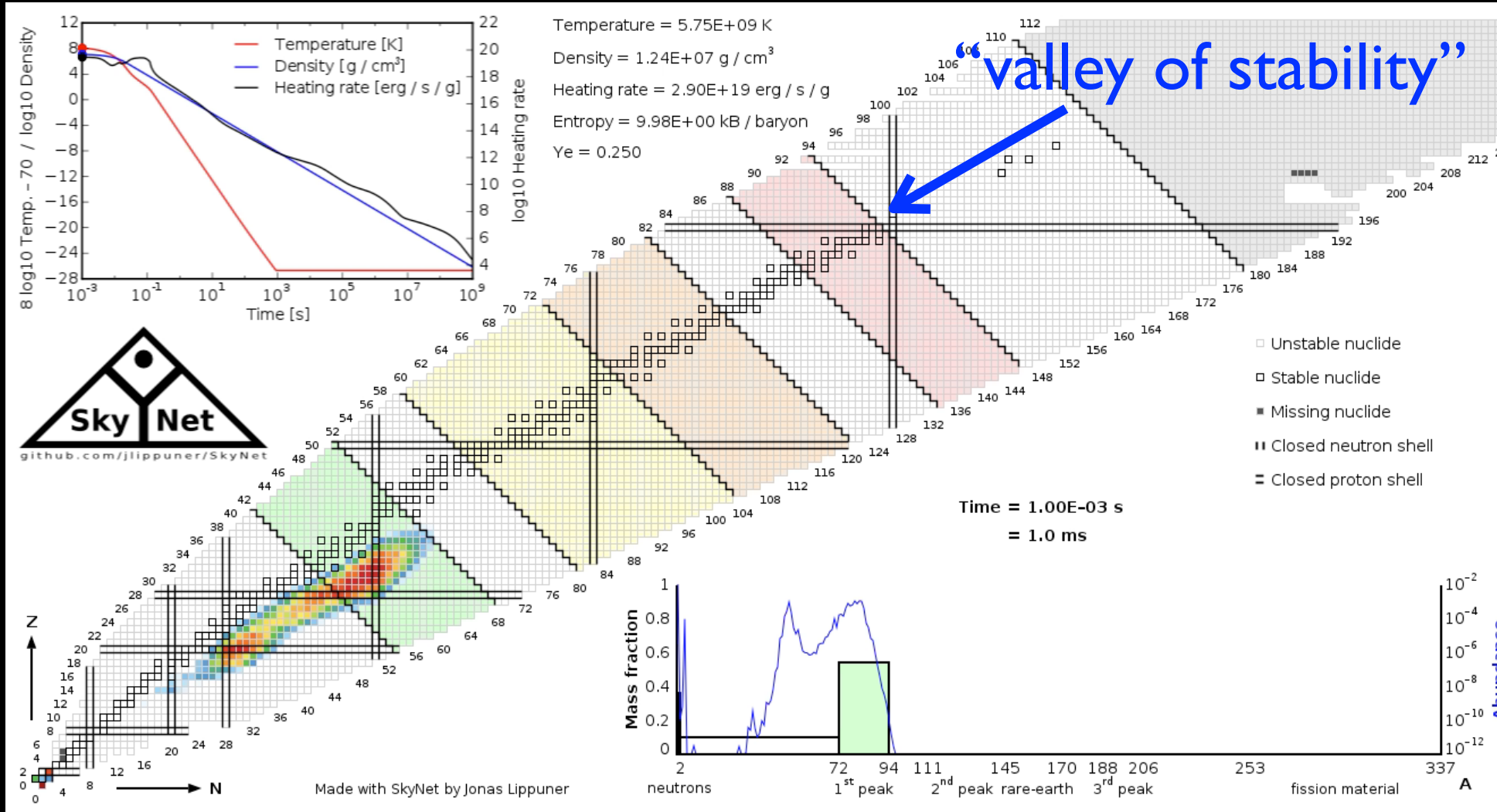
Figure 6. Changes in the current surface metal content Z across the HR diagram, for a set of isochrones of initial $Z_i = 0.01471$, with ages varying from $\log(t/\text{yr}) = 7.8$ to 10.1 at steps of 0.1 dex, and for $n_{\text{inTPC}} = 0$.

r-process

Rapid accretion of multiple neutrons,
before eventual β decay

r-process in action

more protons ↑



more neutrons →

NS-NS merger kilonova simulation: <https://stellarcollapse.org/lippunerroberts2015>

R-Process Production: SNe

Type II SNe
($M > 6\text{-}8 M_\odot$)

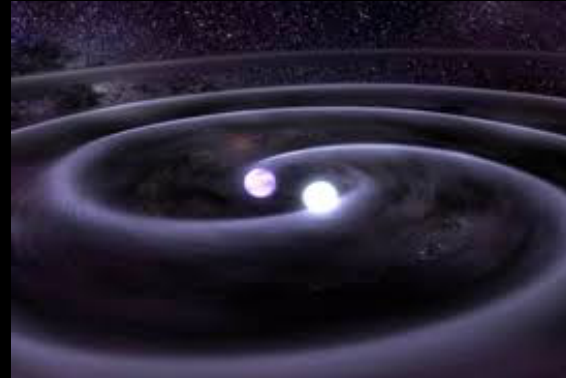
Type Ia SNe
(Range of masses)

- Fast enrichment (<50 Myrs)
- α -element enhanced compared to solar (O, Ne, Mg, Si, S, Ar, Ca, Ti, Cr)
- Some prompt, but most delayed
- Fe-peak elements are dominant products

Both types, but Type II produces more.

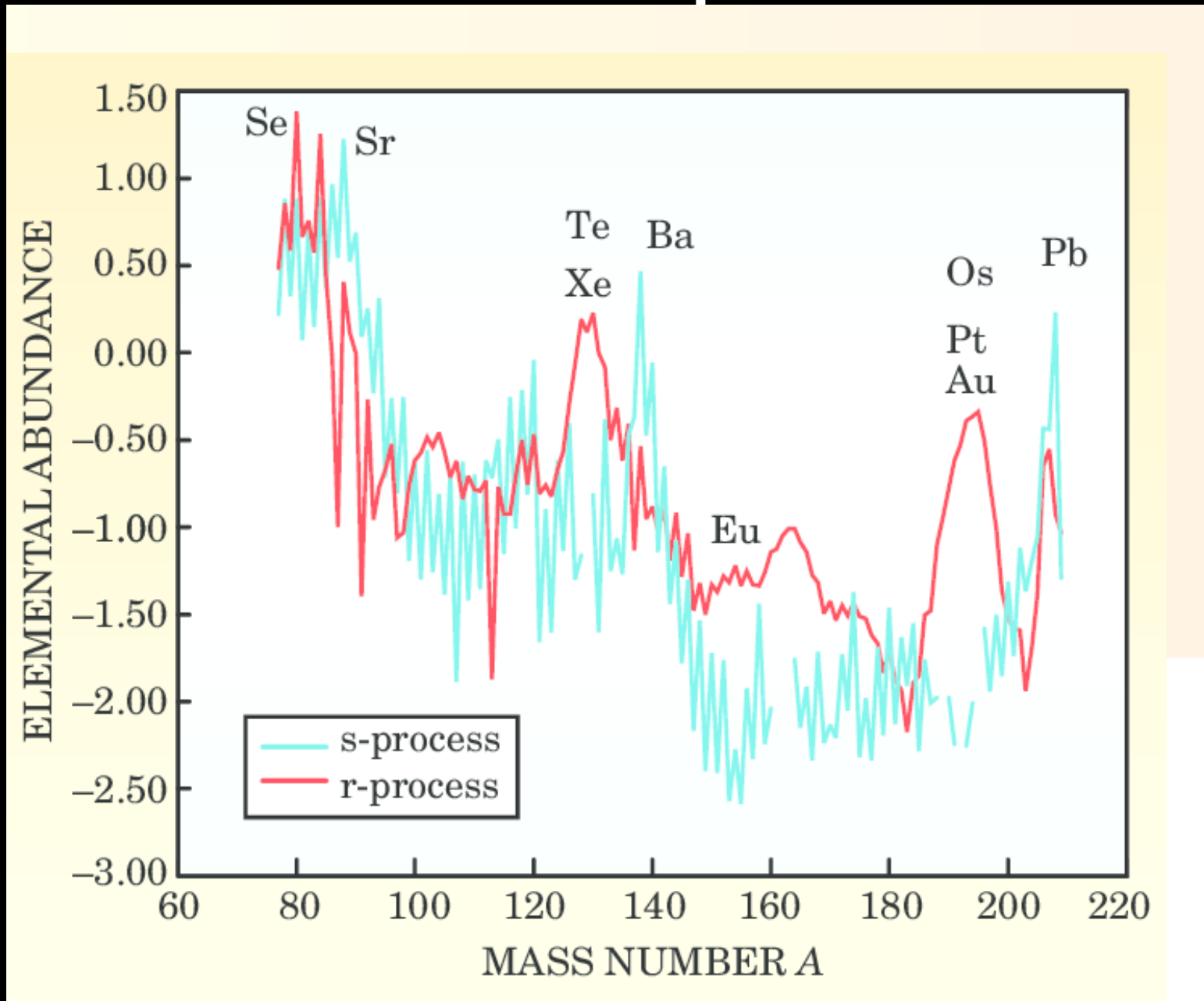
R-Process Production: “kilonovae”

Neutron Star
Mergers



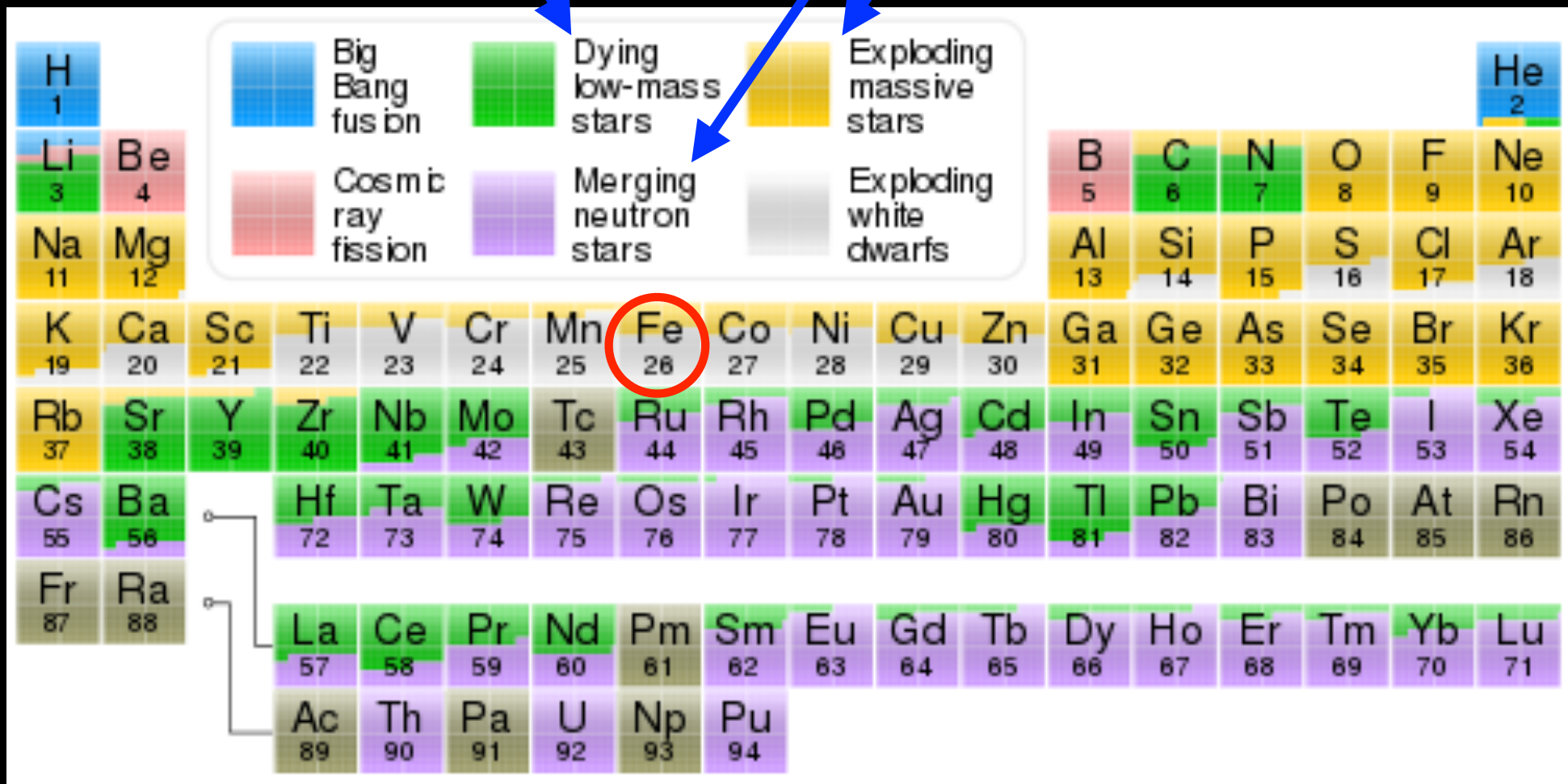
- Timescale depends on binary evolution
- Can also produce r-process elements
- Rarer, but bigger yield per event than SNe
- Produces dispersion in r-process/Fe at low Fe

r- and s-process produce different enrichment patterns



s-process

r-process



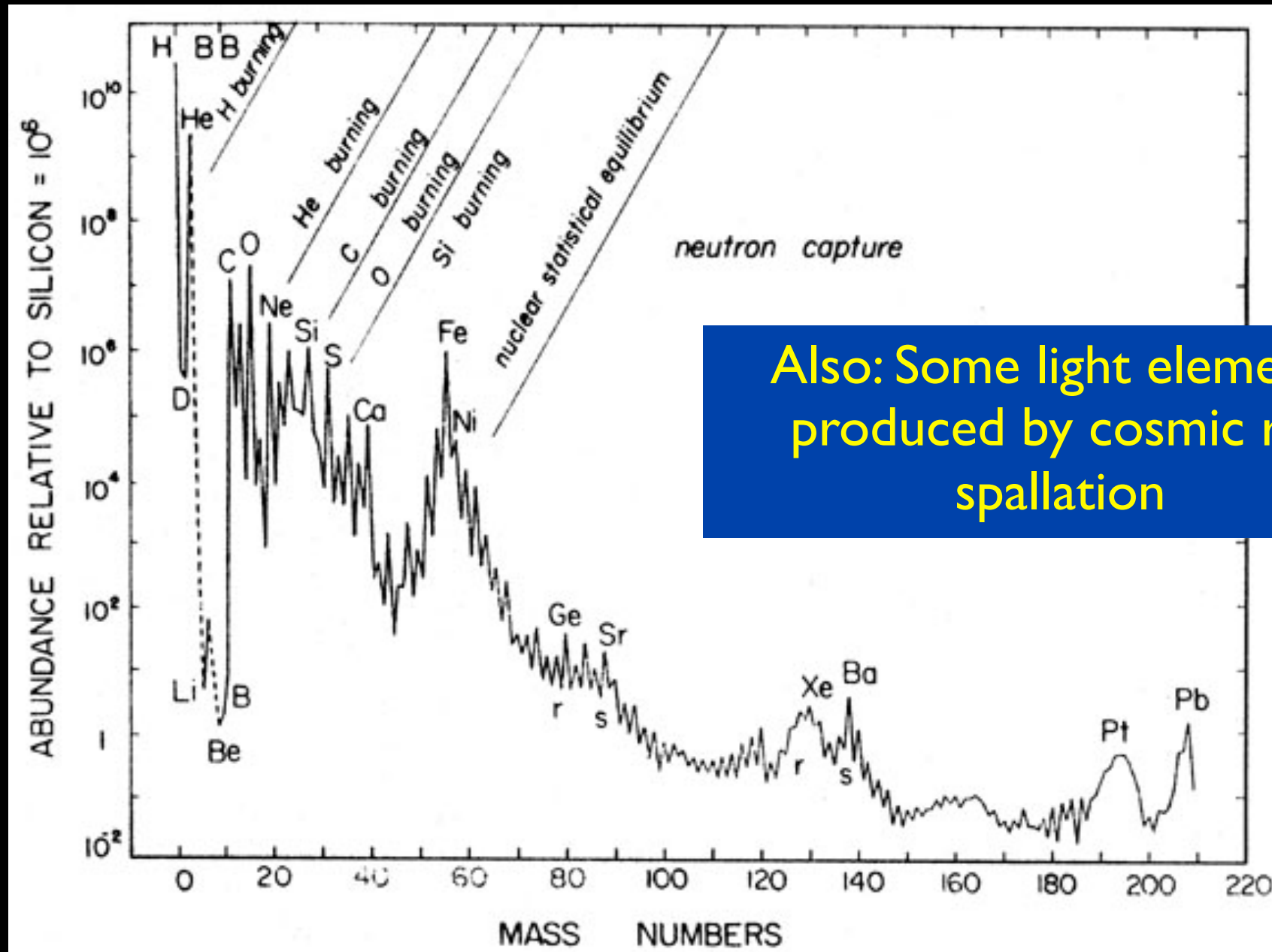
Nucleosynthesis Questions

- Have we correctly identified the sites of nucleosynthetic production?
- What are the actual yields in SNe and NS mergers?
- What are the timescales of Type Ia and NS production?
- How does the fate of massive stars depend on their mass (Type II SNe? direct collapse? pair instability?)

All nucleosynthetic channels operate
in galaxies.

Resulting abundance pattern is
complex but informative.

For elements less massive than Fe, solar abundance is combination of Type II, Type Ia, and s-process



The relative importance of Type II and Type Ia SNe is a particularly informative diagnostic

Type II SNe
($M > 6\text{-}8 M_{\odot}$)

Fast, Makes α
elements

Type Ia SNe
(range of masses)

Extended
timescale, Makes
Fe-peak elements

Interpret $[\alpha/\text{Fe}]$ vs $[\text{Fe}/\text{H}]$ using timescales

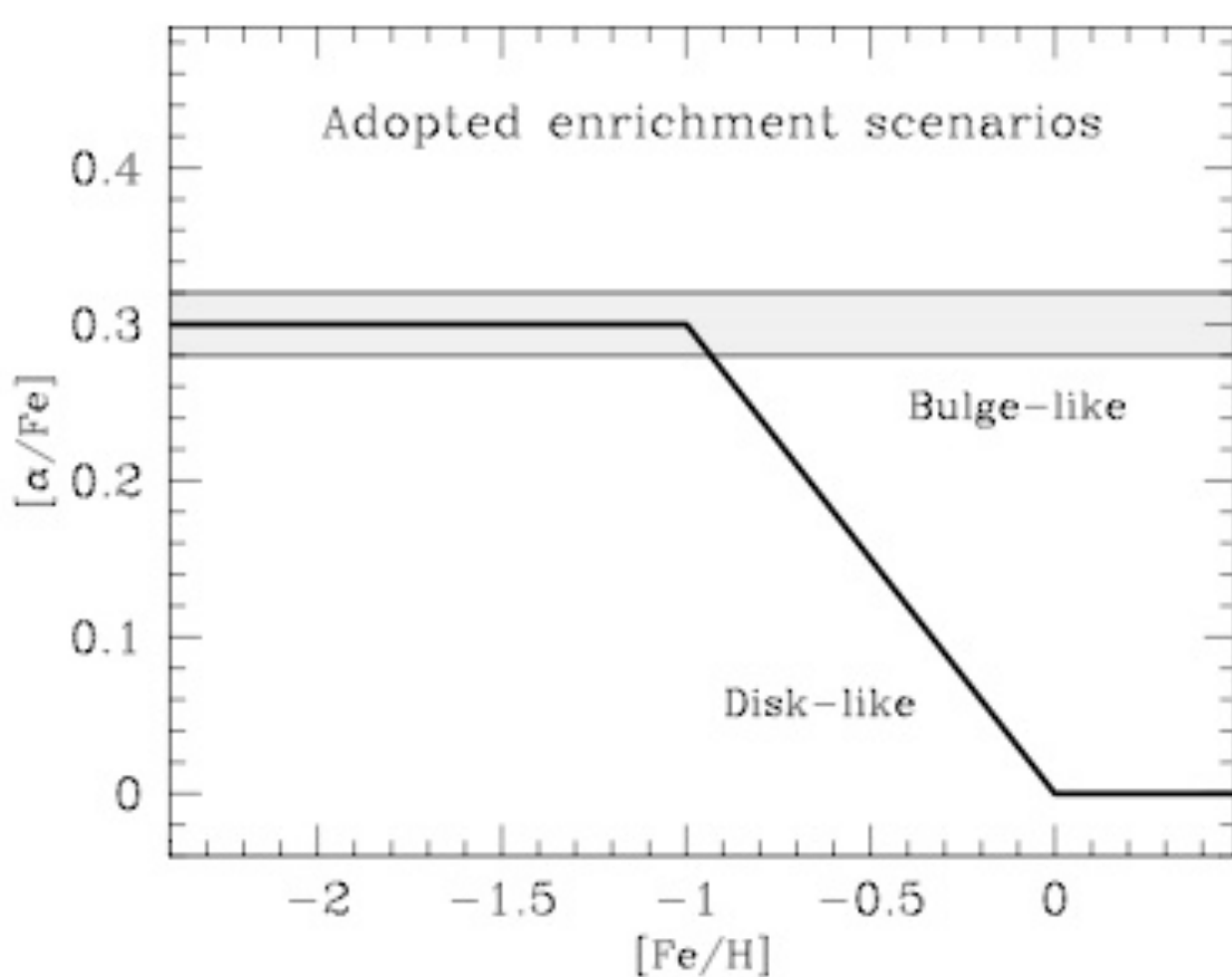


FIG. 1.—Sketched diagram of the $[\alpha/\text{Fe}]$ vs. $[\text{Fe}/\text{H}]$ trend in the disk-/bulge-like enrichment scenarios, as adopted in our computational routine.

Fast enrichment:
no time for Type Ia,
so only Type II
products

Slow enrichment:
Extended SF history
allows enrichment of
Type Ia iron peak
elements

Extended SF lowers α/Fe while increasing Fe/H

Different locations have different α -enhancement

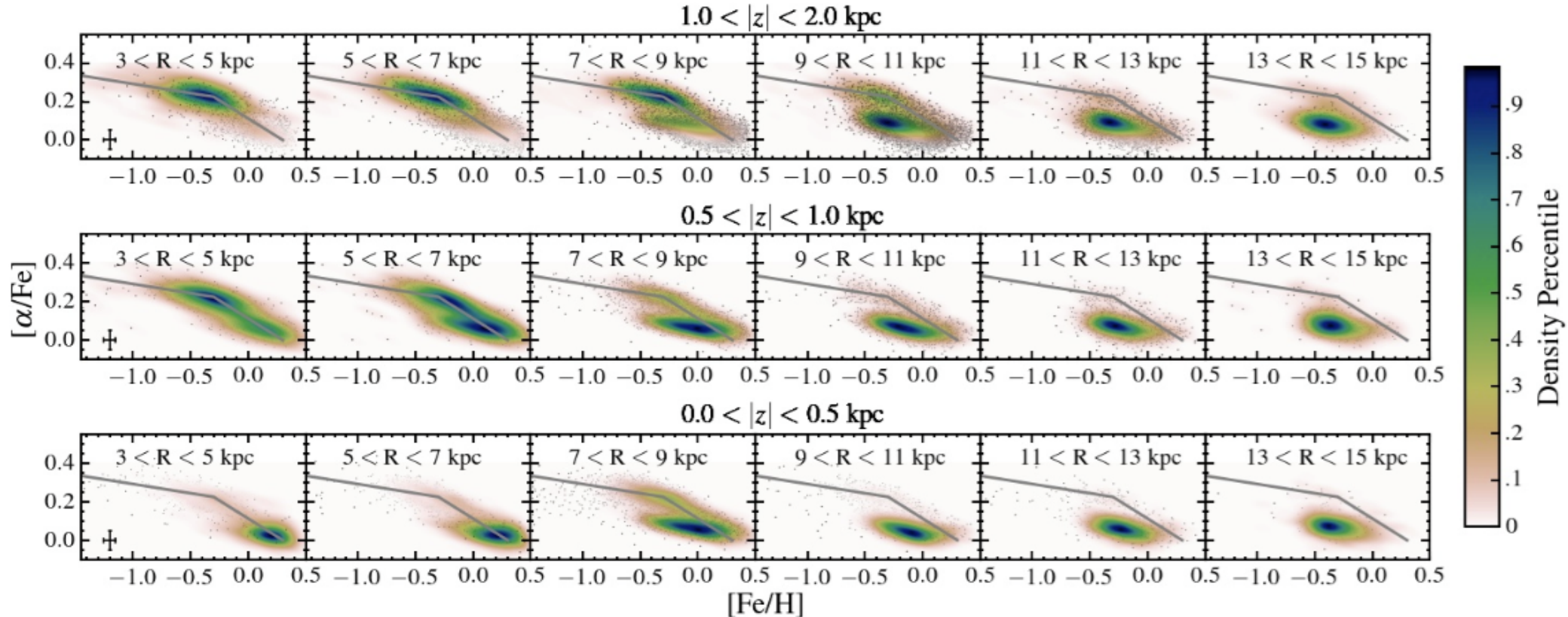
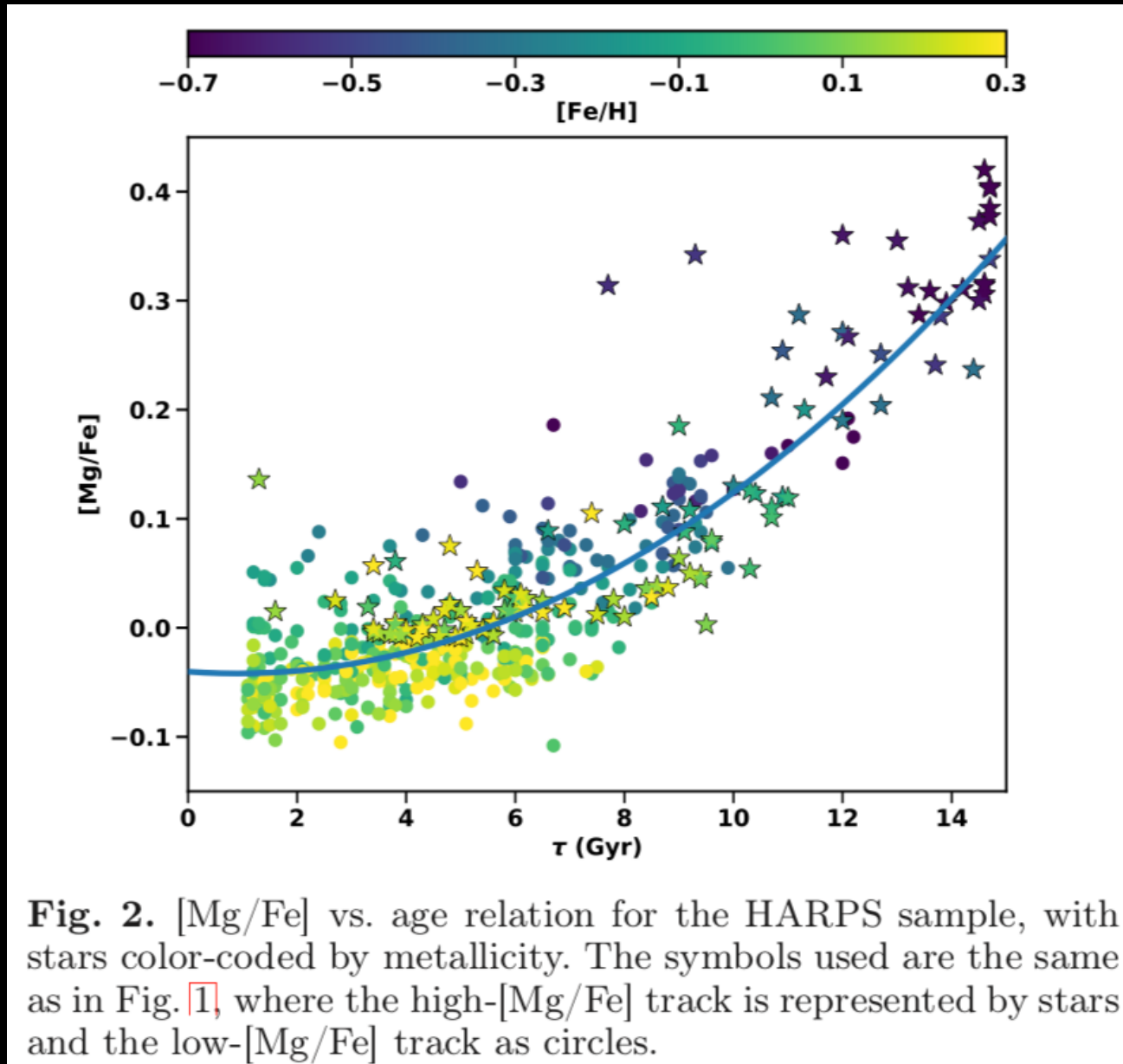


Figure 4. The stellar distribution of stars in the $[\alpha/\text{Fe}]$ vs. $[\text{Fe}/\text{H}]$ plane as a function of R and $|z|$. **Top:** The observed $[\alpha/\text{Fe}]$ vs. $[\text{Fe}/\text{H}]$ distribution for stars with $1.0 < |z| < 2.0 \text{ kpc}$. **Middle:** The observed $[\alpha/\text{Fe}]$ vs. $[\text{Fe}/\text{H}]$ distribution for stars with $0.5 < |z| < 1.0 \text{ kpc}$. **Bottom:** The observed $[\alpha/\text{Fe}]$ vs. $[\text{Fe}/\text{H}]$ distribution for stars with $0.0 < |z| < 0.5 \text{ kpc}$. The grey line on each panel is the same, showing the similarity of the shape of the high- $[\alpha/\text{Fe}]$ sequence with R . The extended solar- $[\alpha/\text{Fe}]$ sequence observed in the solar neighborhood is not present in the inner disk ($R < 5 \text{ kpc}$), where a single sequence starting at high- $[\alpha/\text{Fe}]$ and low metallicity and ending at solar- $[\alpha/\text{Fe}]$ and high metallicity fits our observations. In the outer disk ($R > 11 \text{ kpc}$), there are very few high- $[\alpha/\text{Fe}]$ stars.

APOGEE: Higher α -enhancement above the plane, and towards the center of the galaxy.

In the MW, stars that formed early, formed with high α/Fe



More on-going SF in disk and disks' outer regions

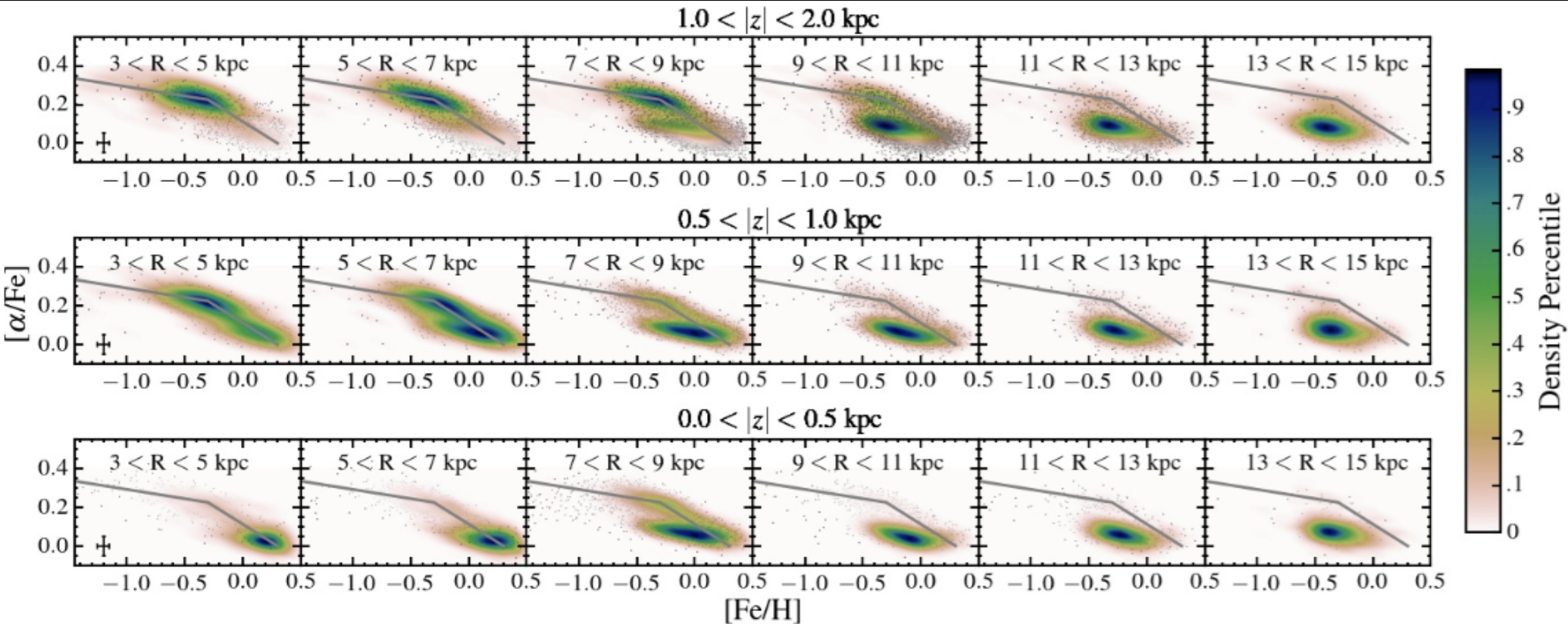
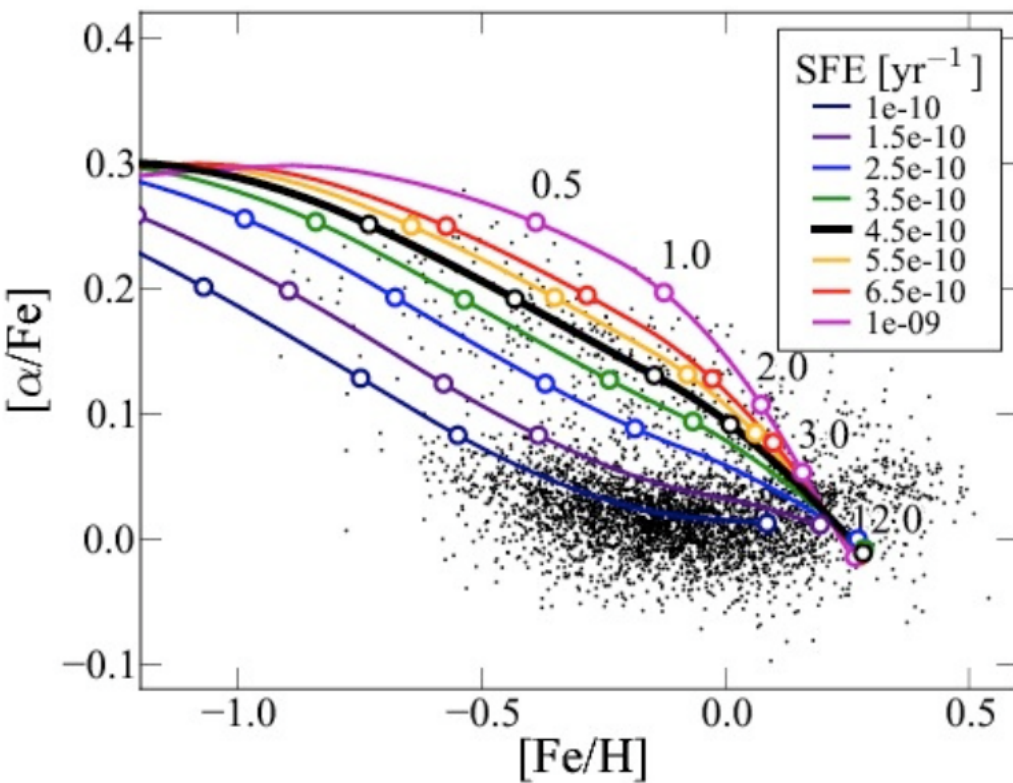


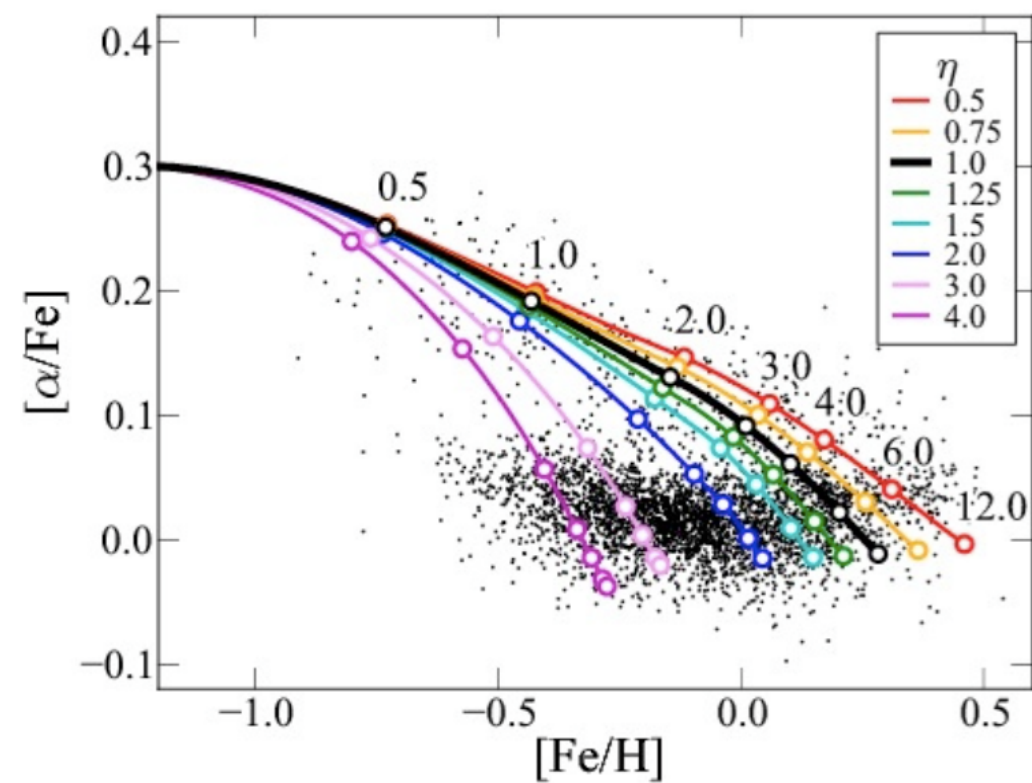
Figure 4. The stellar distribution of stars in the $[\alpha/\text{Fe}]$ vs. $[\text{Fe}/\text{H}]$ plane as a function of R and $|z|$. **Top:** The observed $[\alpha/\text{Fe}]$ vs. $[\text{Fe}/\text{H}]$ distribution for stars with $1.0 < |z| < 2.0 \text{ kpc}$. **Middle:** The observed $[\alpha/\text{Fe}]$ vs. $[\text{Fe}/\text{H}]$ distribution for stars with $0.5 < |z| < 1.0 \text{ kpc}$. **Bottom:** The observed $[\alpha/\text{Fe}]$ vs. $[\text{Fe}/\text{H}]$ distribution for stars with $0.0 < |z| < 0.5 \text{ kpc}$. The grey line on each panel is the same, showing the similarity of the shape of the high- $[\alpha/\text{Fe}]$ sequence with R . The extended solar- $[\alpha/\text{Fe}]$ sequence observed in the solar neighborhood is not present in the inner disk ($R < 5 \text{ kpc}$), where a single sequence starting at high- $[\alpha/\text{Fe}]$ and low metallicity and ending at solar- $[\alpha/\text{Fe}]$ and high metallicity fits our observations. In the outer disk ($R > 11 \text{ kpc}$), there are very few high- $[\alpha/\text{Fe}]$ stars.

α/Fe vs Fe/H also affected by galaxy evolution

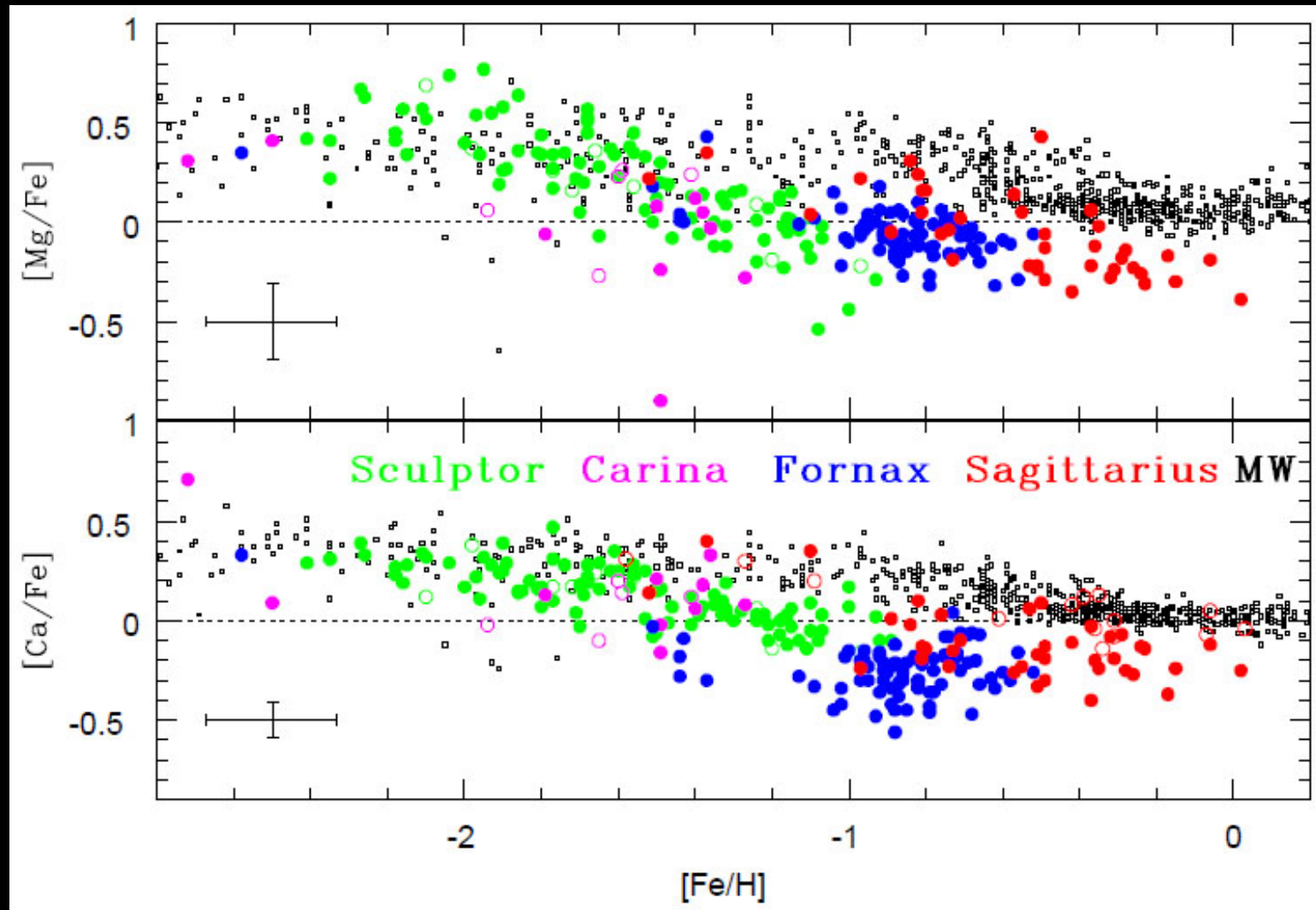
Star Formation Efficiency



Outflow Rate



Application: Stars in dwarfs



Dwarfs: Fe enrichment does not progress as far before SN II
 α -enhancement becomes diluted. Winds?

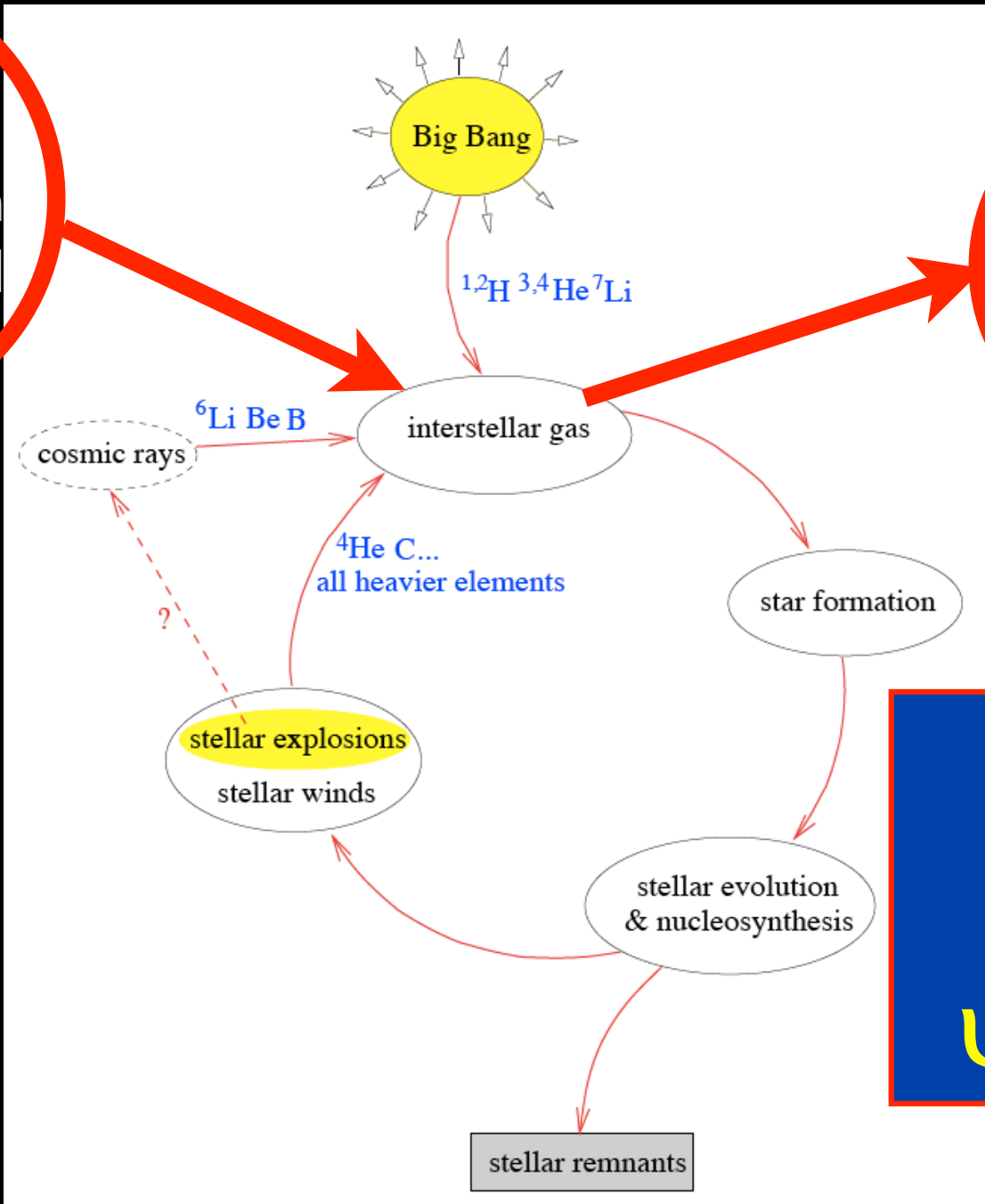
What sets overall metallicity?

“Chemical Evolution”

Chemical Evolution

Metal and gas accretion from CGM and IGM

Metal & gas loss in galactic winds



Goals:
 $Z_{\text{gas}}(t)$
 $\Psi(Z_{\text{stars}}; t)$

Complex accounting problem

Masses

M_g : Total mass of interstellar gas

M_s : Total mass of stars

M_w : Total mass of stellar remnants (white dwarfs)

M_t : Total mass of the system

$$M_t = M_g + M_s + M_w$$

Rates

E : the rate of mass ejection from stars

E_Z : the rate of metal ejection from stars

W : the creation rate of stellar remnants.

Ψ : Rate of star formation

f : Rate of infall or outflow of material from the system

Z_f : Metal abundance of the infall (or outflow) material

$\phi(m)$: the Initial Mass Function

Stellar Evolution & Nucleosynthesis

w : the mass of a stellar remnant

τ_m : the main-sequence lifetime of a star

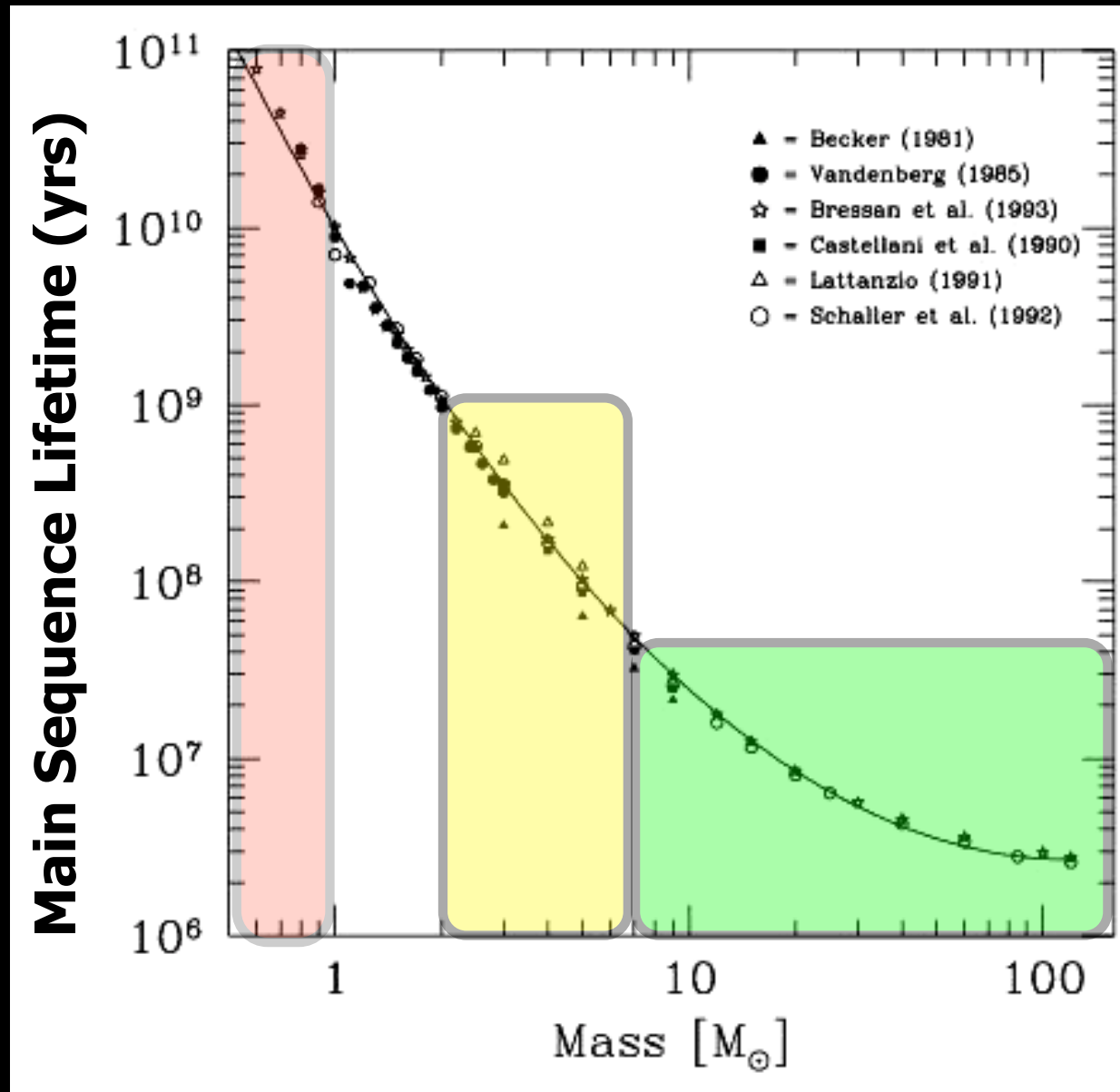
m_{tn} : the turnoff mass of a population with $t = \tau$

p_z : the stellar recyclable mass fraction that is converted to metal z and then ejected into space.

Classic references: Tinsley 1980 (Fundamentals of Cosmic Physics)
Pagel 1997 (Textbook)

“Instantaneous Recycling Approximation”

Low mass stars essentially live “forever”



Intermediate mass stars aren't quite “instant”, but still fast on astrophysical timescales

High mass stars that go SNe die “instantly”

Assume SF instantly injects metals into the ISM from SNe

Key, unfamiliar quantities:

Return Fraction
 (R)

The mass fraction of a generation of stars that is returned to the ISM. Depends on time, but typically 0.2-0.3

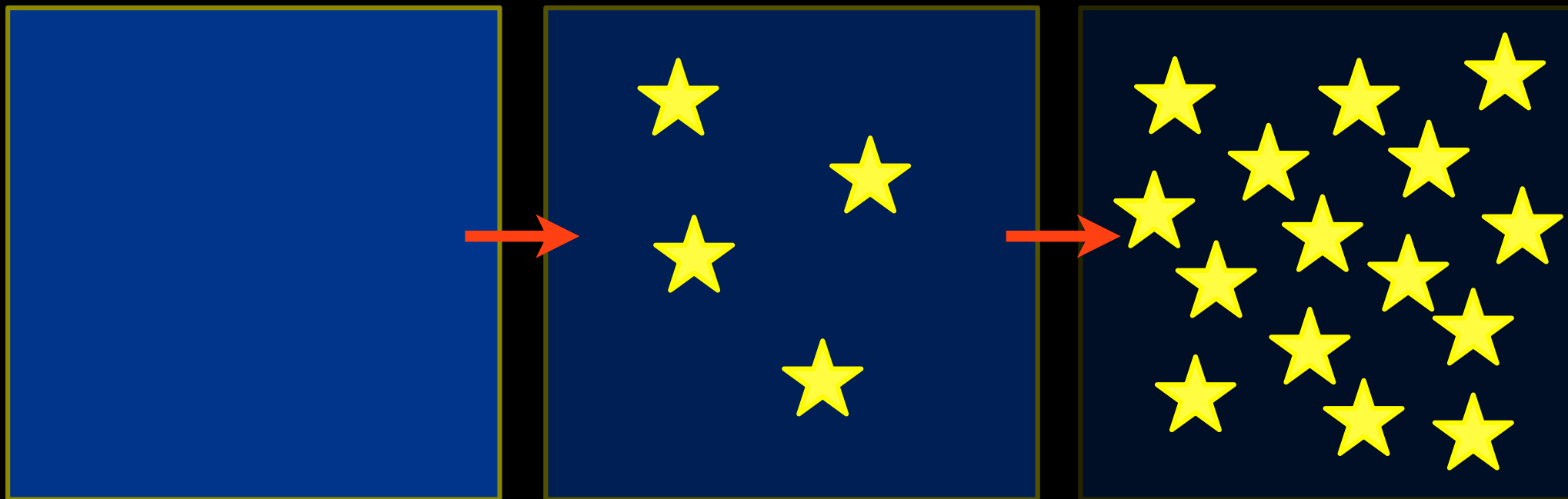
Lock up fraction
 $(\alpha = 1-R)$

The mass fraction of a generation of stars that is locked up in long-lived stars or remnants.

“Nucleosynthetic yield” (y or p)

The mass in newly formed elements ejected by a generation of stars, in units of the mass locked up in long-lived stars and stellar remnants

Simplest Form: “Closed Box”



$$Z_{\text{gas}} = 0$$

$$f_{\text{gas}} = 1$$

$$Z_{\text{gas}} > 0$$

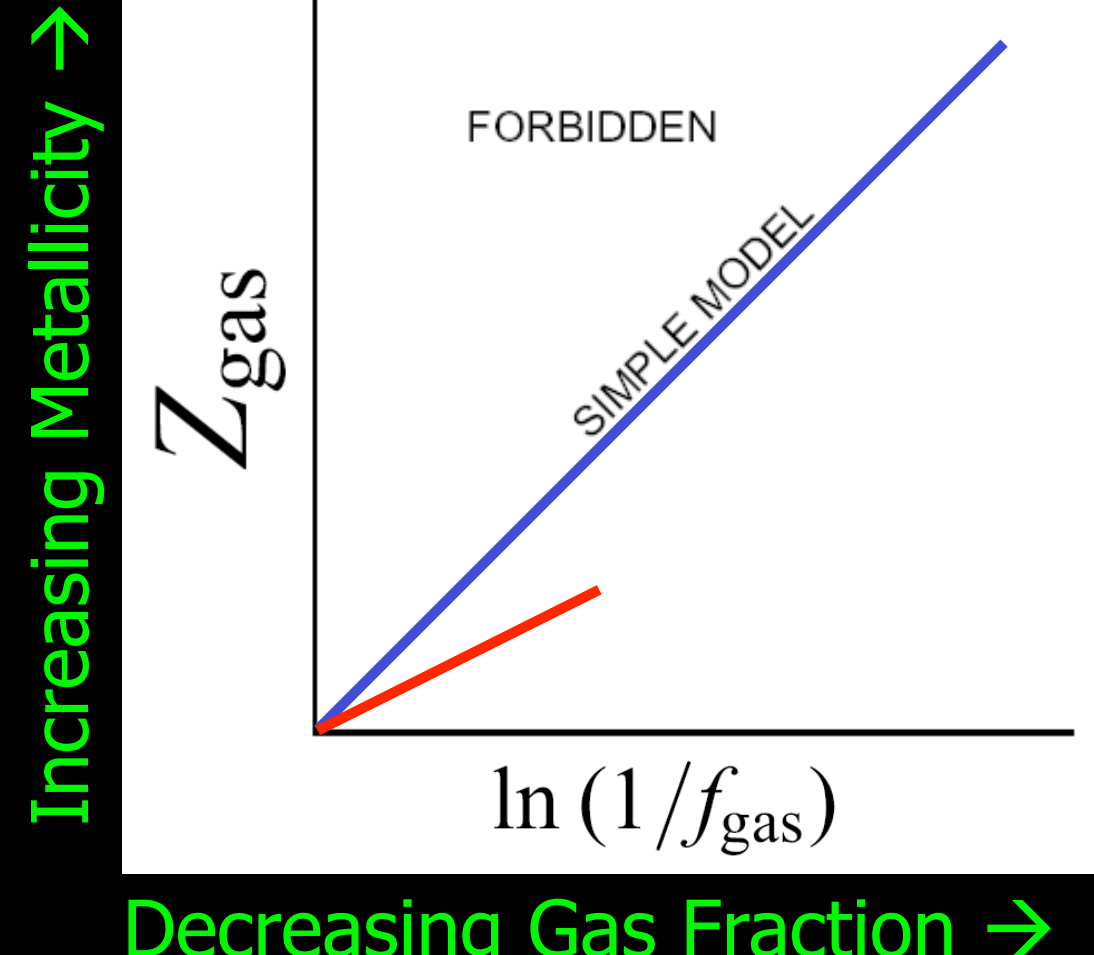
$$f_{\text{gas}} = 0.5$$

$$Z_{\text{gas}} \gg 0$$

$$f_{\text{gas}} = 0.1$$

- No infall or outflow
- Assume “instantaneous recycling” for massive stars

Closed Box Model



$f_{\text{gas}} = \text{gas fraction} = M_{\text{gas}}/M_{\text{baryon}}$

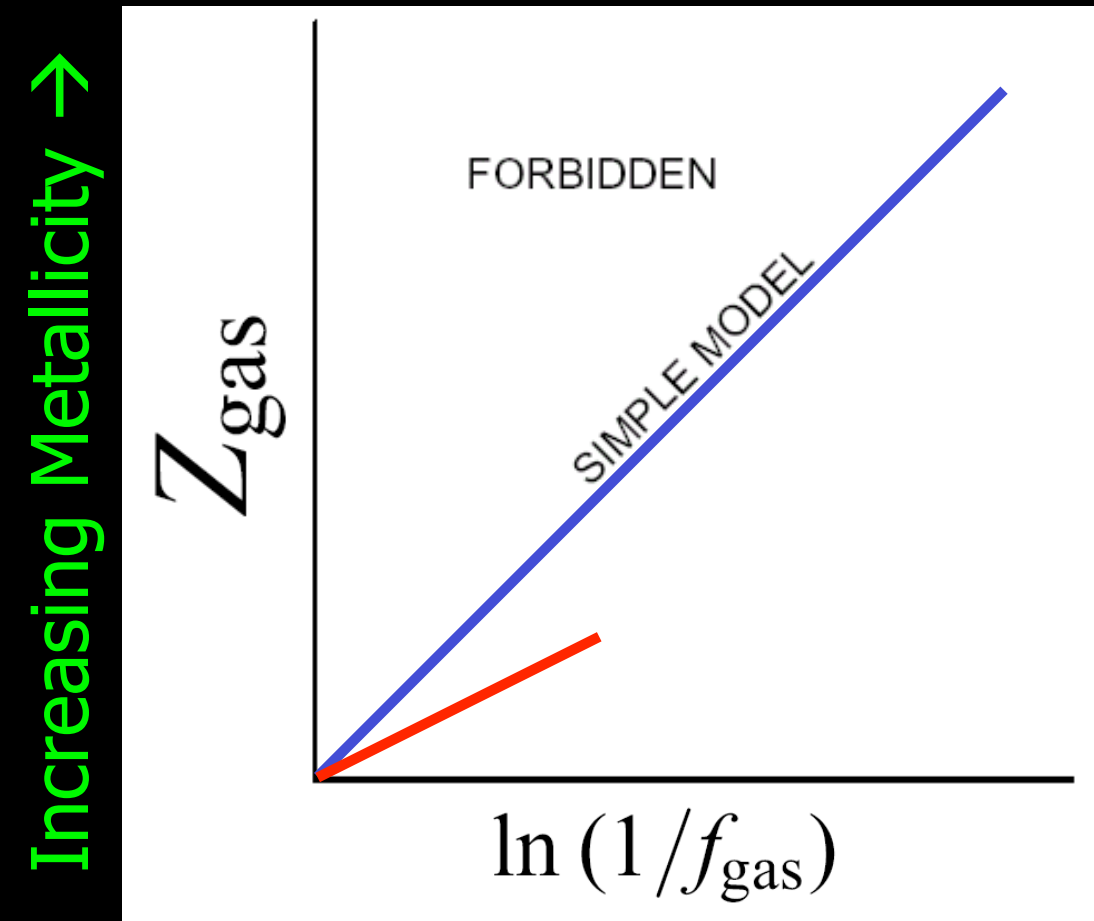
$$Z = y_Z \ln(\mu^{-1})$$

Nucleosynthetic
“yield”

$$y_{\text{eff}} = \frac{Z(\text{obs})}{\ln(\mu^{-1})}$$

“Effective Yield”

If $y_{\text{eff}} \sim y_Z$, evolved like “closed box”



Decreasing Gas Fraction →

$$f_{\text{gas}} = \text{gas fraction} = M_{\text{gas}}/M_{\text{baryon}}$$

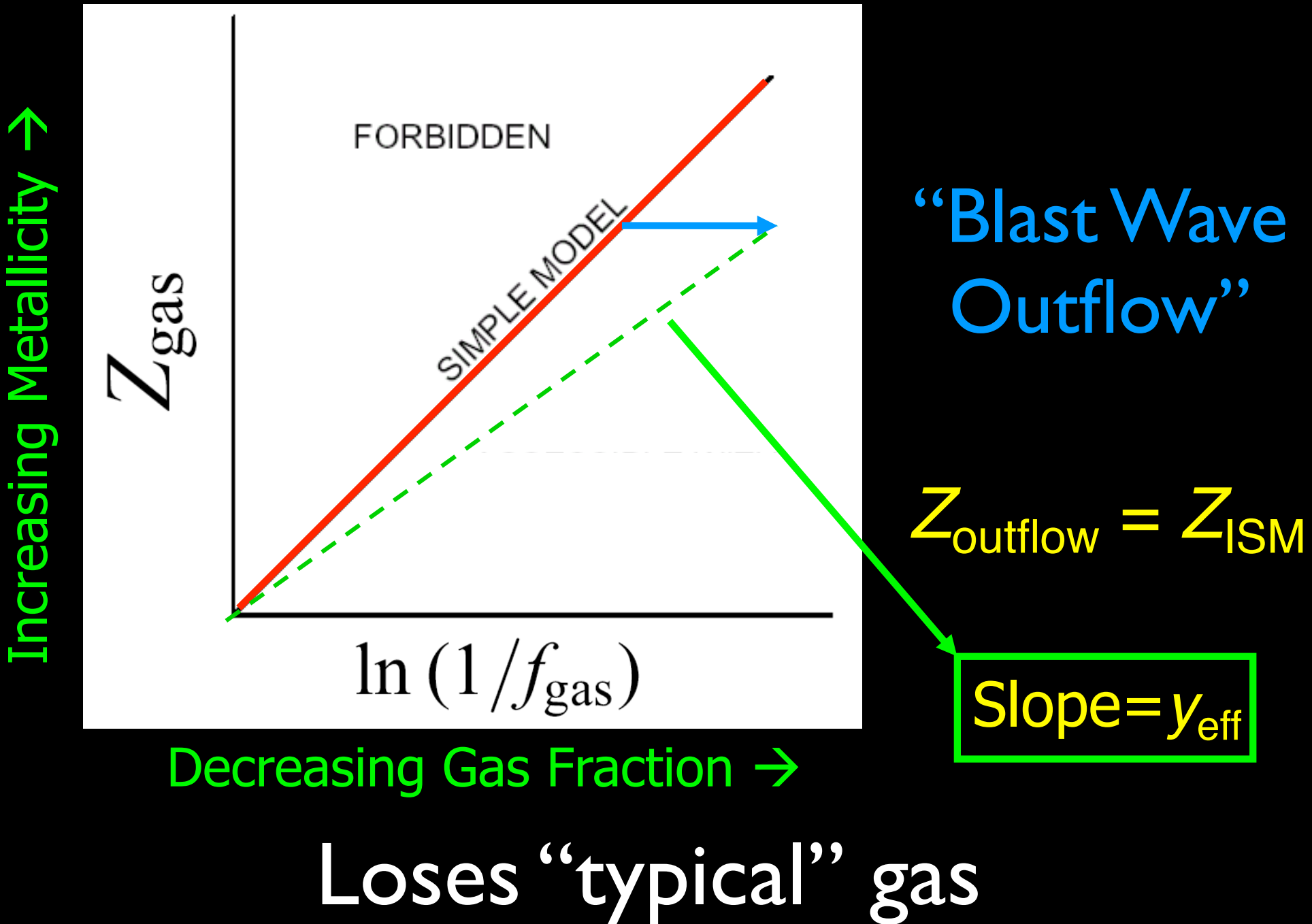
$$Z = y_Z \ln(\mu^{-1})$$

Nucleosynthetic
“yield”

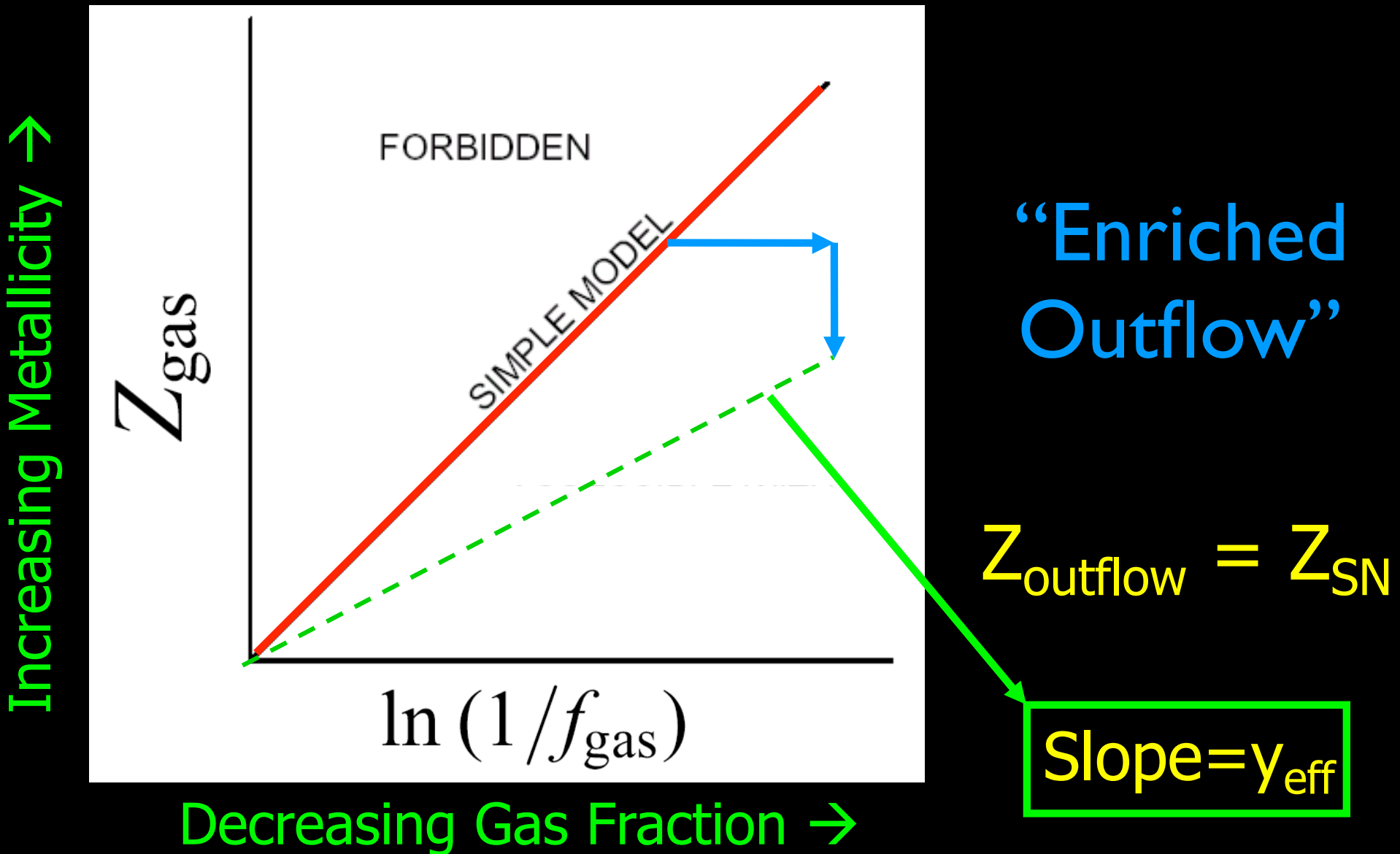
$$y_{\text{eff}} = \frac{Z(\text{obs})}{\ln(\mu^{-1})}$$

“Effective Yield”

Deviations from closed box

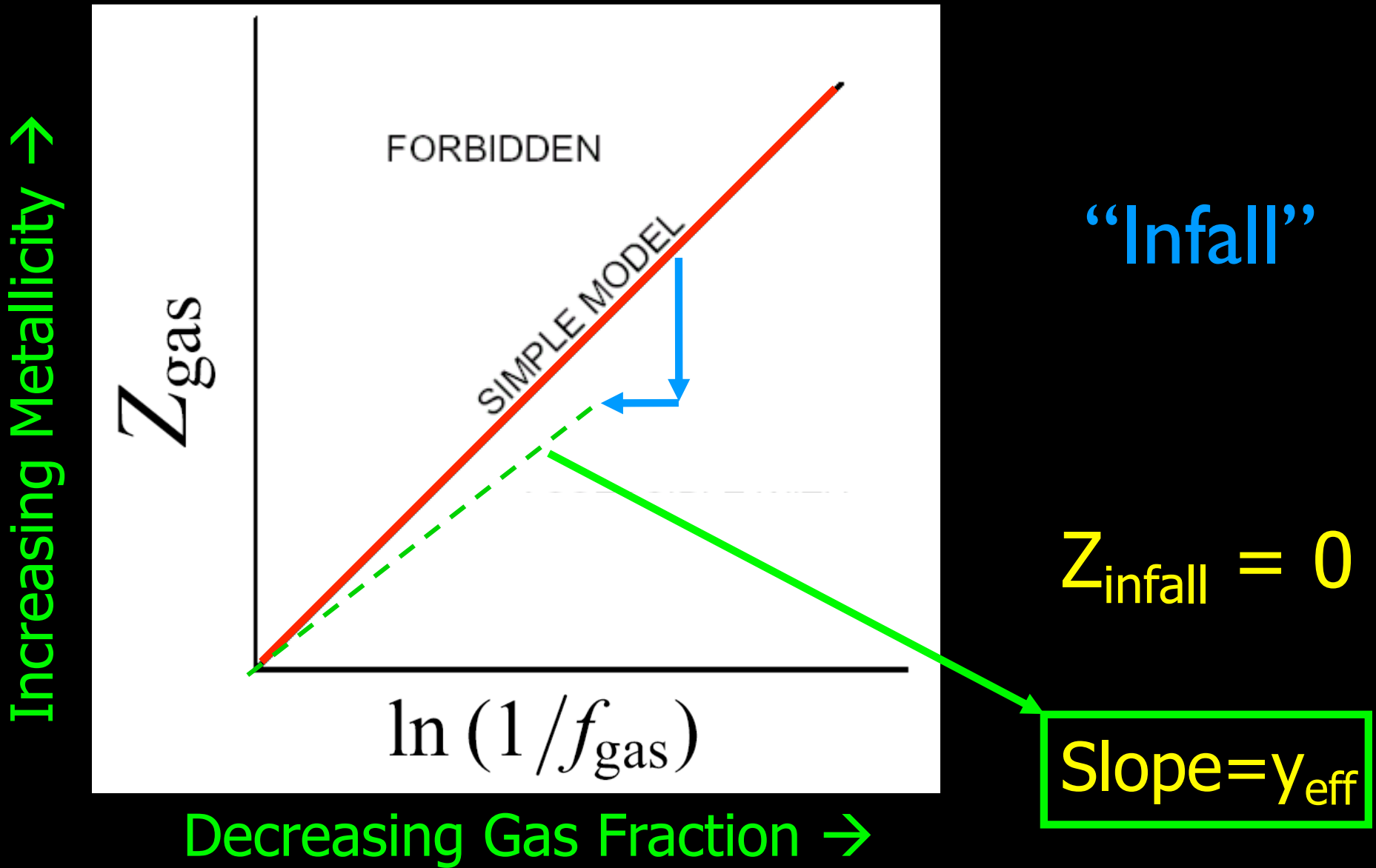


Deviations from closed box



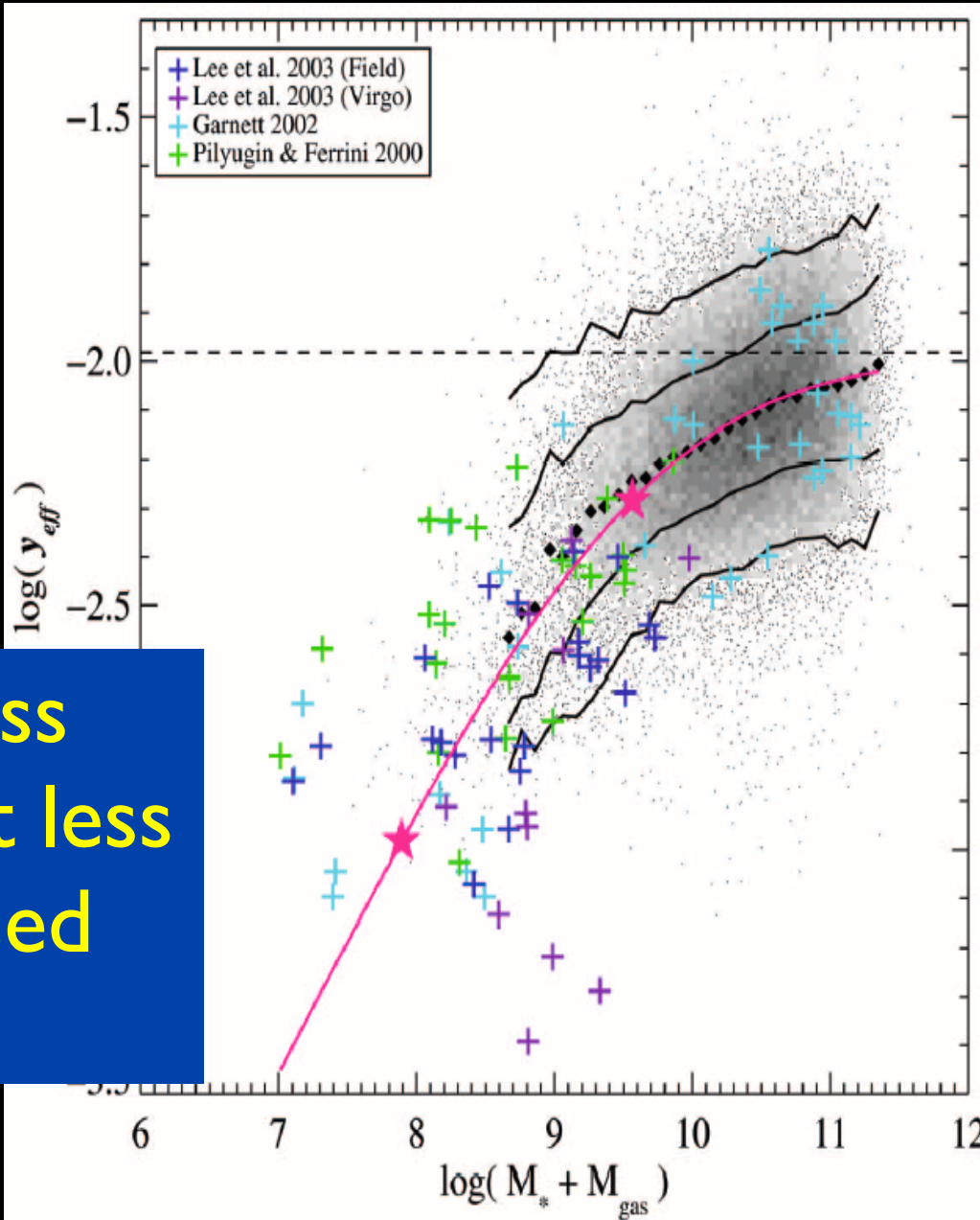
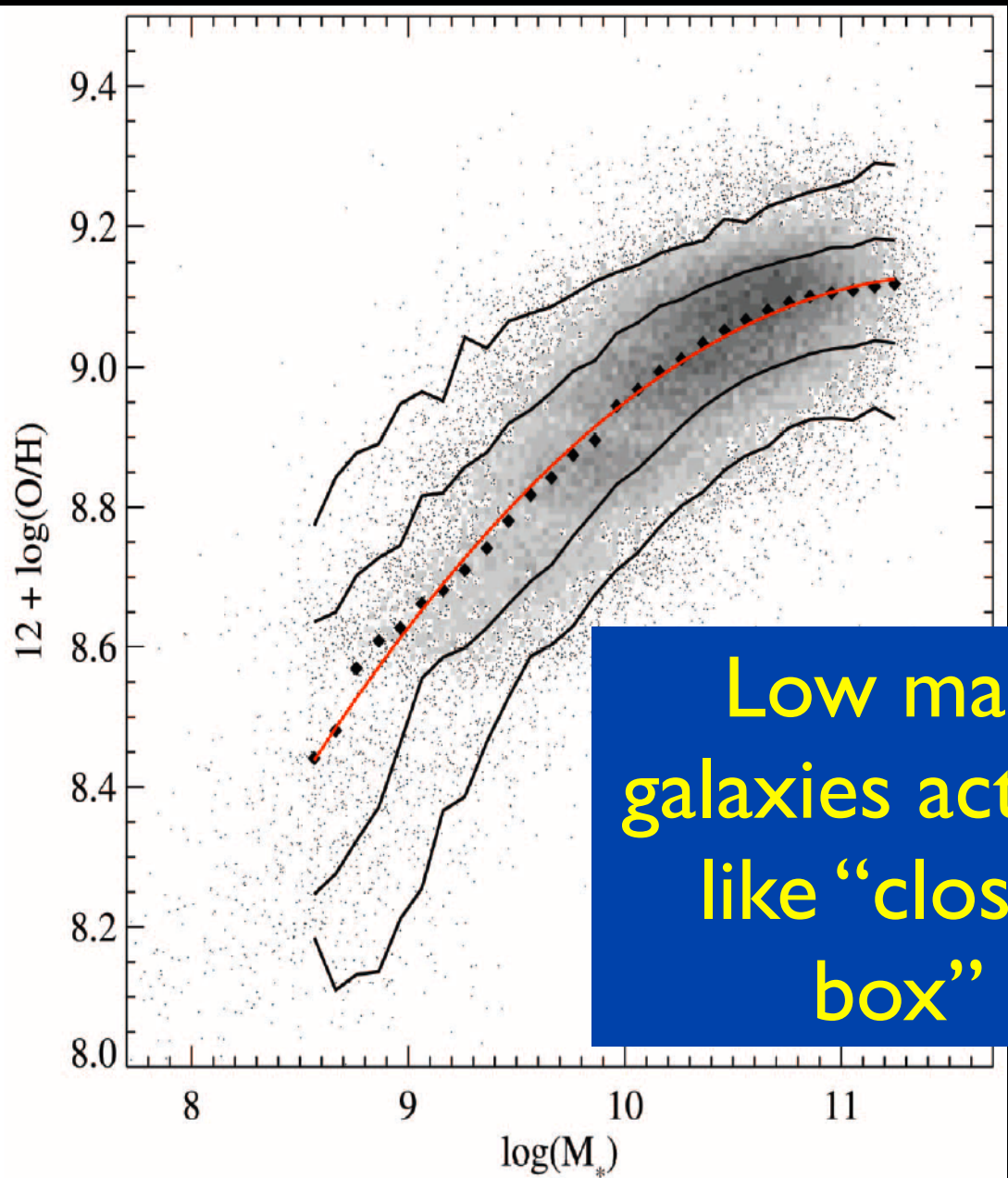
Loses metal-rich gas (SNe ejecta)

Deviations from closed box

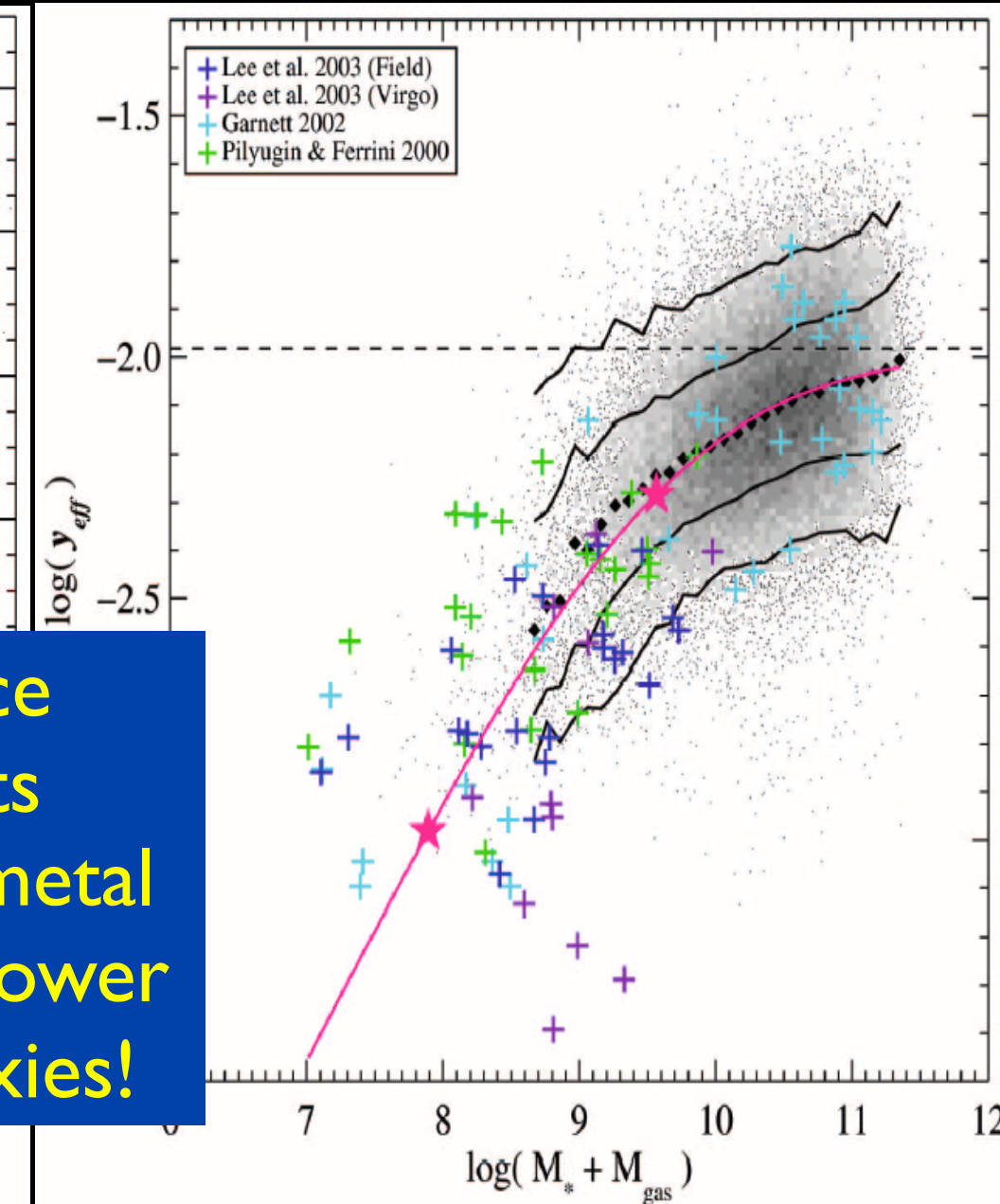
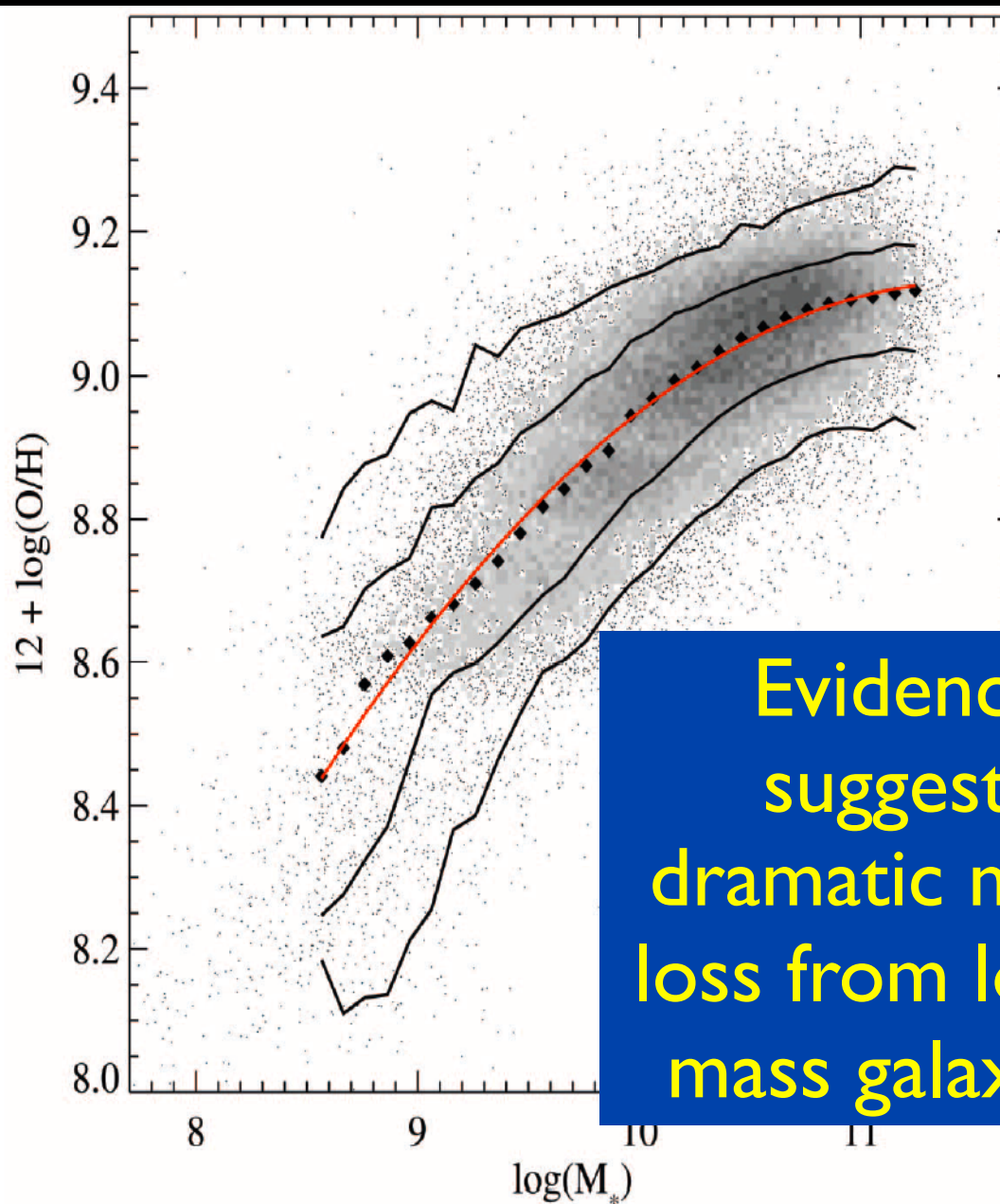


Accretes metal-poor gas (IGM)

Mass-Metallicity vs Effective Yield

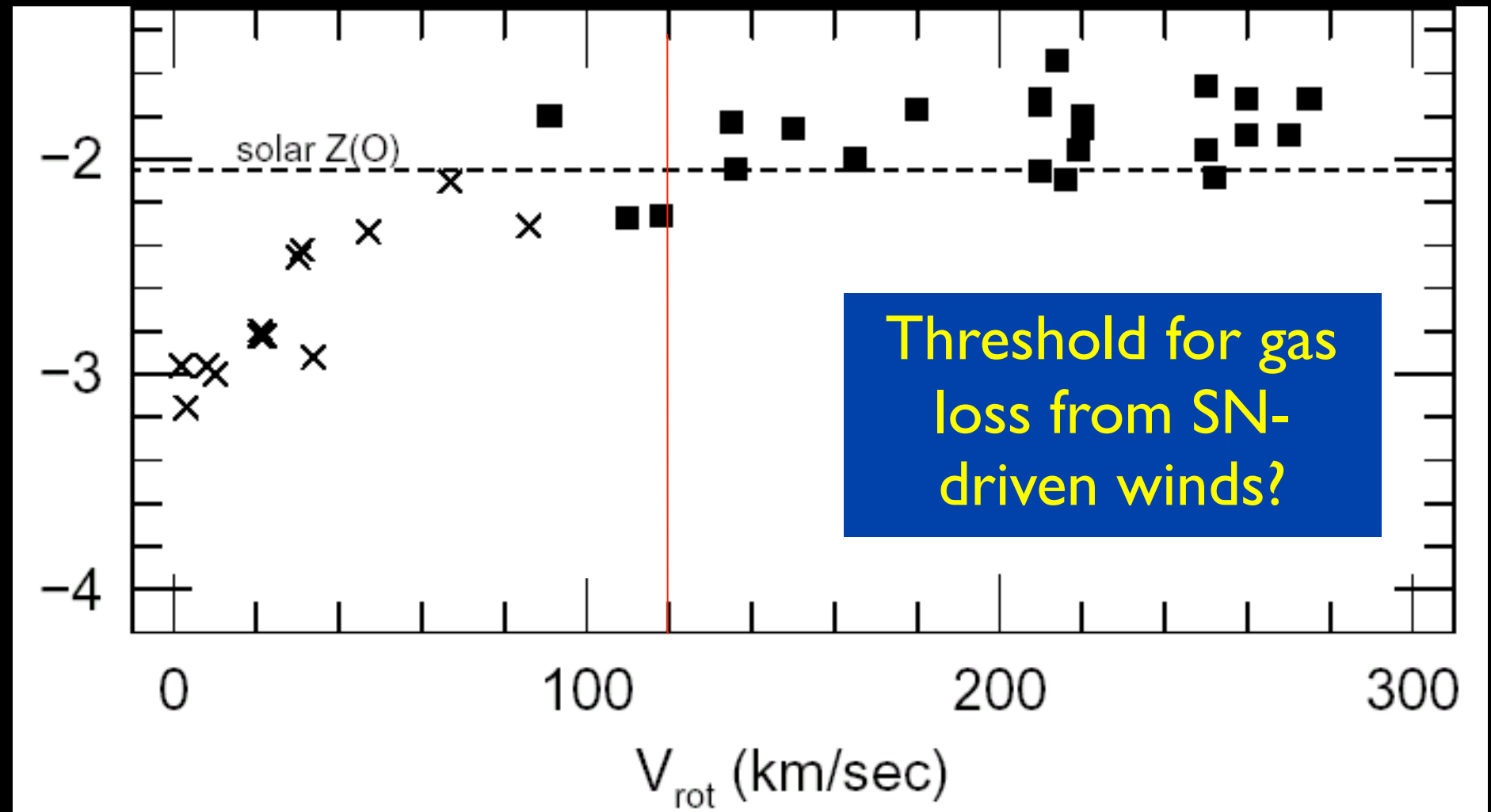


Mass-Metallicity vs Effective Yield



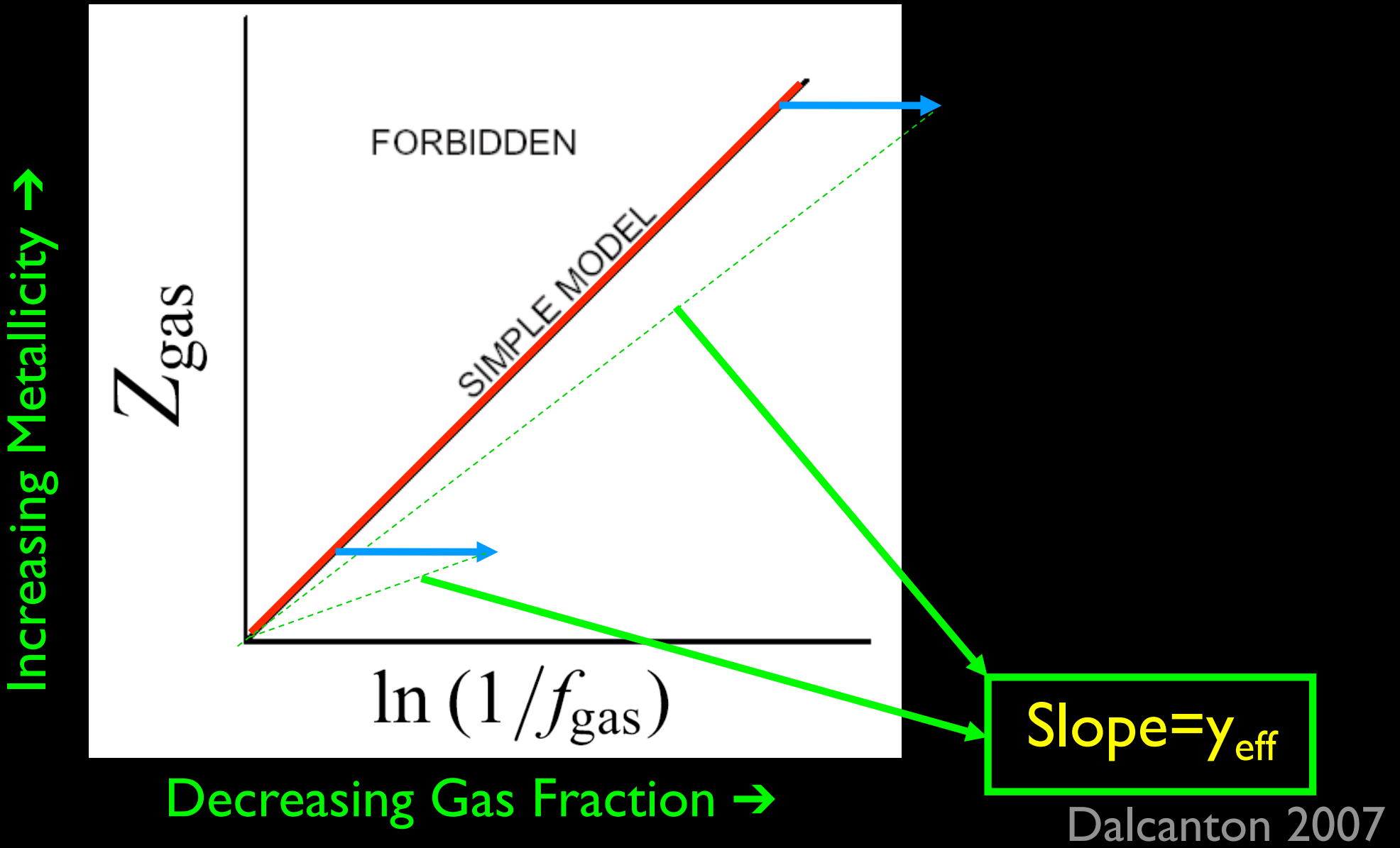
But note, metal loss \neq gas mass loss loss...

Effective yield is constant for $V > 120$ km/s

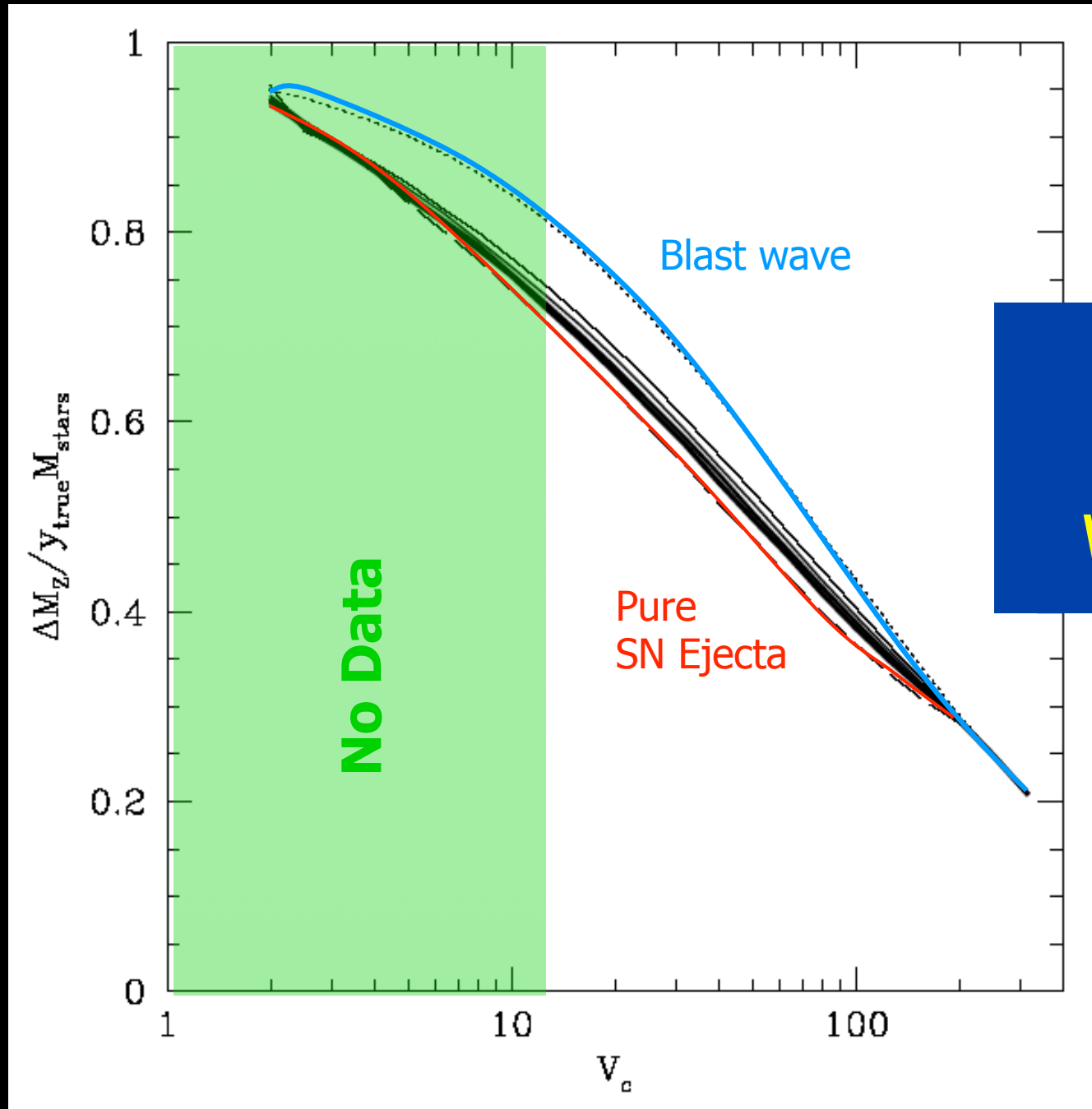


Garnett 2002

No. It's just hard to change effective yield of gas poor systems



Inferred metal loss is high, increases steadily



No clear
feature at
 $V_c=120 \text{ km/s}$

For dSph and
ultrafaints, more like
99% metal loss
(Kirby et al 2013)

In LG dwarfs metal loss is near total

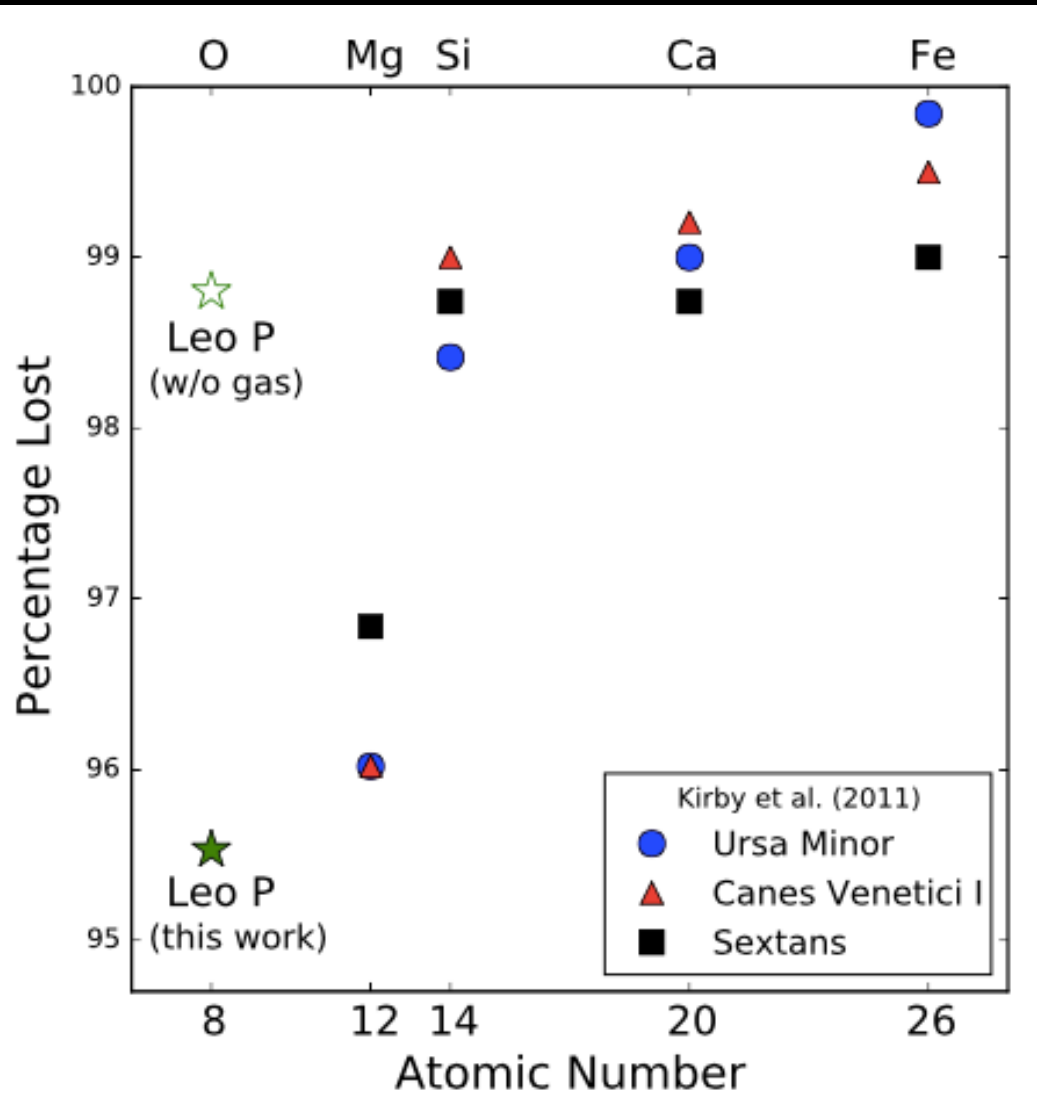


Figure 2. Percentage of O lost in Leo P compared to the percentage of metals lost in 3 Milky Way dSphs of comparable stellar mass from Kirby et al. (2011). Leo P has retained its gas content and thus a larger fraction of O. If the O atoms in the gas phase are ignored, the percentage of O lost is comparable to gas-poor dSphs (unfilled star point). Also note the discrepant low value for Mg loss in the dSphs.

- Measure stellar mass & SFH
- Infer production of elements (mass formed) M_{form}
- Measure stellar metallicities to infer mass in metals locked up M_{kept}
- Calculate M_{kept} / M_{form}

McQuinn et al 2015
see Telford et al 2019 for M3I

Chemical Evolution Questions

- How much infall or outflow of gas and metals is needed to explain mass-metallicity relation?
- How metal rich are outflows (pushing out mean ISM vs metal-enriched SN ejecta)?
- Does internal metallicity structure constrain how metals move radially (i.e., galactic fountains & circulation within the near CGM, migration of stars before Type Ia SNe)?
- Can different element tracers give more detailed information on history of gas flows?

How do we infer metallicity?

“Metallicity Indicators”

Metallicity Indicators

Stars:
Tracks [Fe/H] at time
luminosity-weighted
stellar population formed

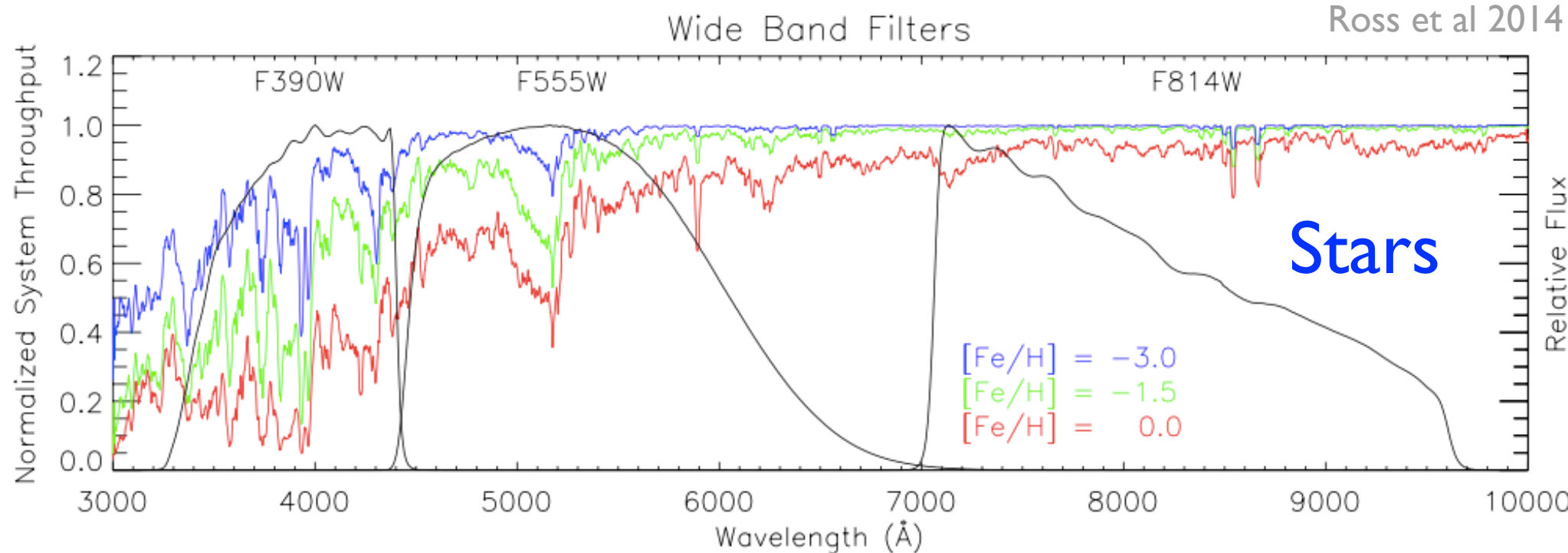
- Broadband colors — particularly NIR
- Spectral fitting (i.e. fit template to whole spectrum)
- Strength of specific spectral features (in absorption)

Gas:
Tracks current metallicity
of ISM

- Emission lines from metals in gas (HII regions, CGM)
- Absorption lines from interstellar gas

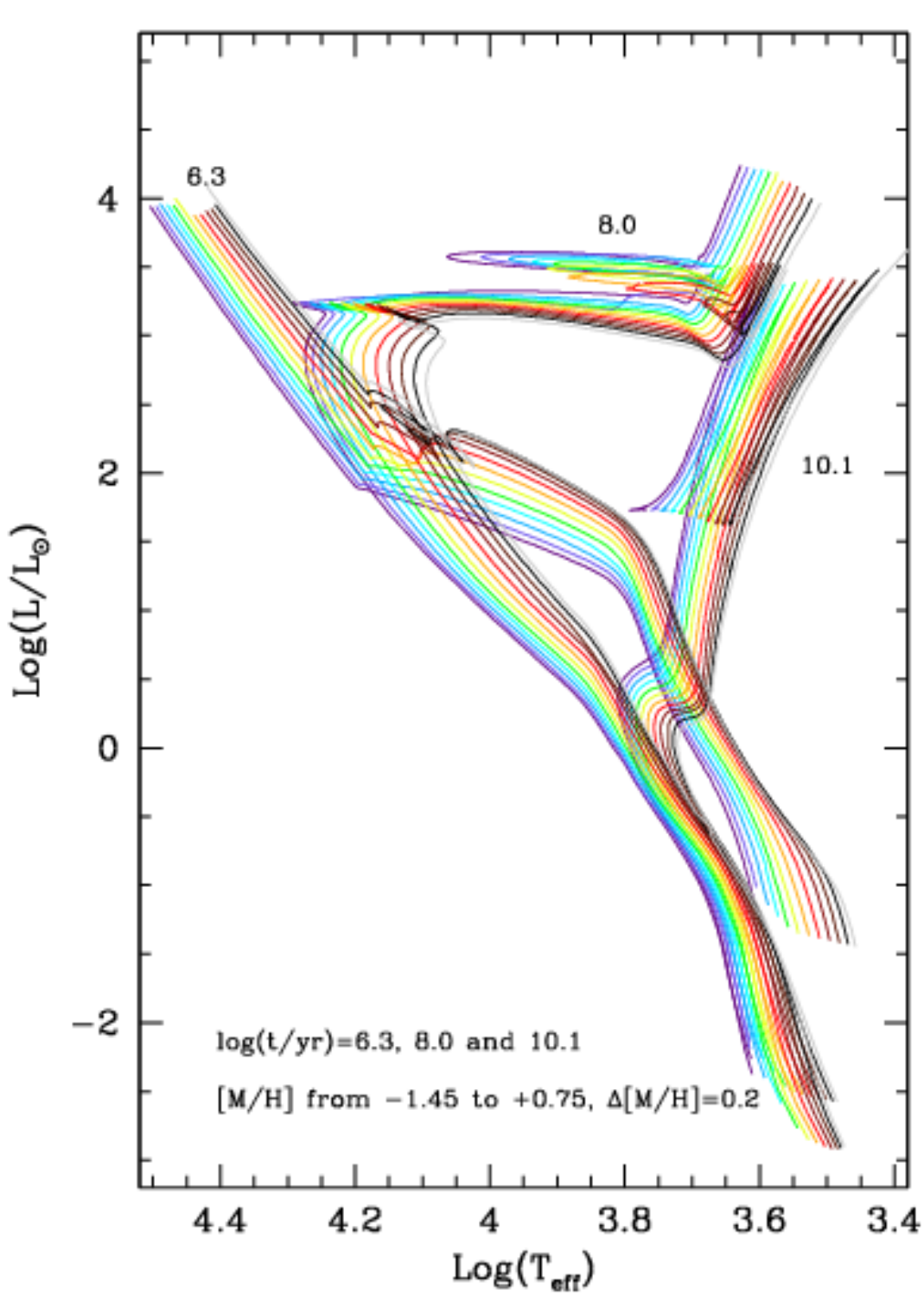
Stellar metallicity indicators

More Metals = More absorption



- More absorption lines in the blue
- Redder = More metal rich
- But, age effects in composite populations
- Colors more robust metallicity indicator in NIR, but spectral fitting more robust in optical

Metallicity-dependence of stellar evolution & atmospheres



Examples of theoretical isochrones in the HR diagram. {bf Left panel:} A sequence of solar-metallicity isochrones for ages going from $\log t = 6$ to 10.2 at equally spaced intervals of $\Delta \log t = 0.1$. {bf Right panel:} Three sequences of isochrones for a fixed age and at varying metallicity. The ages are $\log t = 6.3$, 8.0 and 10.1. The sequence of metallicities goes from $[\text{M}/\text{H}] = -1.45$ to $+0.75$ at equally spaced intervals of $\Delta[\text{M}/\text{H}] = 0.2$. In all cases, the mass-loss parameter is assumed to be $\eta = 0.2$, and the sequences are completed down to $0.1 \sim \text{Msun}$. Notice the presence of the PMS phase in the youngest isochrones.

Bressan et al 2012

“Age-Metallicity Degeneracy”

Ross et al 2014

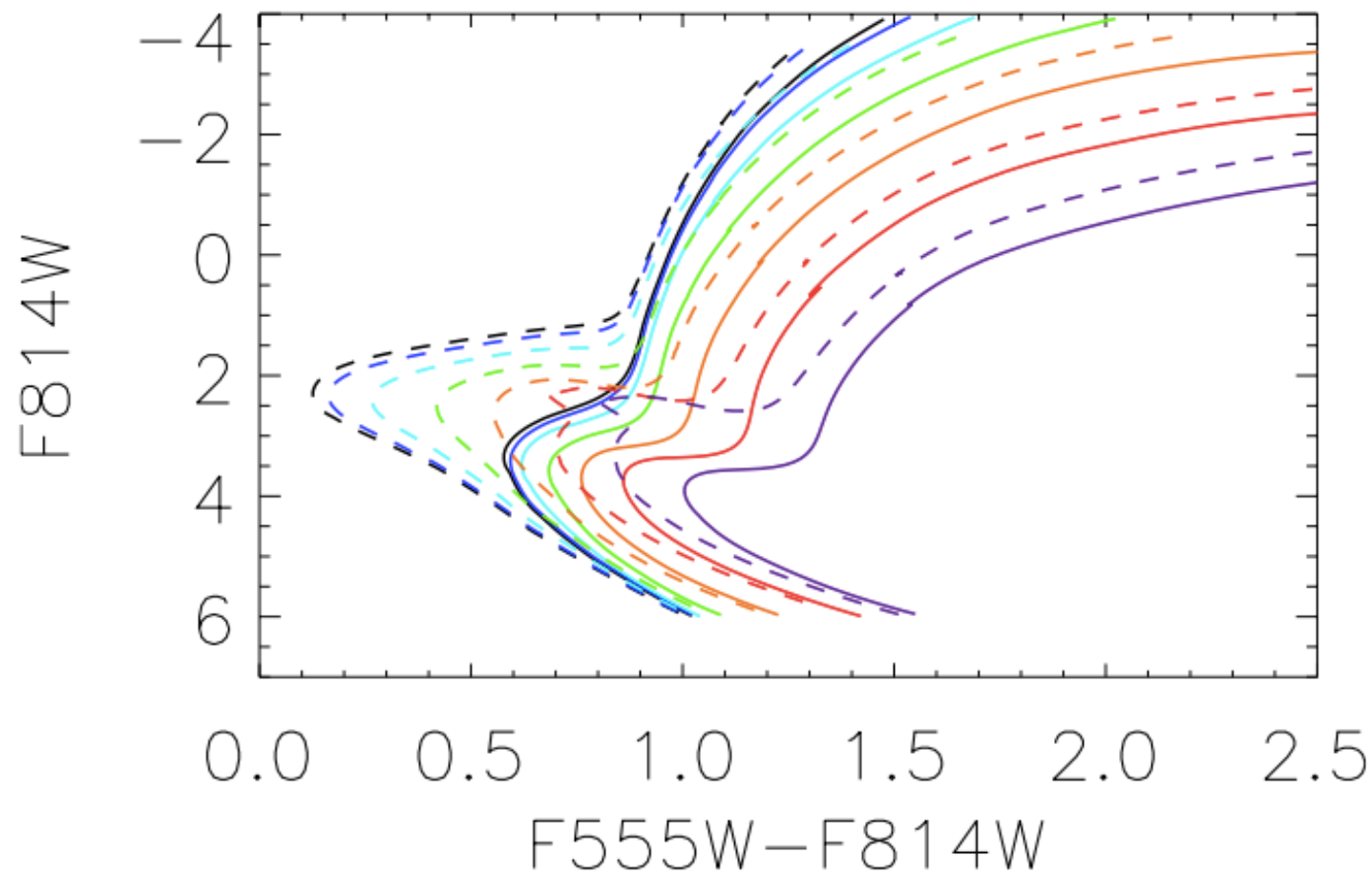
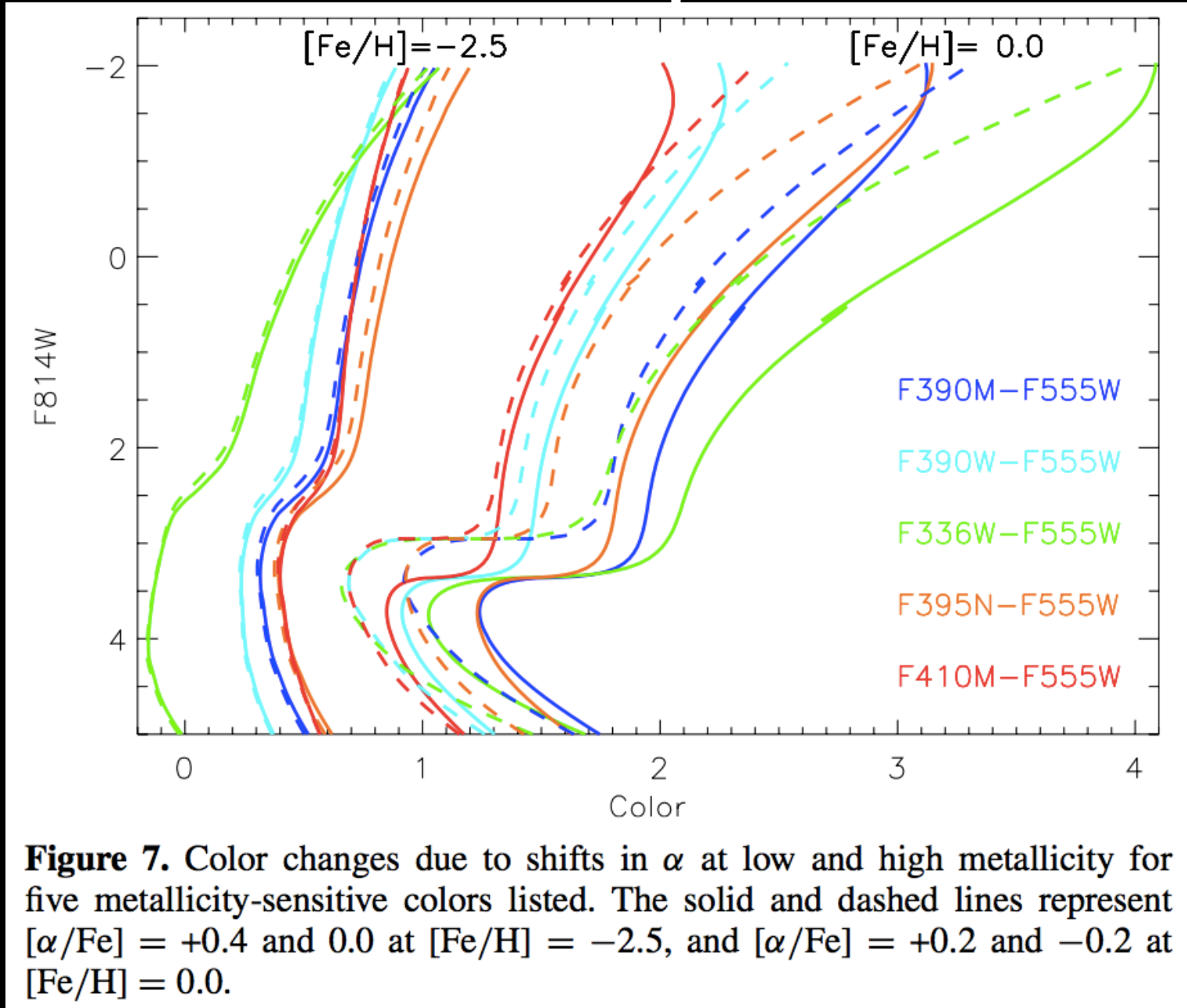
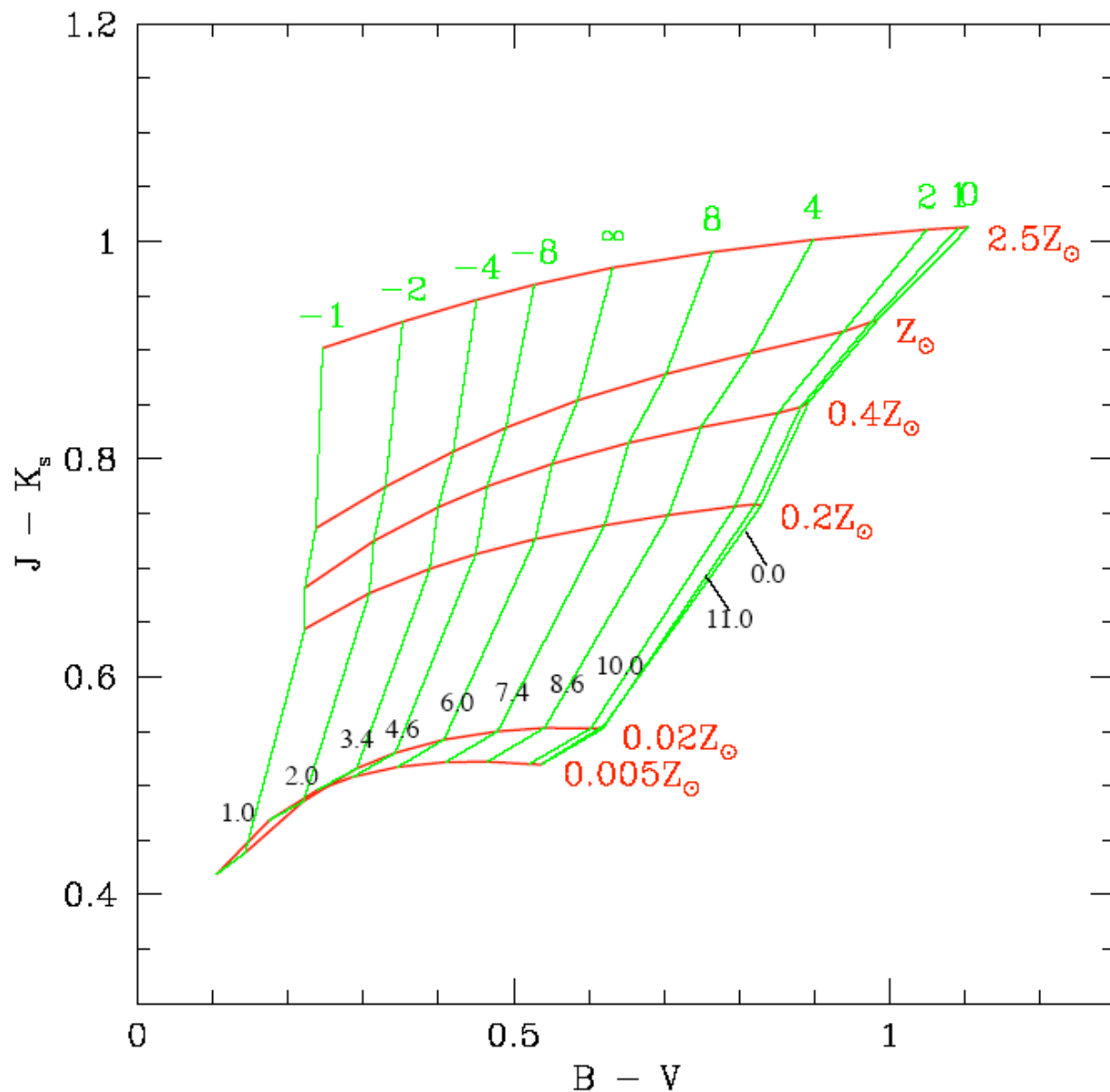


Figure 2. Age–metallicity degeneracy is shown here with isochrones of different ages covering a range of metallicity $-2.5 < [\text{Fe}/\text{H}] < +0.5$; black represents the most metal-poor, purple the most metal-rich, with each color in between representing a 0.5 increment in $[\text{Fe}/\text{H}]$; the solid lines represent an age of 12.5 Gyr and the dashed lines represent 4 Gyr.

Caveat: Color also depends on abundance patterns





Combine colors
to interpret age
& metallicity

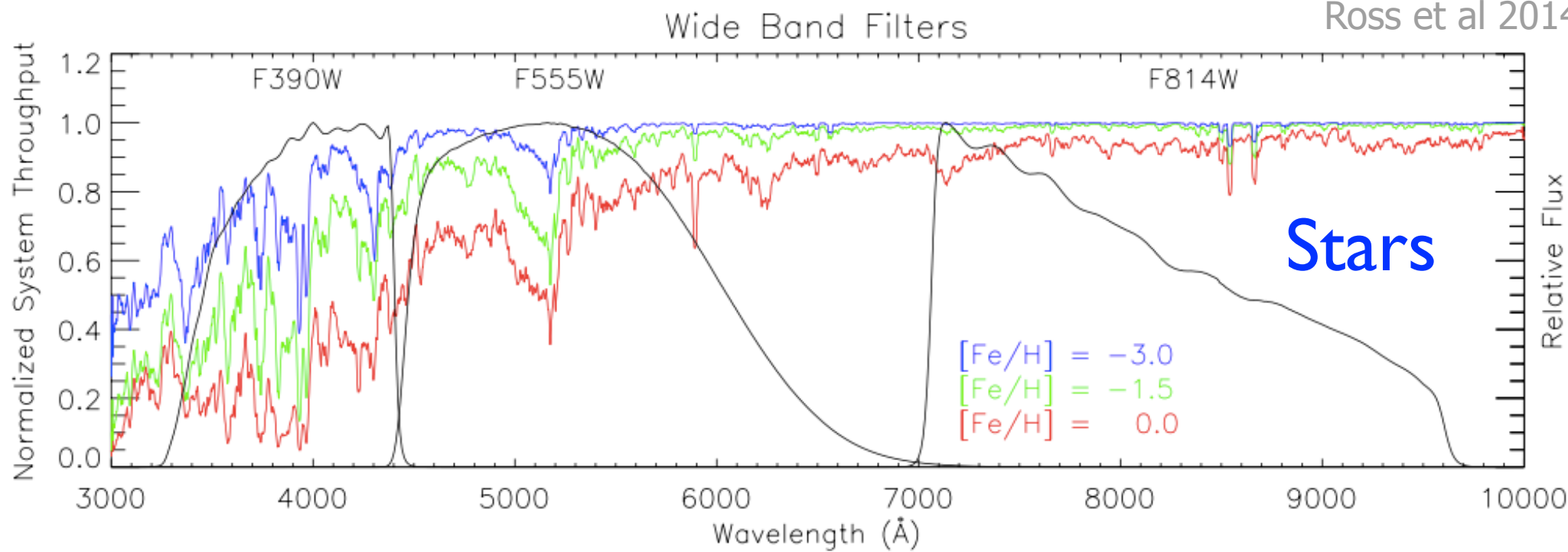
Lines of constant
metallicity (red) have
nearly *constant* $J-K$
colors.

Lines of constant **age**
(green) have relatively
constant $B-V$ colors

Fig. 15.— Color grid for the $J - K_s$ index as a function of the $B - V$ index, for different stellar formation rates and metallicities. Metallicities range from $0.005Z_\odot$ to $2.5Z_\odot$. Top labels denote different exponential star-formation rates, where ∞ denotes a constant star-formation rate. Bottom labels denote mean ages in Gyr. The star-formation started 12 Gyr ago for all bursts.

Caveats

Ross et al 2014



- Stellar metallicity indicators are light-weighted
- Different galaxies will have different age stars dominating light-weighted spectrum
- Comparing stellar metallicity is not tracking identical age across galaxies.

INDEX DEFINITIONS

Name (2)	Index Bandpass (3)	Pseudocontinua (4)	Units (5)	Measures ^a (6)
CN ₁	4142.125–4177.125	4080.125–4117.625 4244.125–4284.125	mag	C, N, (O)
CN ₂	4142.125–4177.125	4083.875–4096.375 4244.125–4284.125	mag	C, N, (O)
Ca4227	4222.250–4234.750	4211.000–4219.750 4241.000–4251.000	Å	Ca, (C)
G4300	4281.375–4316.375	4266.375–4282.625 4318.875–4335.125	Å	C, (O)
Fe4383	4369.125–4420.375	4359.125–4370.375 4442.875–4455.375	Å	Fe, C, (Mg)
Ca4455	4452.125–4474.625	4445.875–4454.625 4477.125–4492.125	Å	(Fe), (C), Cr
Fe4531	4514.250–4559.250	4504.250–4514.250 4560.500–4579.250	Å	Ti, (Si)
C ₂ 4668	4634.000–4720.250	4611.500–4630.250 4742.750–4756.500	Å	C, (O), (Si)
H β	4847.875–4876.625	4827.875–4847.875 4876.625–4891.625	Å	H β , (Mg)
Fe5015	4977.750–5054.000	4946.500–4977.750 5054.000–5065.250	Å	(Mg), Ti, Fe
Mg ₁	5069.125–5134.125	4895.125–4957.625 5301.125–5366.125	mag	C, Mg, (O), (Fe)
Mg ₂	5154.125–5196.625	4895.125–4957.625 5301.125–5366.125	mag	Mg, C, (Fe), (O)
Mgb	5160.125–5192.625	5142.625–5161.375 5191.375–5206.375	Å	Mg, (C), (Cr)
Fe5270	5245.650–5285.650	5233.150–5248.150 5285.650–5318.150	Å	Fe, C, (Mg)
Fe5335	5312.125–5352.125	5304.625–5315.875 5353.375–5363.375	Å	Fe, (C), (Mg), Cr
Fe5406	5387.500–5415.000	5376.250–5387.500 5415.000–5425.000	Å	Fe
Fe5709	5696.625–5720.375	5672.875–5696.625 5722.875–5736.625	Å	(C), Fe
Fe5782	5776.625–5796.625	5765.375–5775.375 5797.875–5811.625	Å	Cr
Na D	5876.875–5909.375	5860.625–5875.625 5922.125–5948.125	Å	Na, C, (Mg)
TiO ₁	5936.625–5994.125	5816.625–5849.125 6038.625–6103.625	mag	C
TiO ₂	6189.625–6272.125	6066.625–6141.625 6372.625–6415.125	mag	C, V, Sc

Metallicity Sensitive Absorption Features

“Lick Indices”

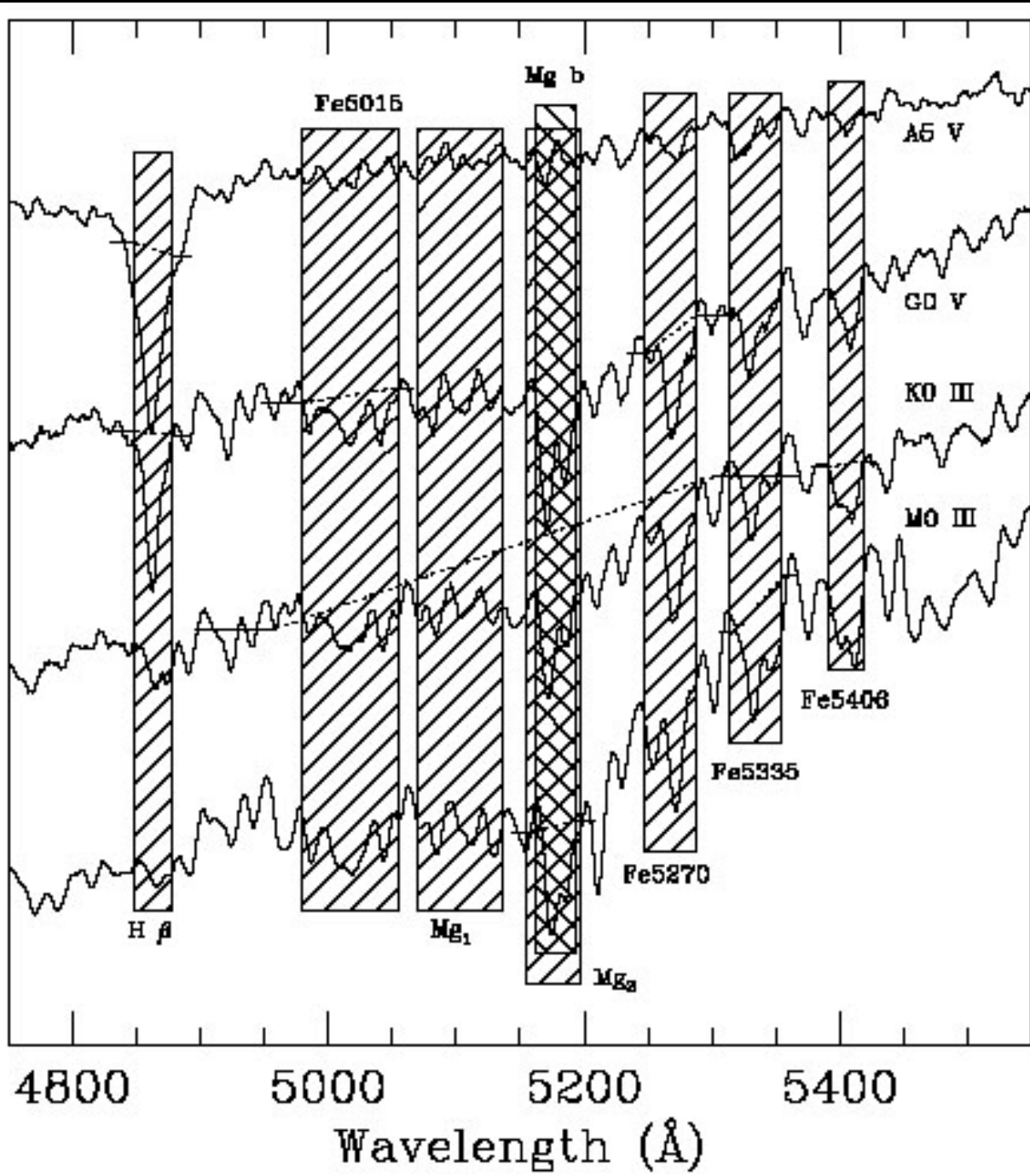
Characterize strength of optical absorption features

Age & Metallicity Sensitive

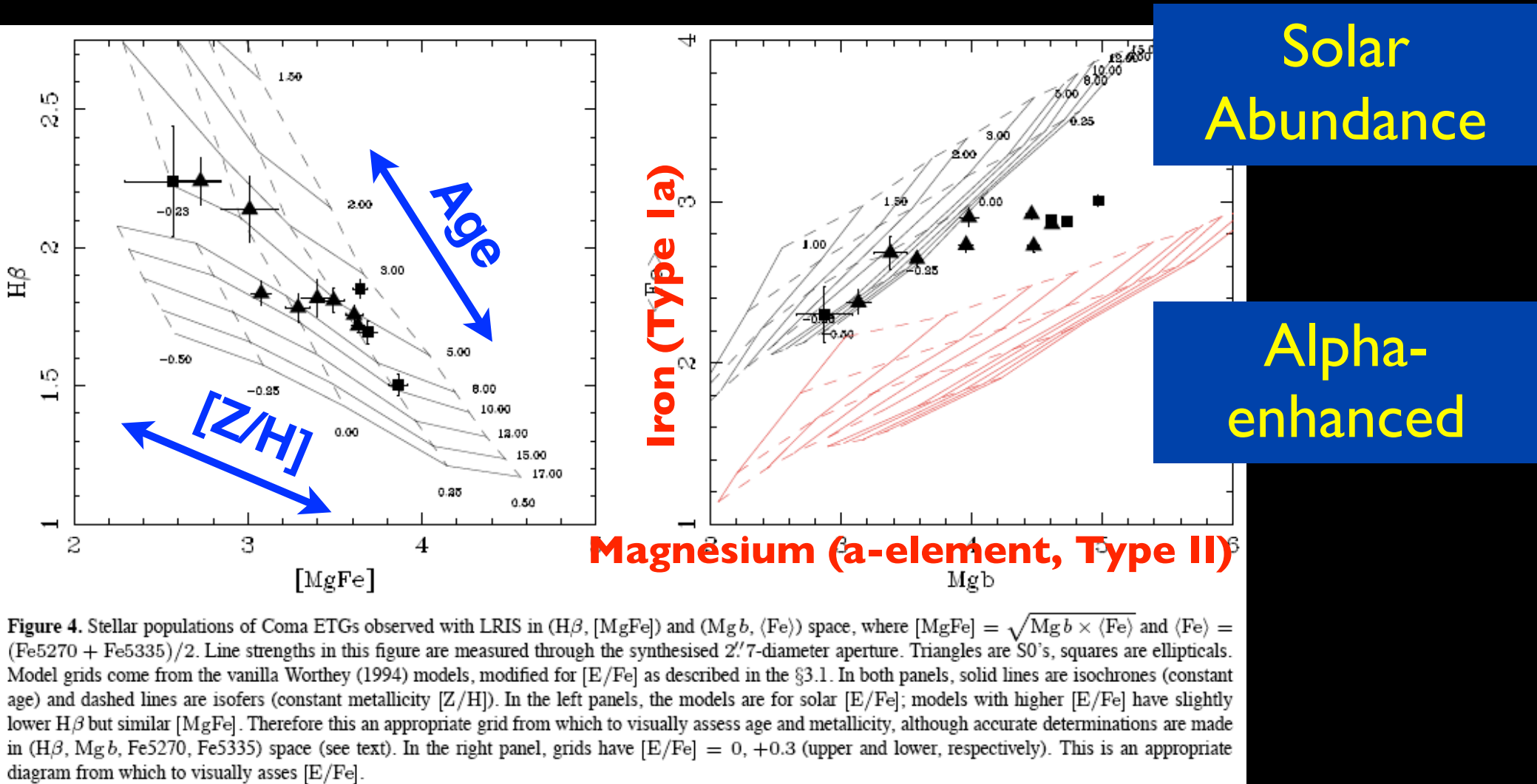
Note that the name sometimes has no connection to what elements are actually dominating the absorption!

Trager et al 1998

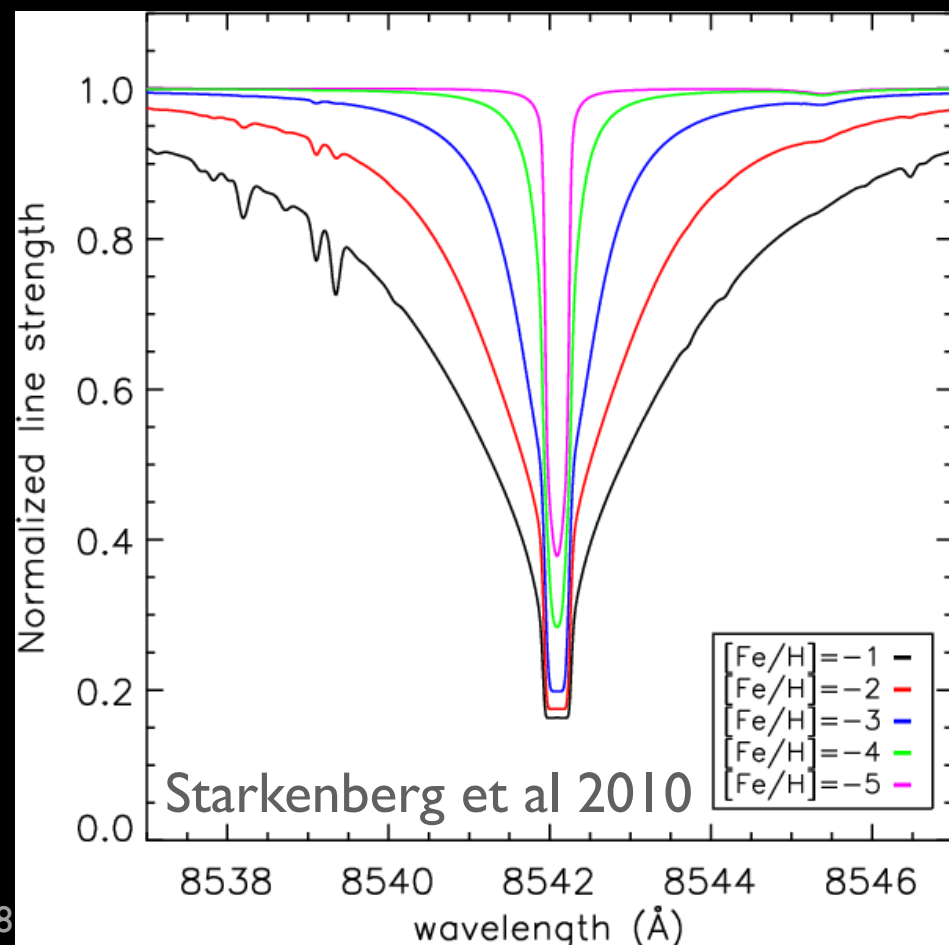
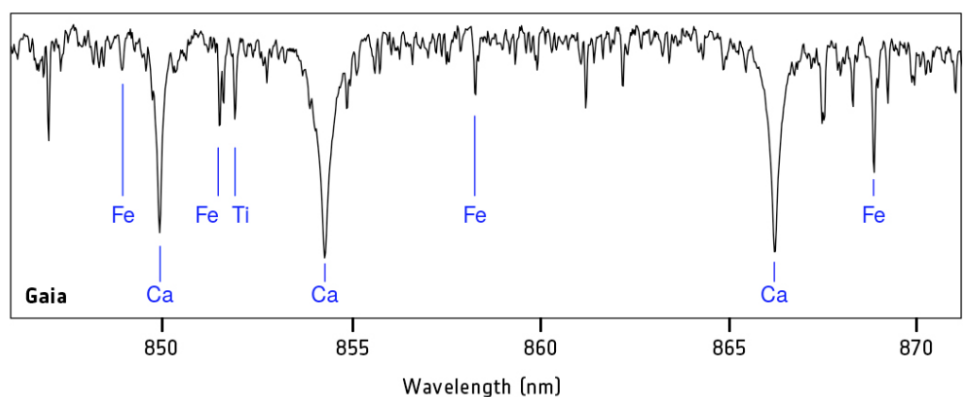
- Most useful for old stellar populations
- Tied to specific properties of spectrograph at Lick
- Resolution & velocity-broadening dependent



Lick indices are good probes of α -enhancement for unresolved galaxies



Metallicity Sensitive Absorption Features:



“Calcium Triplet”

- Strong and easily measured at red optical wavelengths
- Depends on metallicity
- Ca is an α -element, so also depends on $[\alpha/\text{Fe}]$

The change of the shape of the CaT line at λ 8542 Å with changing metallicity (metallicity is decreasing as the line narrows). Non-LTE effects are not taken into account. These lines are obtained from synthetic spectra from MARCS models with $T_{\text{eff}} = 4500$ K and $\log(g) = 1.5$ as described in the text. The flattening in the core at higher metallicities arises because the models do not cover small enough optical depths in the outer layers, where the core of the line is formed. This is a problem within the modeling itself, and not related to the non-LTE effects which are described in Sect. 3.2. Because of the broad wings, the area of the core of the line that is missing is a negligible fraction of the total equivalent width.

Gas metallicity indicators

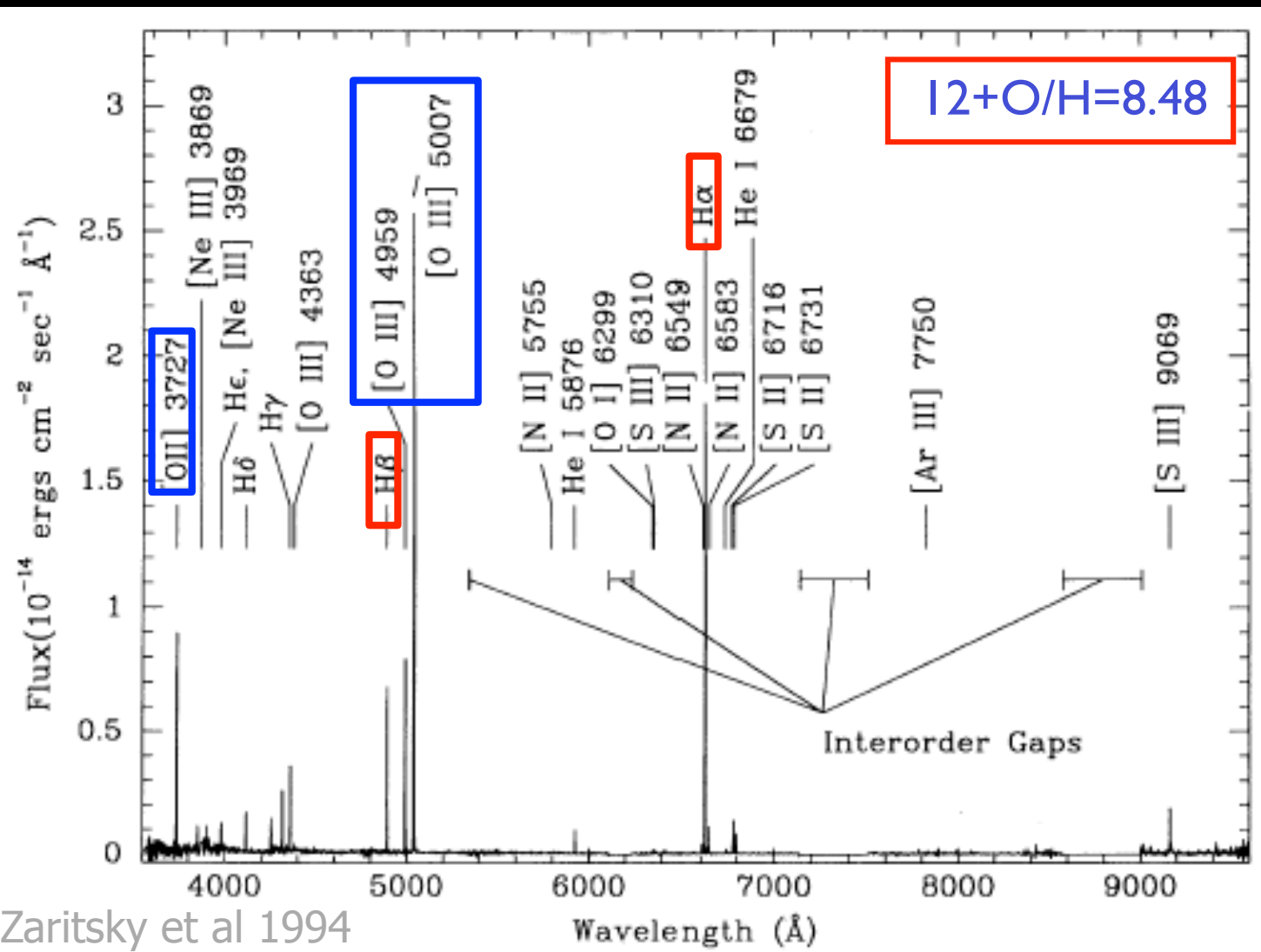
Metallicity-sensitive indicators

Gas:

Tracks Z of current gas reservoir

- Ratios of “strong” emission lines
- Detailed fitting of weak+strong emission lines (like [OIII] “auroral” line; discussed in A54I)
- X-ray spectroscopy
- UV absorption spectroscopy (discussed in A54I)

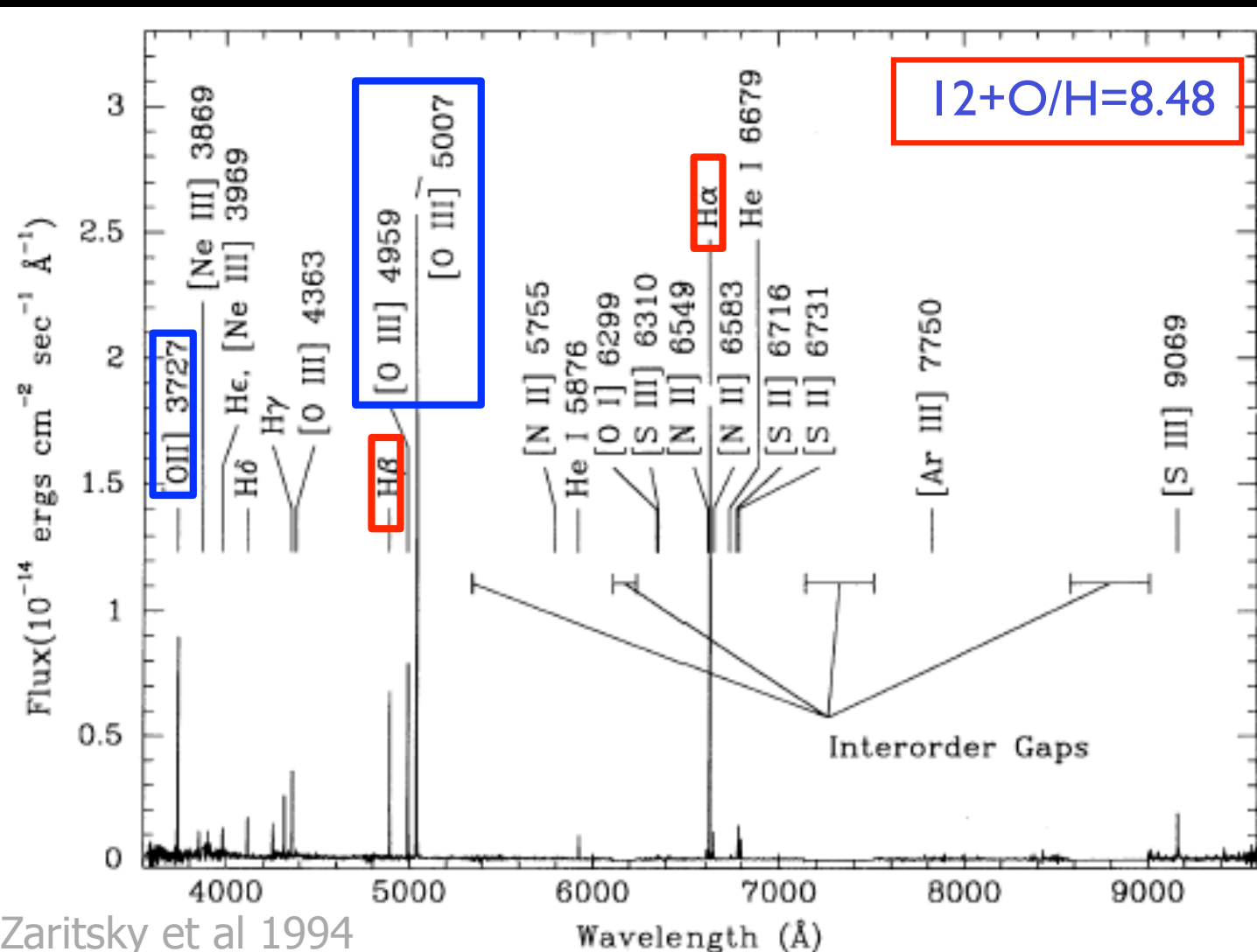
Measuring gas-phase metallicity



Need way of translating line ratios to elemental abundances.

Not as simple as taking ratio of O lines to H lines

Measuring gas-phase metallicity

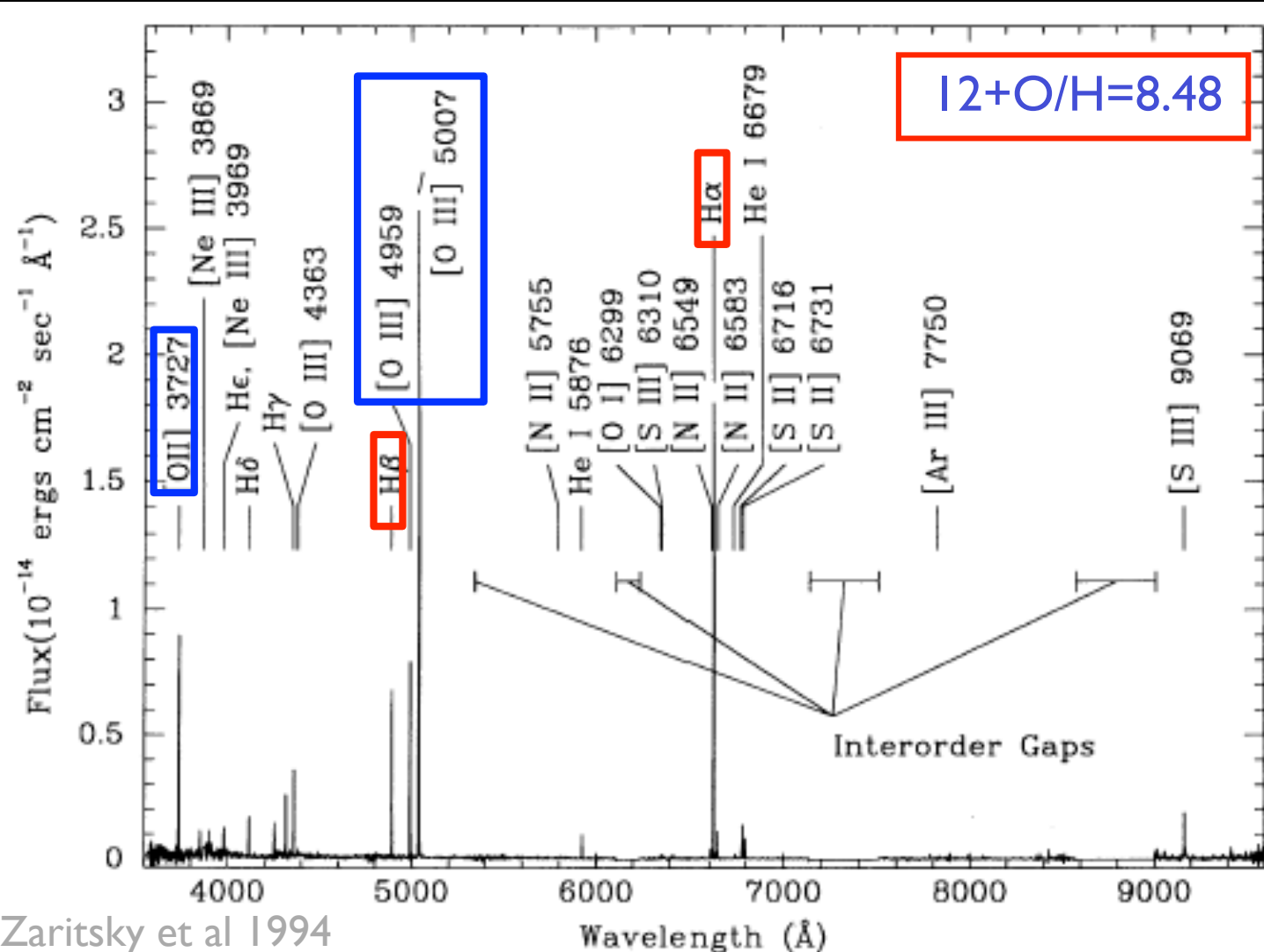


Hydrogen:
recombination
radiation

Oxygen:
Collisionally
excited
forbidden lines

These are different physical processes. Their ratios don't immediately tell you much.

Measuring gas-phase metallicity

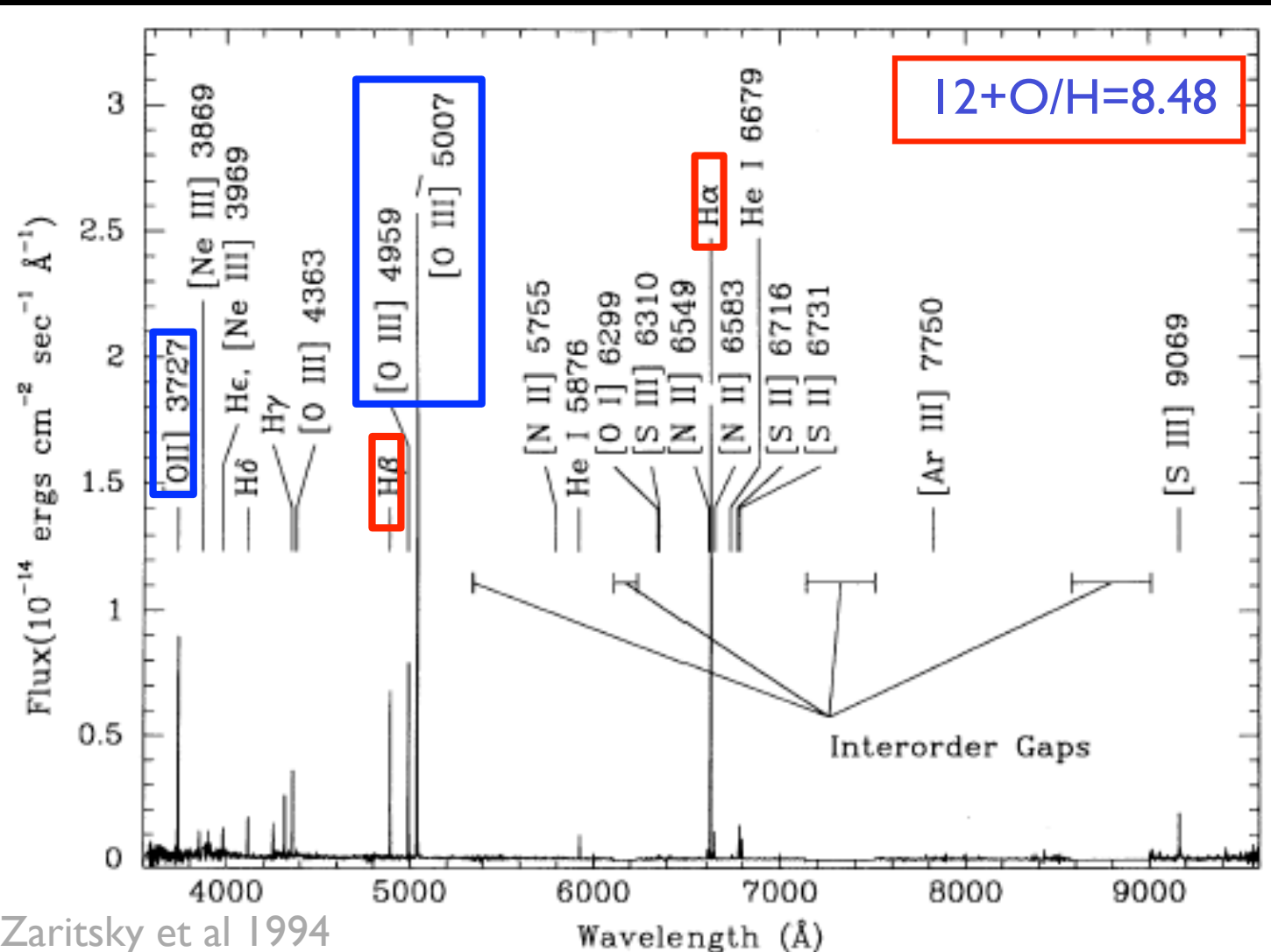


Hydrogen: recombination radiation

Line strength depends on n_e , Q_{ion} (electron density, ionizing flux).

Dependence on n_e , Q_{ion} often combined into an “ionization parameter” $U=n_Y/n_e$ where n_Y is # density of photons at Ly edge

Measuring gas-phase metallicity

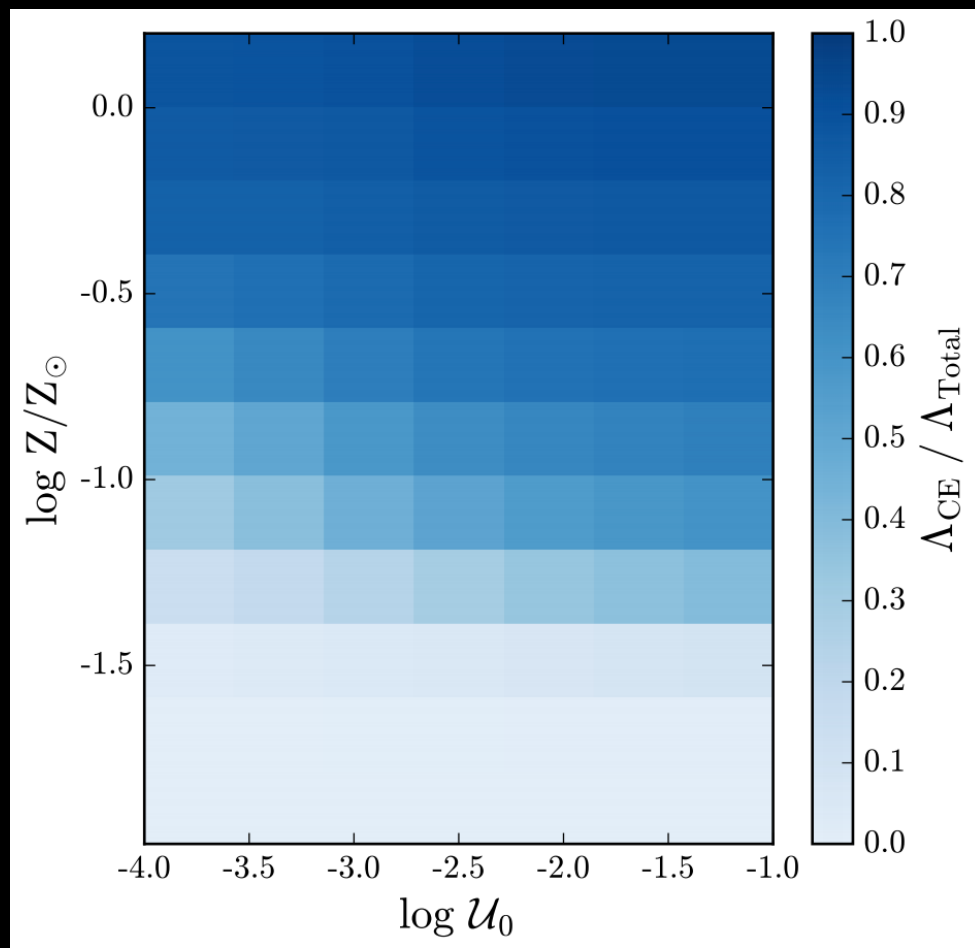


Also will depend on degree of ionization,
which also is affected by U

Oxygen:
Collisionally*
excited
forbidden lines

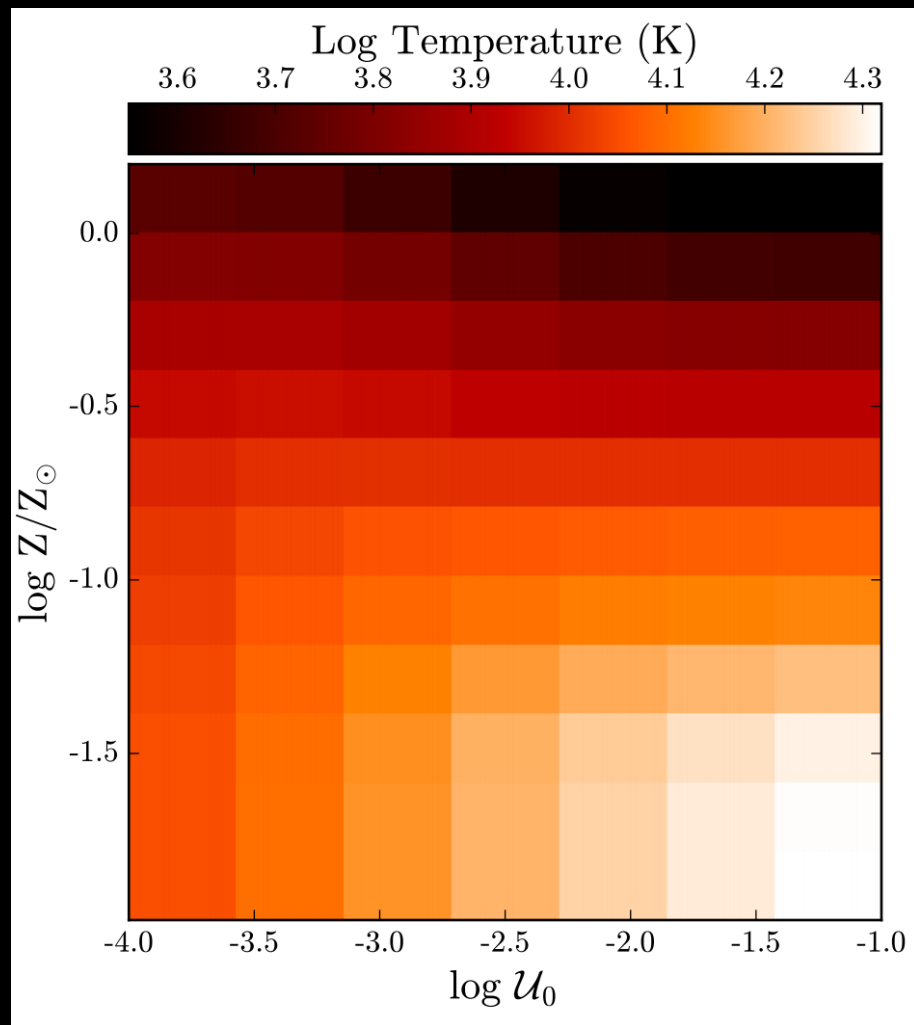
Line strength
depends on n_e ,
 T_e
(electron density,
temperature)

Metallicity impact on HII regions



Metals increase the cooling rate through collisionally-excited lines...

Figure 5. The fractional contribution of collisionally-excited metal lines to the total cooling in a 1 Myr population as a function of metallicity and ionization parameter. Metal lines are the dominant coolant for models with metallicities above $\sim \log_{10} Z/Z_\odot = -1.0$, and can provide as much as 90% of the cooling emission at the highest model metallicities. For models with metallicities below $\sim \log_{10} Z/Z_\odot = -1.0$, the bulk of the cooling emission is through Ly α , recombination lines, and the bound-free continuum. Cooling from free-free emission contributes at most $\sim 10\%$ of the total cooling.



...so metal rich HII regions are cooler

Figure 6. Top: The volume-averaged electron temperatures (T_e) of model HII regions as a function of \mathcal{U}_0 and $\log_{10} Z/Z_\odot$ at a fixed age (2 Myr). Above $\log_{10} Z/Z_\odot = -1$, metal line cooling dominates and T_e is primarily a function of metallicity. Below $\log_{10} Z/Z_\odot = -1$, Ly α , free-bound, and free-free continuum emission provide most of the cooling radiation and T_e depends primarily on \mathcal{U}_0 . **Bottom:**

Line ratios depend on Z , U , and t

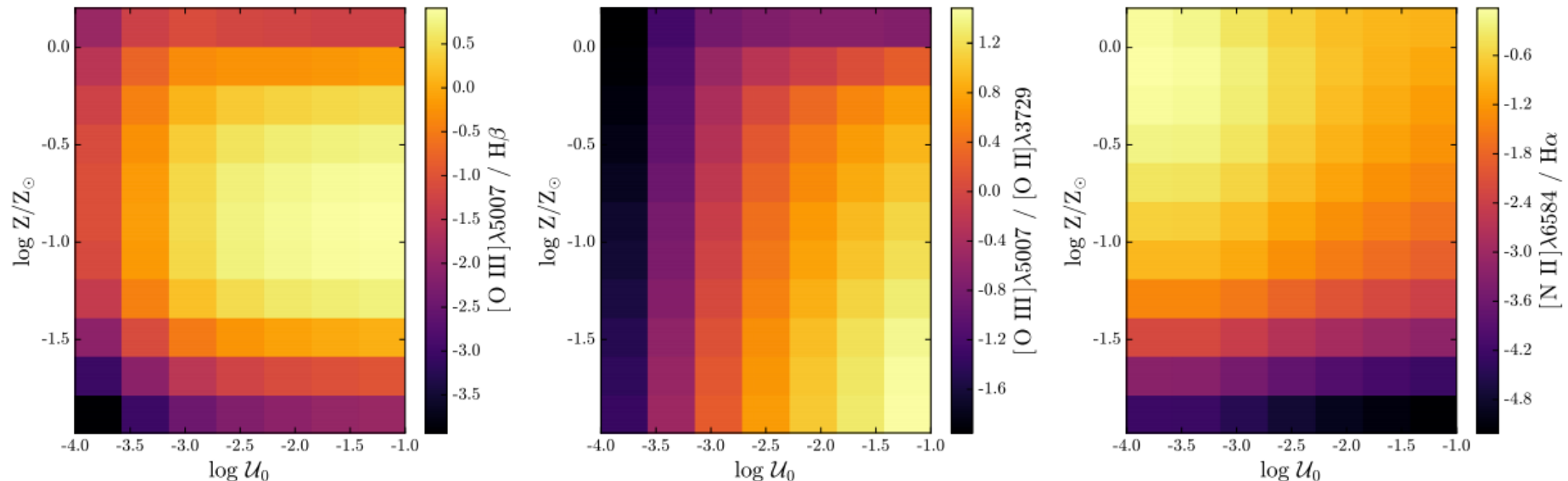


Figure 14. Line ratios as a function of metallicity and ionization parameter for a 1 Myr model: $[\text{O III}]\lambda 5007/\text{H}\beta$ (left); $[\text{O III}]/[\text{O II}]$ (middle); $[\text{N II}]\lambda 4865/\text{H}\alpha$ (right).

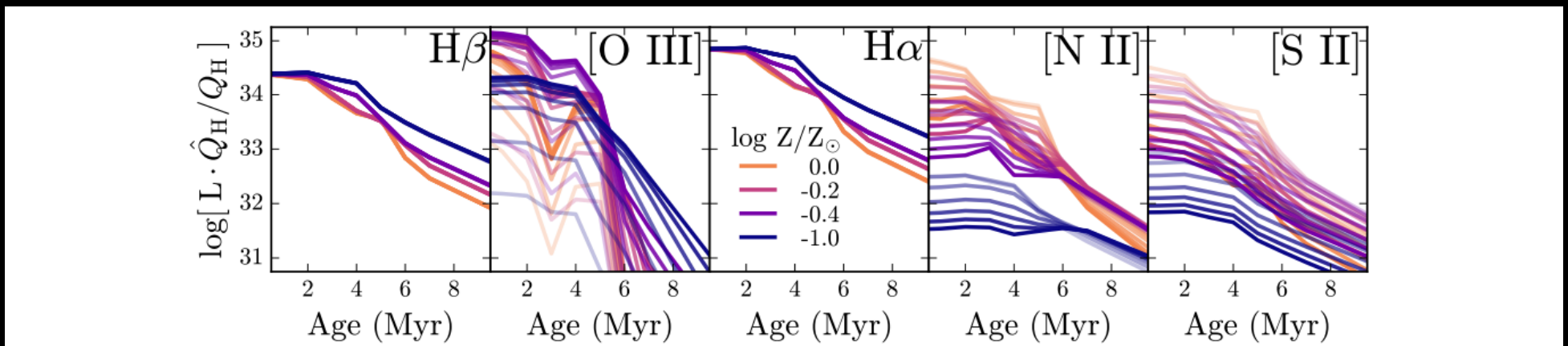


Figure 13. Emission line strength for $\text{H}\beta \lambda 4861\text{\AA}$, $[\text{O III}] \lambda 5007\text{\AA}$, $\text{H}\alpha \lambda 6563\text{\AA}$, $[\text{N II}] \lambda 6584\text{\AA}$, and $[\text{S II}] \lambda 6731\text{\AA}$ as a function of model age, color-coded by model metallicity. The transparency of the line indicates the ionization parameter, which varies from $\log_{10} U_0 = -1$ (opaque) to $\log_{10} U_0 = -4$ (transparent).

Line ratios depend on Z , U , and t

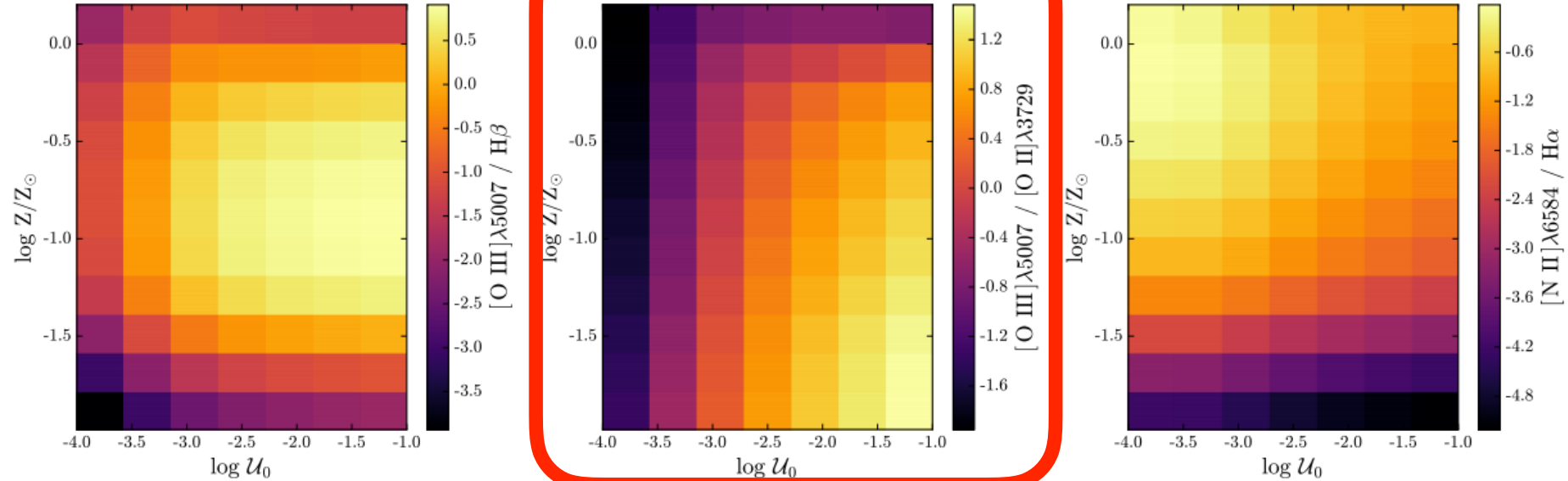


Figure 14. Line ratios as a function of metallicity and ionization parameter for a 1 Myr model: $[\text{O III}]\lambda 5007/\text{H}\beta$ (left); $[\text{O III}]/[\text{O II}]$ (middle); $[\text{N II}]\lambda 4865/\text{H}\alpha$ (right).

OIII/OII is sensitive to ionization parameter

Line ratios depend on Z , U , and t

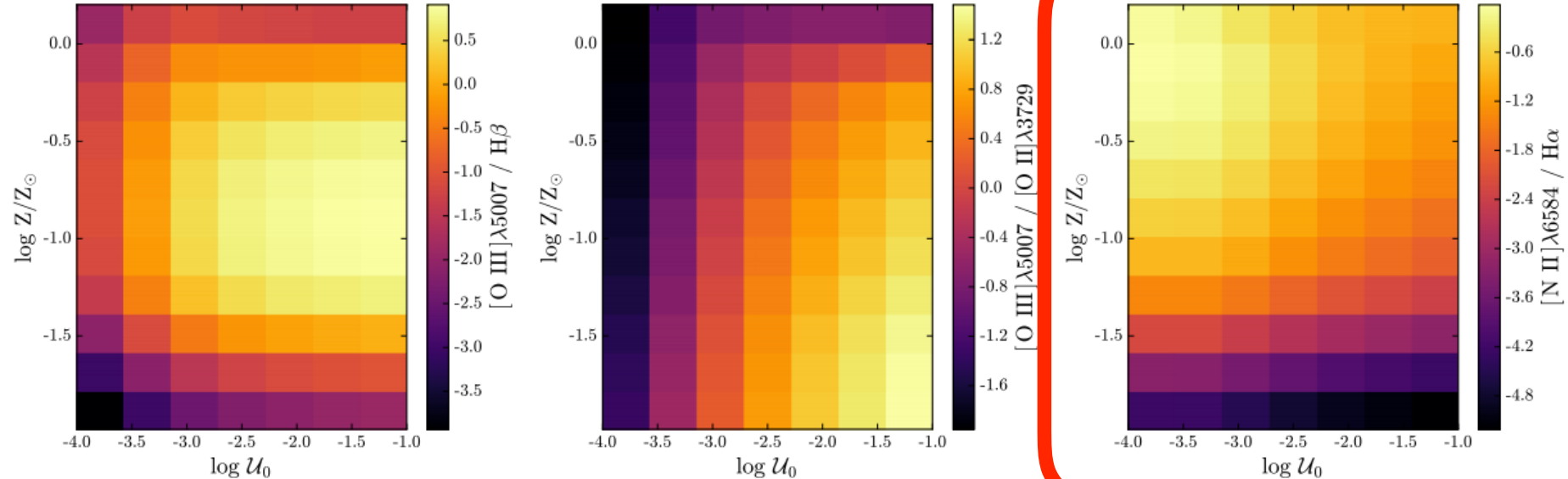


Figure 14. Line ratios as a function of metallicity and ionization parameter for a 1 Myr model: $[\text{O III}]\lambda 5007/\text{H}\beta$ (left); $[\text{O III}]/[\text{O II}]$ (middle); $[\text{N II}]\lambda 6584/\text{H}\alpha$ (right).

NII/H α is sensitive to metallicity

Line ratios depend on Z , U , and t

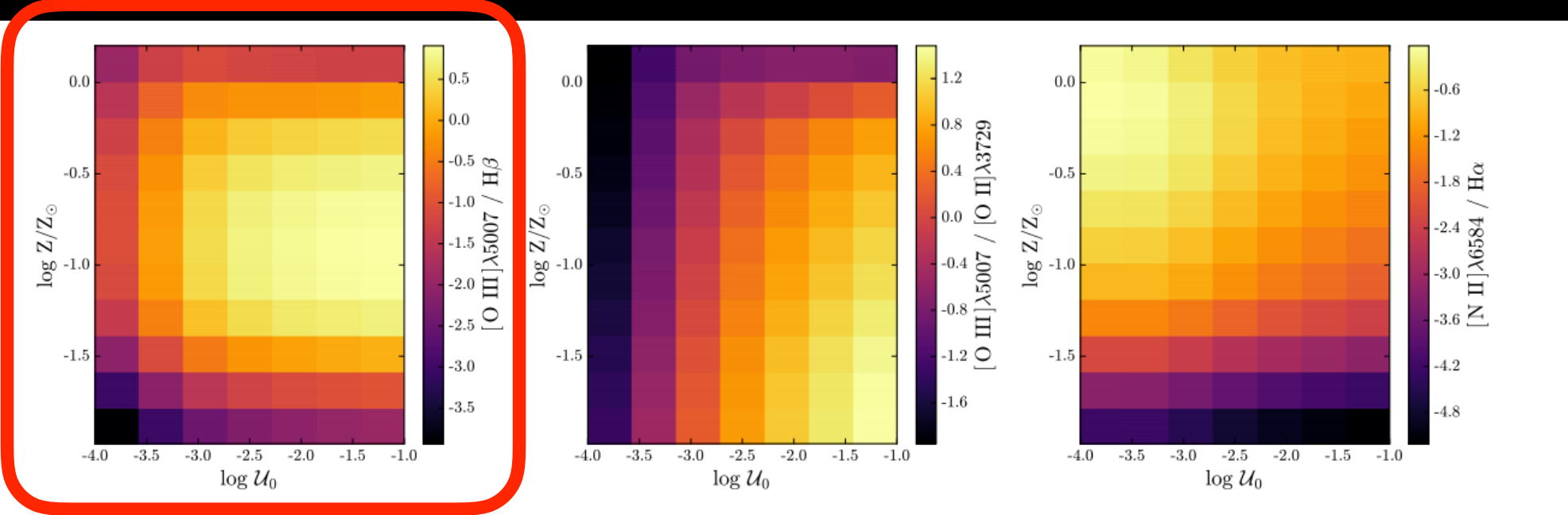


Figure 14. Line ratios as a function of metallicity and ionization parameter for a 1 Myr model: $[\text{O III}]\lambda 5007/\text{H}\beta$ (left); $[\text{O III}]/[\text{O II}]$ (middle); $[\text{N II}]\lambda 6584/\text{H}\alpha$ (right).

OIII/H β is complicated

For most nearby galaxies, $Z > -1$,
so stronger OIII/H β means lower metallicity

Two approaches to deriving Z from lines

Weak Line Methods

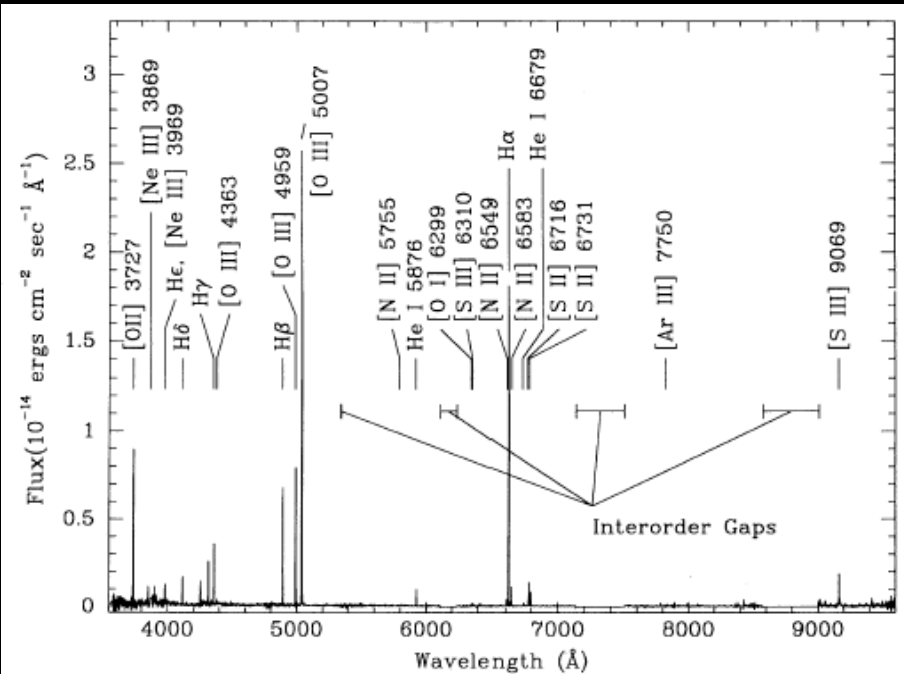
- Requires high SNR spectra to detect faint diagnostic lines
- Solves in detail for properties of individual HII regions (T_e, n_e)

Strong Line Methods

- Easy to measure
- Depends on calibrations (from data or theory)

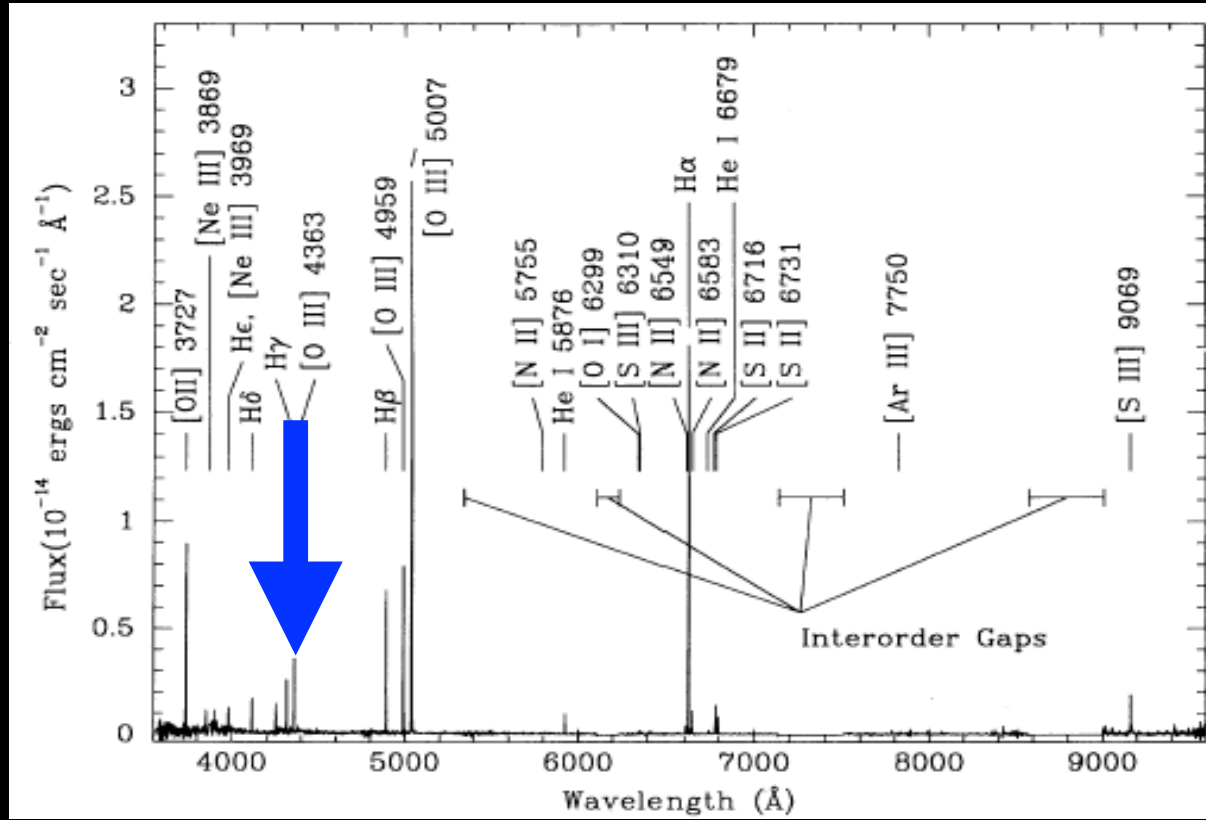
Weak Line Methods

require measuring
 T_e , n_e , Q_{ion}



- Q_{ion} : Constrain using photoionization models (usually constrains U instead)
- n_e : Use “density sensitive” line ratios like [SII]6716Å, 6731Å, or [OII]3727 doublet
- T_e : Use “temperature sensitive” line ratios like [OIII]4363Å, 5007Å

Difficulty measuring T_e with [OIII]4363Å



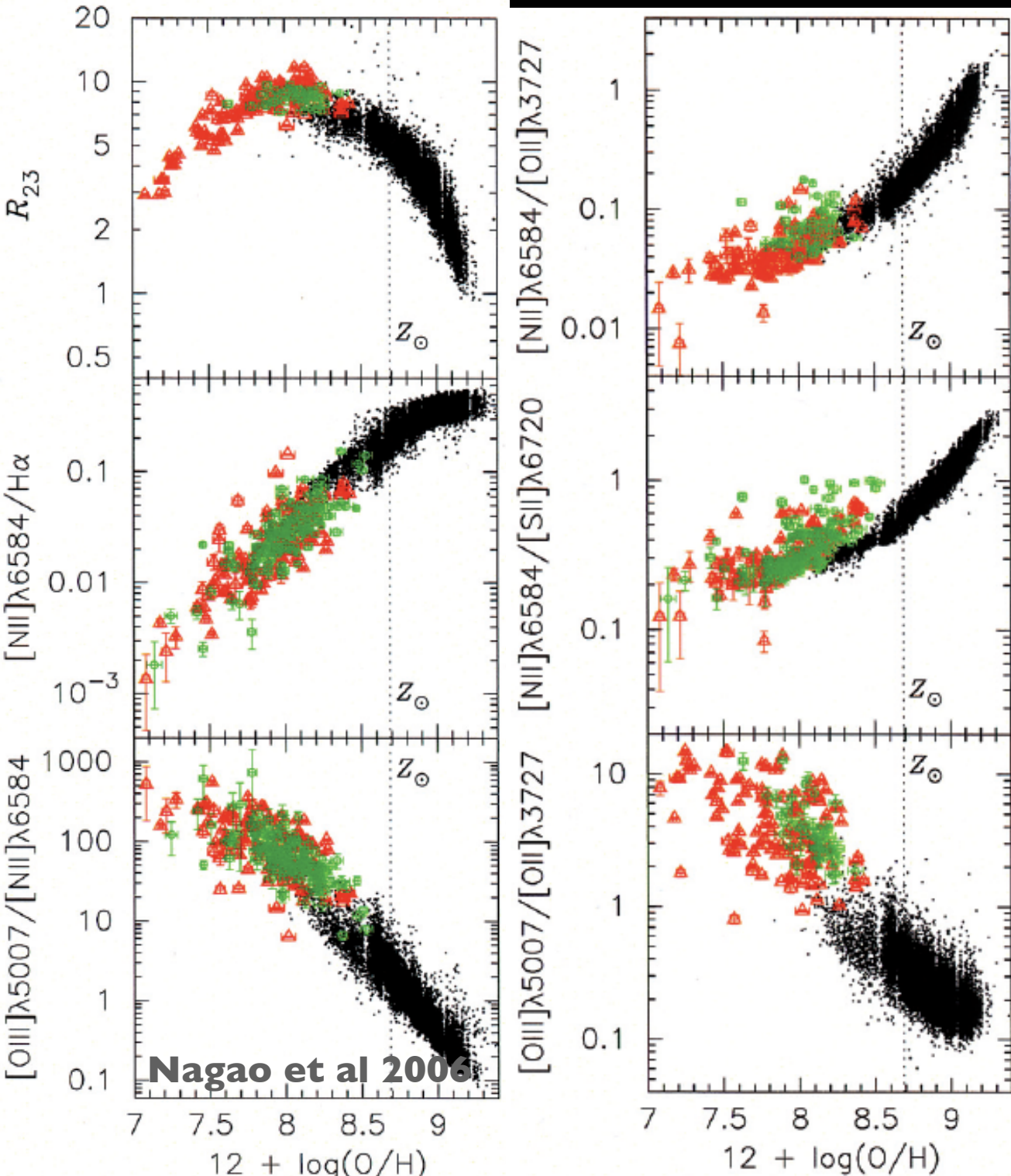
- This is a **weak line!** Needs high SNR
- Usual approach: Use “weak line” methods to calibrate techniques **only** using strong lines
- Or, use theoretical “grids” of line ratios as a function of U and Z .

Strong Line Methods

- “R23” method -- Uses $[\text{OII}]$, $[\text{OIII}]$, $\text{H}\beta$ lines
- Pilyugin P-Method -- like R23, but with empirical correction for ionization parameter
- “N2” -- $[\text{NII}]/\text{H}\alpha$
- “O3N2” -- $([\text{OIII}]/\text{H}\beta) / ([\text{NII}]/\text{H}\alpha)$
- “N2O2” -- $[\text{NII}]/[\text{OII}]$

Note: Should correct for stellar absorption lines, particular for Balmer lines

Calibrating Strong-Line Methods



Red: SDSS w/
[OIII]4363

Ivotov et al 2006

Green: Literature w/
[OIII]4363

Black: SDSS from
strong lines+models

Tremonti et al 2006

Fig. 6. Emission-line flux ratios of $R_{23}(=[F([OII]\lambda 3727) + 1.327 \times F([OIII]\lambda 5007)]/F(H\beta))$, $F([NII]\lambda 6584)/F(H\alpha)$, and $F([OIII]\lambda 5007)/F([NII]\lambda 6584)$ for galaxies in sample A (red triangles), in sample B (green circles) and in sample C (black dots), as a function of the oxygen abundance. The compiled low-metallicity galaxies with an error of the oxygen abundance larger than 0.05 dex are not plotted. Dotted lines denote the solar metallicity [$12 + \log(O/H) = 8.69$].

Calibrating Strong Line Methods:

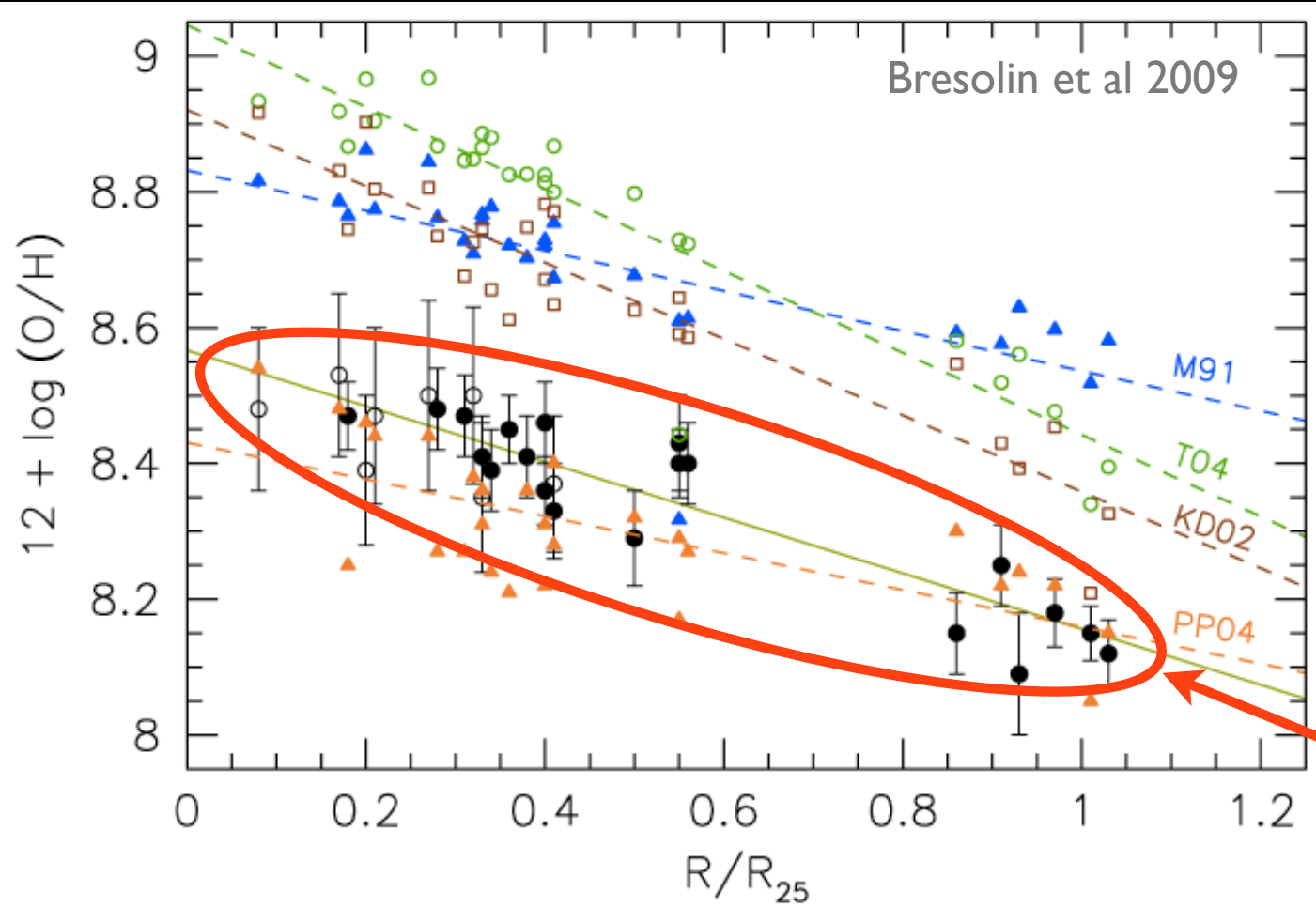
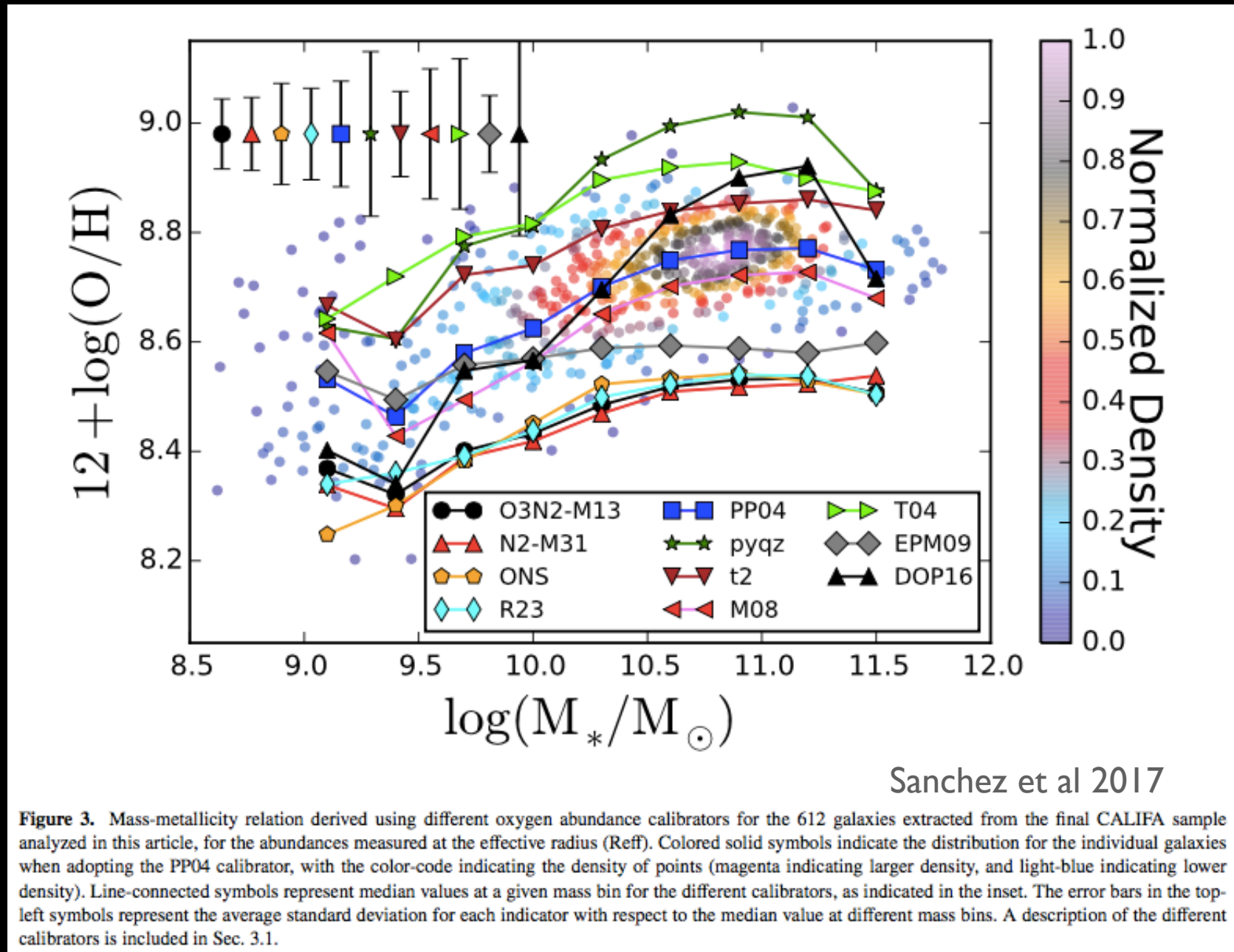


Figure 12. Galactocentric distribution of the abundance values obtained from different strong-line methods and calibrations: R_{23} (McGaugh 1991: M91, blue triangles; Tremonti et al. 2004: T04, green circles), $[N\text{ II}]/[O\text{ II}]$ (Kewley & Dopita 2002: KD02, open squares), and N2 (Pettini & Pagel 2004: PP04, orange triangles). Linear least-squares fits are shown by the dashed lines, and labeled with the appropriate reference. The direct abundances determined from our work are shown by the full and open circle symbols, and the corresponding linear fit is shown by the continuous line (same as in Figure 10).

- Many common strong line indicators are biased high

Ground truth
from stellar
spectroscopy
of young stars
+ weak line
methods

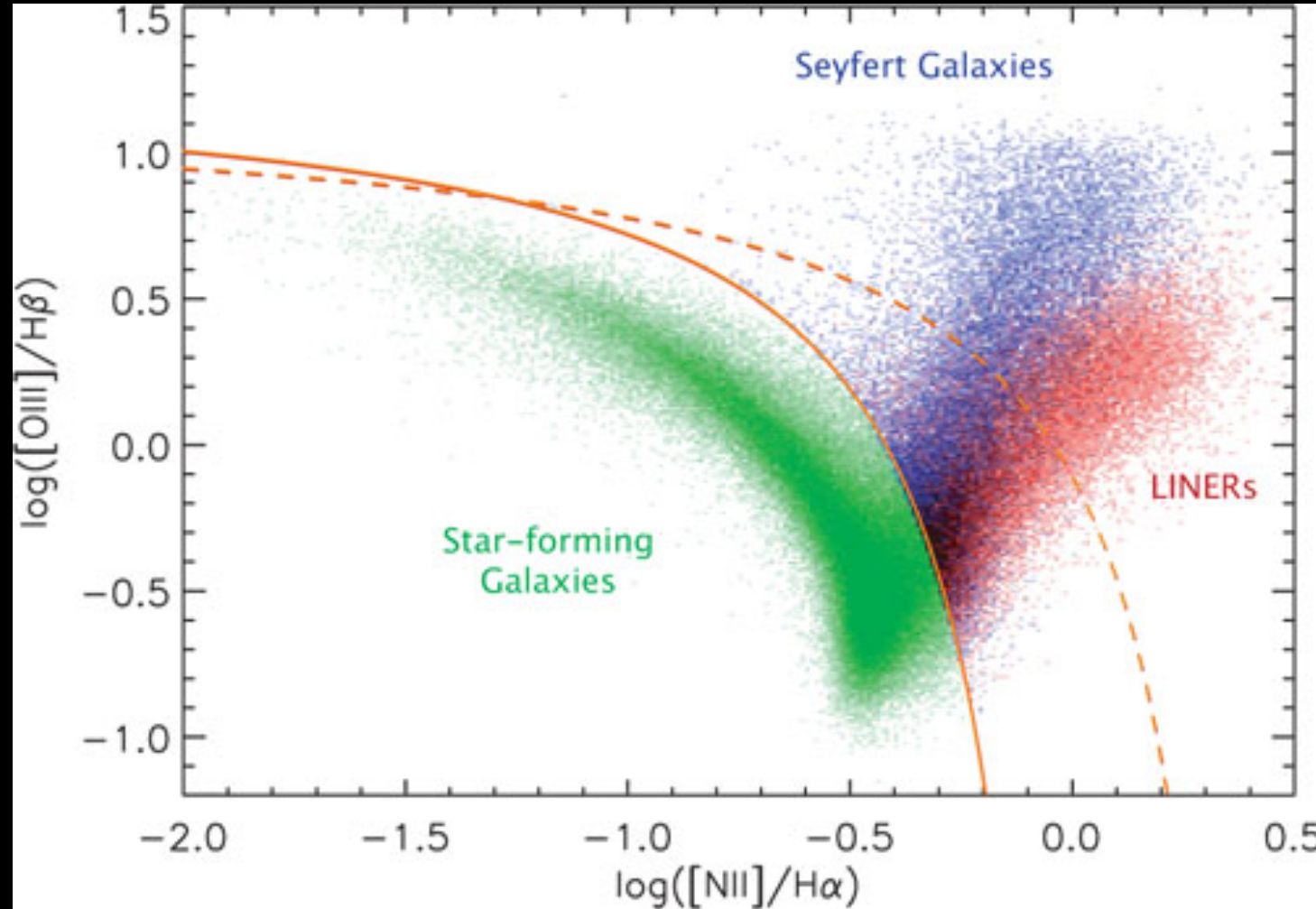
Mass-Metallicity Relation can look different by 0.2 dex with different strong-line methods



Caveats: Line ratios also affected by AGN (shocks+photoionization)

SDSS: Based on Kewley et al 2006

http://www.eso.org/~rfsbury/research/AGN2-07/AGN2-07_Messenger_v5.1.html



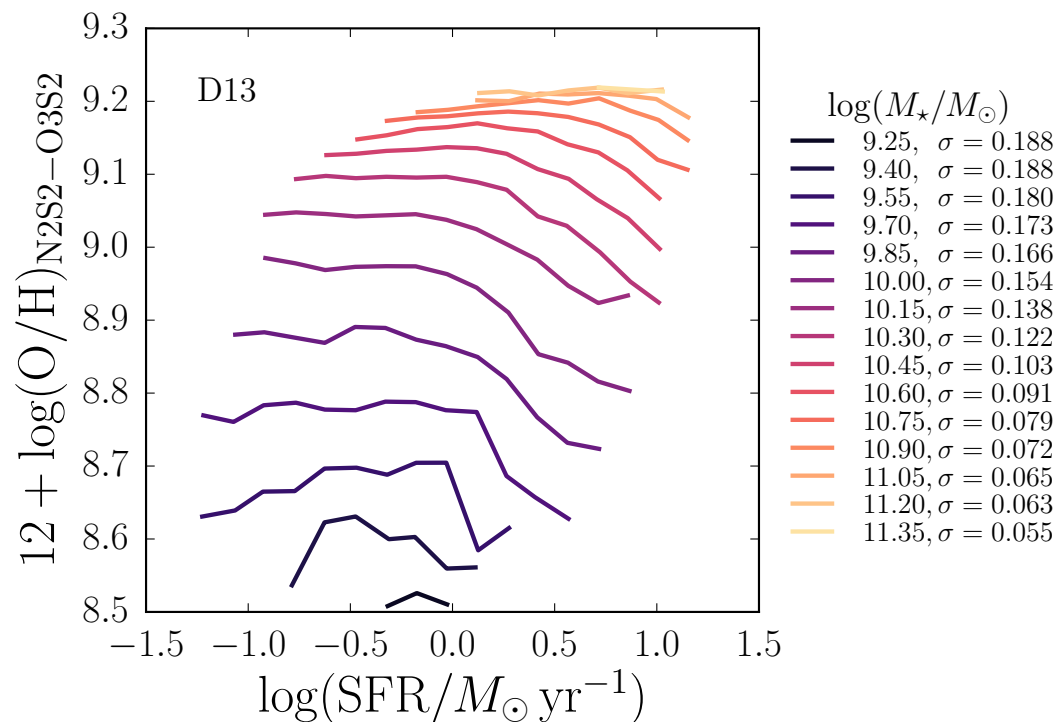
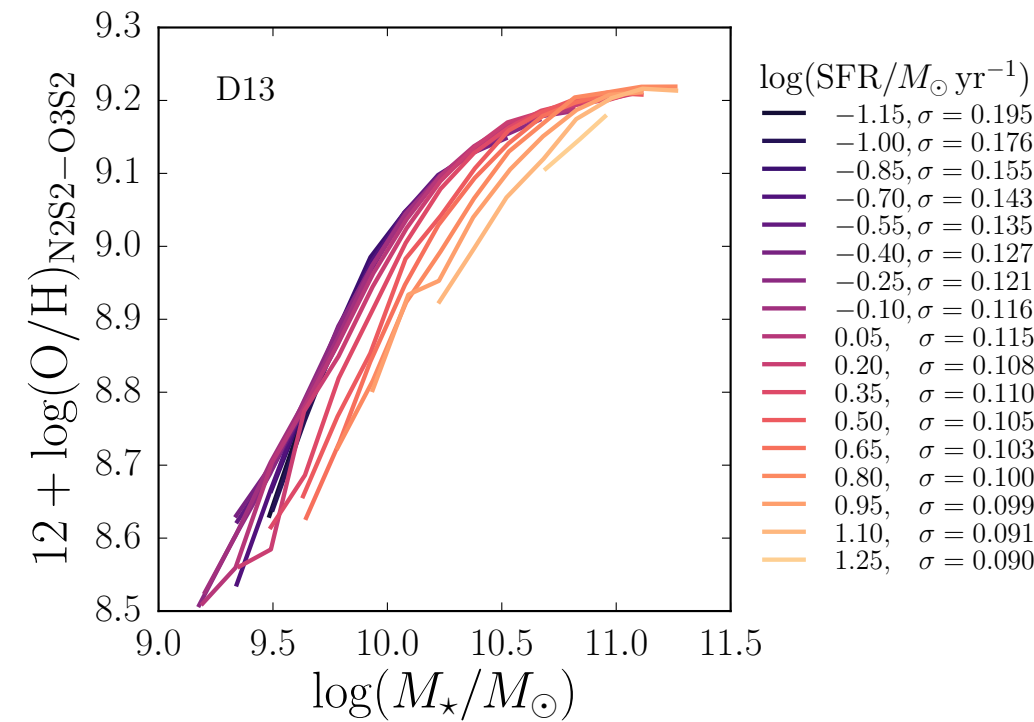
Other groups using SDSS calibration to create line ratio + color or line ratio + mass AGN vs SF galaxy classification for high-z work. (Juneau et al 2011, Yan 2011)

“BPT Diagram”: Baldwin, Phillips, & Terlevich 1981

Basic Metallicity Results

- Mass-metallicity correlation
 - Evidence for mass dependent metal loss
 - Possible correlation w/ SFR
 - Evolves w/ redshift
- Bulge vs disk metallicities
- Metallicity gradients within disks
- Metallicity and α -enhancement in ellipticals

Possible secondary dependence of metallicity on SFR



First popularized by Manucci et al 2010
(M-Z-SFR relation)

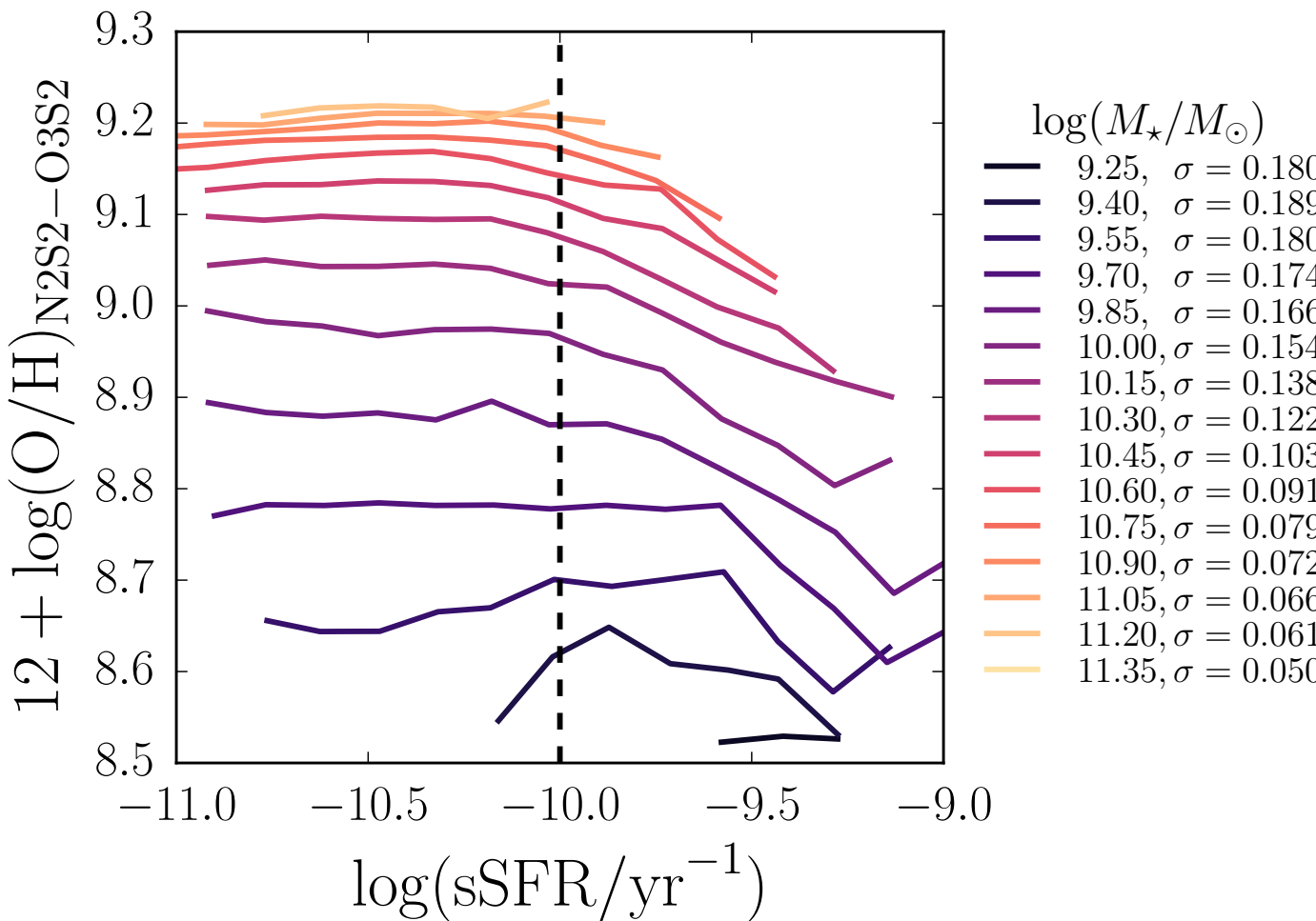
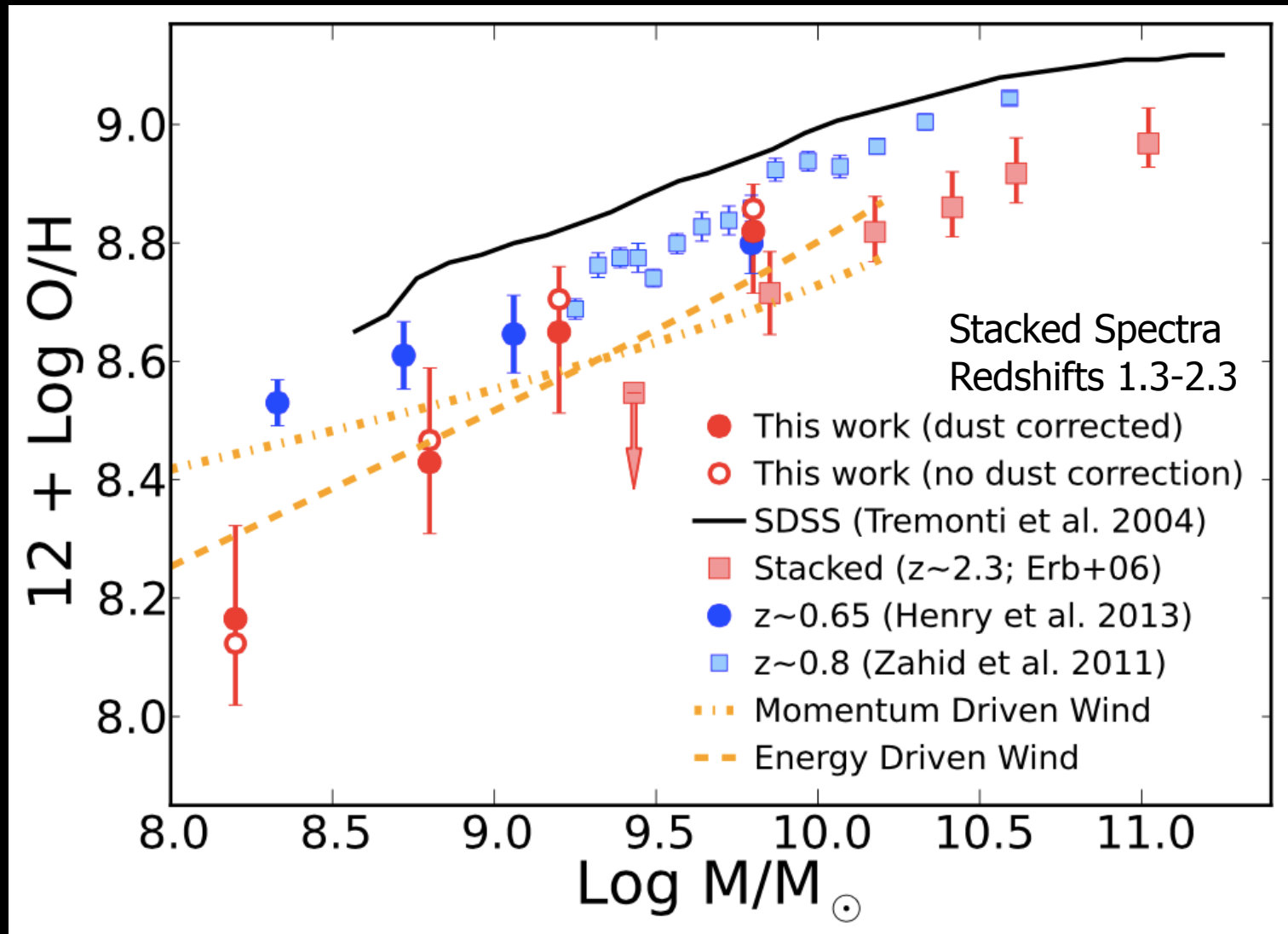


Figure 8. Recasting the M_* – Z – SFR relation in terms of specific SFR. Analogous to the right panel of Figure 5 but using $\log(\text{sSFR})$ instead of $\log(\text{SFR})$. Metallicities are calculated using the fiducial D13 abundance diagnostic grid (N2S2–O3S2). All bins have 0.15 dex width in each $\log(M_*)$ and $\log(\text{sSFR})$ and each bin contains at least 50 galaxies. The dashed line at $\log(\text{sSFR}/\text{yr}^{-1}) = -10$ is shown for reference; 18,960 galaxies (14.5 % of the sample) lie to the right of this line. This figure demonstrates that metallicity is only strongly anti-correlated with sSFR in the high sSFR regime.

Origin and/or strength of effect is unclear.
Some argue infall driven bursts. But, many systematics, effect weak in IFU data

Mass-Metallicity Evolves w/ Redshift



Henry et al 2013

- Fraught with peril, but would be surprised if it didn't evolve.

Example: Disk vs Bulge colors

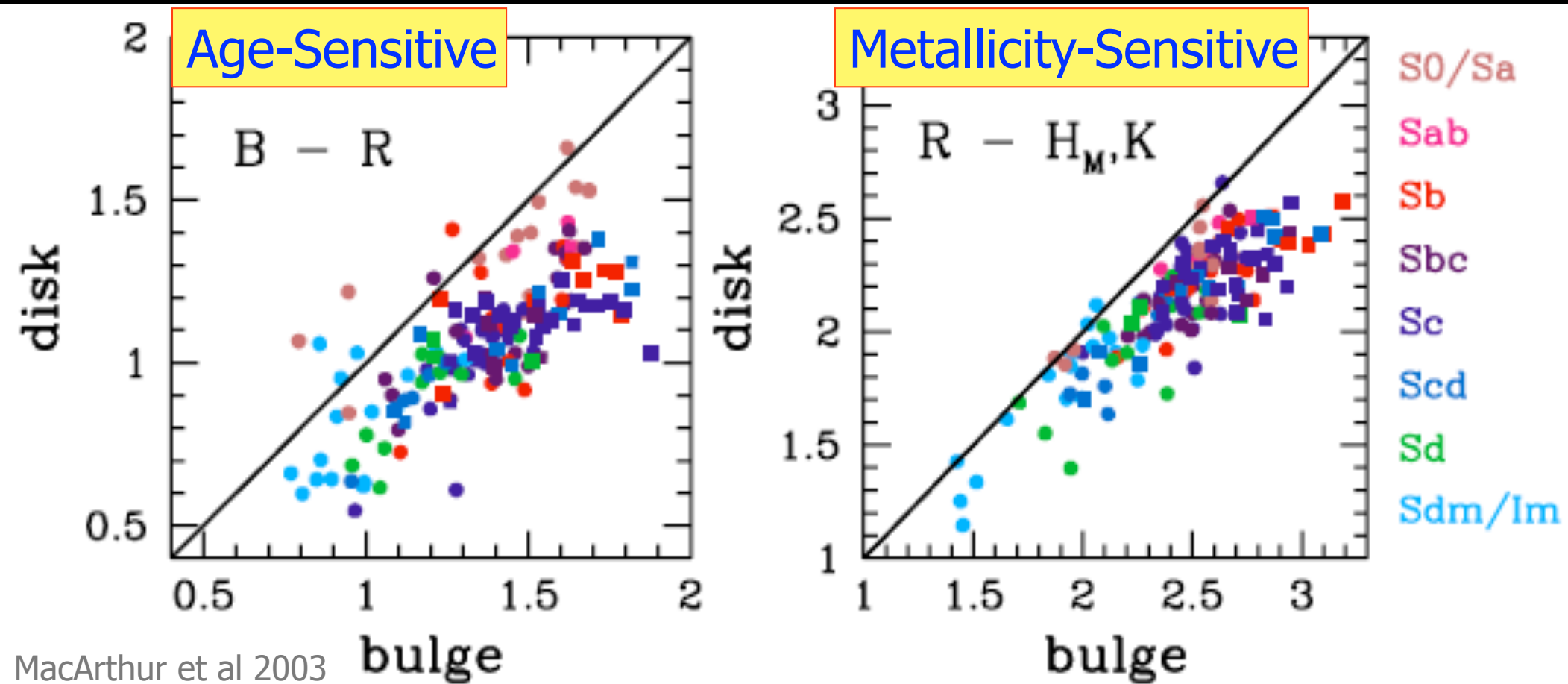
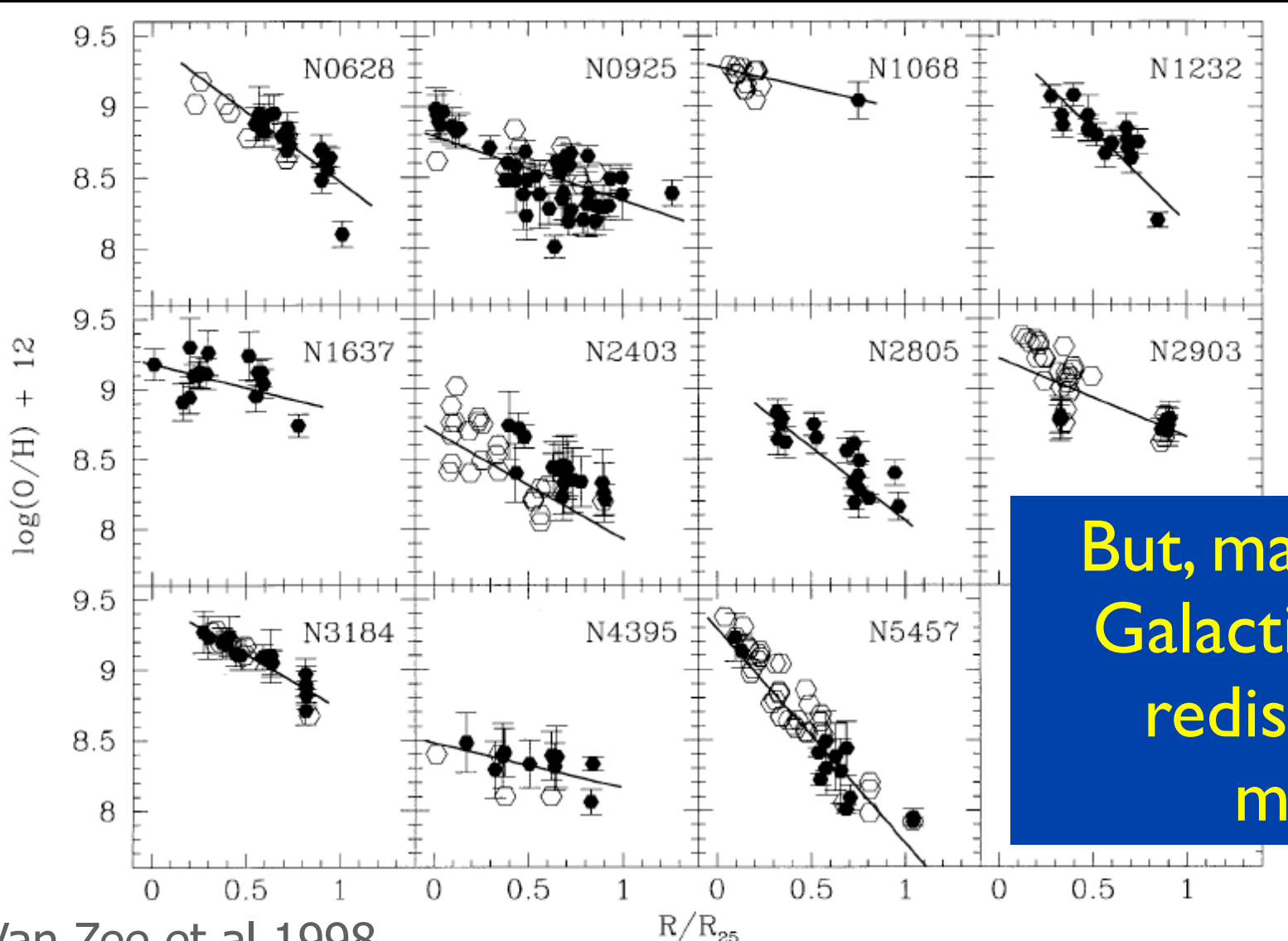


FIG. 8.—Disk colors (average of 1.5–2.5 disk scale length radial bin) as a function of bulge colors (average of 0.0–0.5 disk scale length radial bin). The solid horizontal lines represent a one-to-one mapping (for reference only). H_m is the “modified” H -band magnitude for the Courteau et al. sample, converted to K band with 2MASS $H-K$ colors (see text for details) for direct comparison with the K -band data of the BdJ00 sample.

- Bulges are redder in $B-R$ (older)
- Bulges are redder in $R-K$ (more metal rich)

Within disks, metallicity gradients are common



Non-zero
scatter at
fixed
radius,
however.

But, many are flat.
Galactic fountain
redistributing
metals?

FIG. 12.—Observed oxygen abundance gradients in all 11 spiral galaxies. The filled symbols represent H II regions from the present study. The open circles represent data from the literature: NGC 628, McCall et al. (1985); NGC 925, Zaritsky et al. (1994); NGC 1068, Evans & Dopita (1987), Oey & Kennicutt (1993); NGC 2403, McCall et al. (1985), Fierro et al. (1986), Garnett et al. (1997); NGC 2903, McCall et al. (1985), Zaritsky et al. (1994); NGC 3184, Zaritsky et al. (1994); NGC 4395, McCall et al. (1985); NGC 5457, Kennicutt & Garnett (1996). The solid lines illustrate the derived oxygen abundance gradients.

Internal gradients w/ stars are weaker, and dominated by age

MacArthur et al 2003

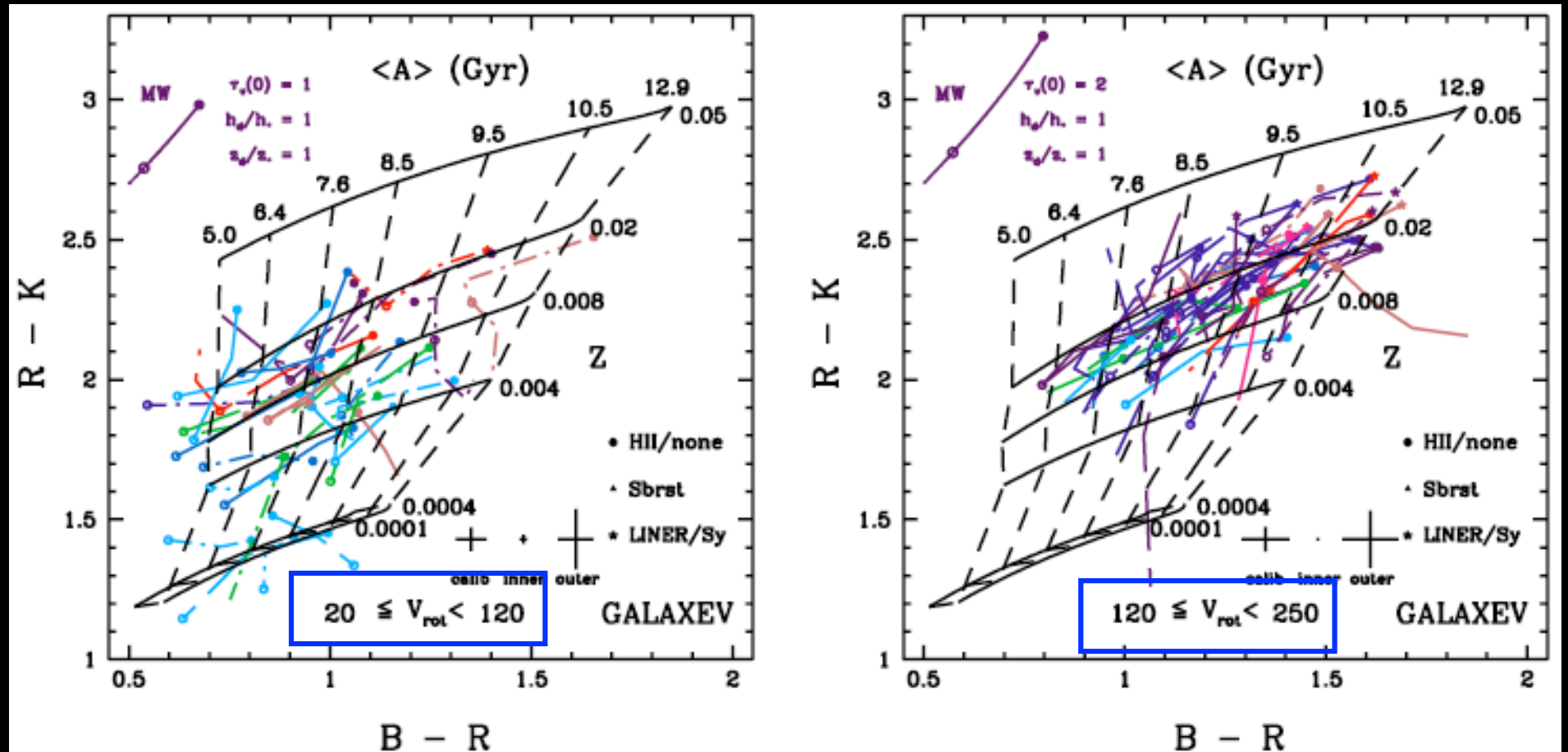
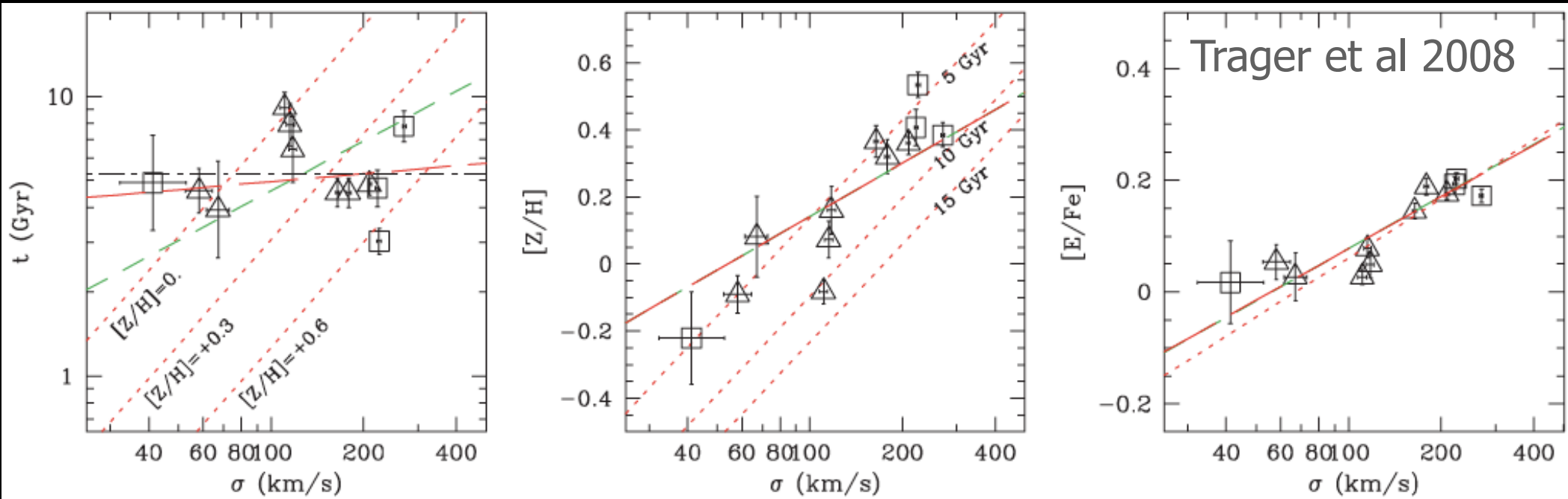


FIG. 11.—Near-IR-optical color-color plots separated by rotational velocity, V_{rot} (km s^{-1}), for the BdJ00 sample. Galaxy center point types correspond to the level of nuclear activity in the galaxies (trends with colors and their gradients with nuclear activity were looked for but none were found, possibly because of small statistics).

Is this radial differences in metal loss? in gas accretion? in gas fraction?

Application: Ellipticals in Coma



More Massive Ellipticals have:

- Higher metallicity
- More alpha-enhancement

(No trend with age apparent, but luminosity weighted, so small “frosting” of SF at $z \sim 0.3$ could mask underlying age trend)